National Library of Canada
Bibliothèque nationale du Canada

Canadian Theses Service
Service des thèses canadiennes

Ottawa, Canada
K1A 0N4

NOTICE

The quality of this microform is heavily dependent upon the quality of the original thesis submitted for microfilming. Every effort has been made to ensure the highest quality of reproduction possible.

If pages are missing, contact the university which granted the degree.

Some pages may have indistinct print especially if the original pages were typed with a poor typewriter ribbon or if the university sent us an inferior photocopy.

Previously copyrighted materials (journal articles, published tests, etc.) are not filmed.

Reproduction in full or in part of this microform is governed by the Canadian Copyright Act, R.S.C. 1970, c. C-30.

AVIS

La qualité de cette microforme dépend grandement de la qualité de la thèse soumise au microfilmage. Nous avons tout fait pour assurer une qualité supérieure de reproduction.

S'il manque des pages, veuillez communiquer avec l'université qui a conféré le grade.

La qualité d'impression de certaines pages peut laisser à désirer, surtout si les pages originales ont été dactylographiées à l'aide d'un ruban usé ou si l'université nous a fait parvenir une photocopie de qualité inférieure.

Les documents qui font déjà l'objet d'un droit d'auteur (articles de revue, tests publiés, etc.) ne sont pas microfilmés.

La reproduction, même partielle, de cette microforme est soumise à la Loi canadienne sur le droit d'auteur, SRC 1970, c. C-30.

NL-339 (r. 88/04)

Canada

THE UNIVERSITY OF ALBERTA

A PALEO-GEOMAGNETIC STUDY OF PLEISTOCENE SEDIMENTS IN NORTHWESTERN CANADA

by

KEVIN PAUL GILLEN

A THESIS

SUBMITTED TO THE FACULTY OF GRADUATE STUDIES AND RESEARCH

IN PARTIAL FULFILMENT OF THE REQUIREMENTS FOR THE DEGREE

OF MASTER OF SCIENCE

IN

GEOPHYSICS

DEPARTMENT OF PHYSICS

EDMONTON, ALBERTA

FALL 1988

Permission has been granted to the National Library of Canada to microfilm this thesis and to lend or sell copies of the film.

The author (copyright owner) has reserved other publication rights, and neither the thesis nor extensive extracts from it may be printed or otherwise reproduced without his/her written permission.

L'autorisation a été accordée à la Bibliothèque nationale du Canada de microfilmer cette thèse et de prêter ou de vendre des exemplaires du film.

L'auteur (titulaire du droit d'auteur) se réserve les autres droits de publication; ni la thèse ni de longs extraits de celle-ci ne doivent être imprimés ou autrement reproduits sans son autorisation écrite.

ISBN 0-315-45771-6

THE UNIVERSITY OF ALBERTA

RELEASE FORM

NAME OF AUTHOR KEVIN PAUL GILLEN

TITLE OF THESIS A PALEO-GEOMAGNETIC STUDY OF PLEISTOCENE SEDIMENTS IN NORTHWESTERN CANADA

DEGREE FOR WHICH THESIS WAS PRESENTED MASTER OF SCIENCE

YEAR THIS DEGREE GRANTED FALL 1988

Permission is hereby granted to THE UNIVERSITY OF ALBERTA LIBRARY to reproduce single copies of this thesis and to lend or sell such copies for private, scholarly or scientific research purposes only.

The author reserves other publication rights, and neither the thesis nor extensive extracts from it may be printed or otherwise reproduced without the author's written permission.

(SIGNED) Kevin Gillen

PERMANENT ADDRESS:

2841 DANDURAND BLVD,
WINDSOR, ONTARIO
N9E 2E5

DATED Sept 30 1988

THE UNIVERSITY OF ALBERTA

FACULTY OF GRADUATE STUDIES AND RESEARCH

The undersigned certify that they have read, and recommend to the Faculty of Graduate Studies and Research, for acceptance, a thesis entitled A PALEO-GEOMAGNETIC STUDY OF PLEISTOCENE SEDIMENTS IN NORTHWESTERN CANADA submitted by KEVIN PAUL GILLEN in partial fulfilment of the requirements for the degree of MASTER OF SCIENCE in GEOPHYSICS.

Michael Evans

Supervisor

H. A. K. Charlesworth

J. C. Samson

Douglas P. Hyde

Date.....

Abstract

A total of 626 specimens was collected in two laterally equivalent vertical sections (each approximately 20m in height) from Pleistocene sediments exposed in river bank outcrops on the Old Crow River, Yukon Territory. Paleomagnetic examination revealed remanent magnetization records of both geological and geophysical interest. A sequence of three features appearing in both sections can be correlated with results obtained from previously sampled sections some 5 km upstream. This concordance between previous and present results suggests a geomagnetic perturbing source rather than a sedimentological one.

The remarkable correlation observed allows a date for these sediments to be established paleomagnetically. Previous results come from a site where the Old Crow Tephra is preserved. The unique paleomagnetic signal associated with this tephra is found in both sections of this present study (very good in one, but poorer in the second) and therefore fixes the age of the pertinent level in these sediments as equivalent to that of the tephra (149,000 ±13,000 years B.P.).

The remainders of both sections show features consistent with the idea of a stationary magnetic source in the outer core which has acted intermittently. These features involve perturbations of the remanent magnetization vector, along linear trajectories, in excess of 60° from the ambient position expected from a geocentric axial dipole

field. Elementary magnetostatic modelling shows that even the largest perturbation can be explained by an eccentric radial dipole at the Core-Mantle Boundary (CMB) with moment directed away from the geocentre and as small as about 8% of the moment of the main dipole. Such an outward moment vector would yield a patch of reverse flux at the CMB, very similar in many respects to patches of reverse flux currently existing in the southern hemisphere.

Acknowledgements

I wish to express my deepest appreciation to Dr. M.E. Evans for guidance and stimulating discussion during my work at the University of Alberta. Without his supervision, this thesis could not have been completed.

I am greatly indebted to both the Natural Sciences and Engineering Research Council and the Boreal Institute for Northern Studies for awarding me a Post-graduate scholarship and partially funding my field work respectively. I also wish to thank Dr. C.E. Schweger and Dr. J.V. Matthews for their consultation in the field, my friend Philip Ingenkamp for his help in collecting the samples and Vaslov Frnoch for his help in processing them.

Finally I wish to thank my best friend Esther Methe for her encouragement and patience at all times.

Table of Contents

Chapter	Page
I. INTRODUCTION	1
A. Geomagnetism	1
B. Fossil Magnetism	10
C. Scope of thesis	12
II. SITE DESCRIPTION AND SAMPLING	13
III. NRM AND AF DEMAGNETIZATION RESULTS	20
IV. DECLINATION AND INCLINATION OSCILLATIONS	36
A. Section KGA	36
B. Section KGB	52
V. ANALYSIS OF GEOMAGNETIC SECULAR VARIATION	60
A. Modelling of features A2 and A3	60
B. Comparison with the modern field	69
VI. SUMMARY AND CONCLUSIONS	78
REFERENCES	81
APPENDIX A - Theta	85
APPENDIX B - Data	91

List of Tables

Table		Page
III.1	Table of vector statistics for NRM and 10 mT data of KGA and KGB	35
V.1	Modelling data and results for A2 and A3	62
A.1	Theta values for selected samples on Schonstedt and Molspin magnetometers	89

List of Figures

Figure		Page
I.1	Inclination-declination variations at London and Paris with time	5
I.2	Anomalies in the vertical component of the non-dipole field at 1700 and 1922 A.D.	7
II.1	Location of study area	14
II.2	Location of sites 11 and 11N on the Old Crow River	15
II.3	Composite stratigraphy of the Old Crow Basin	16
III.1	Histogram of NRM intensities for section KGA and KGB combined	21
III.2	Magnetograms of NRM data for section KGA	22
III.3	Magnetograms of NRM data for section KGB	23
III.4	Normalized moment versus demagnetizing field	25
III.5	Typical pilot sample behaviour during demagnetization	26
III.6	Angular shift between successive demagnetization steps normalized by increment of demagnetization field	27
III.7	Zijderveld plots of further demagnetization performed on KGA	30
III.8	Magnetograms for 10 mT data from section KGA	31
III.9	Magnetograms for 10 mT data from section KGB	32
III.10	vector averages for NRM and 10 mT data of KGA and KGB	34
IV.1	Lithology between 10 m and 17 m of section KGA	37
IV.2	Expanded version of Figure 3-8 after removal of sand layers	38
IV.3	Declination-inclination equal area plot for features A2	40

Figure		Page
IV.4	Declination-inclination equal area plot for A3	43
IV.5	Declination-inclination equal area plots for A4	44
IV.6	Calibration curve for susceptibility measurments	45
IV.7	Susceptibility versus elevation for section KGA	46
IV.8	Declination-inclinaton plot of A5	49
IV.9	Declination-inclination equal area plot for A2 with within-pair dispersion criterion removed	51
IV.10	Magnetogram for KGB after correction	53
IV.11	Declination-inclination plots of B1, B2 and B3	55
IV.12	Declination-inclination plot of B4	56
IV.13	Declination-inclination plot for B5	58
V.1	Schematic of model used	61
V.2	Locations and magnitudes of radial dipoles which explain features A2 and A3	66
V.3	Minimum radial dipole moment versus depth below the Core-Mantle interface	68
V.4	Reverse flux patches at Core-Mantle interface in 1945 field	71
V.5	Minimum values of ratio of moments of paleosources to present-day sources	73
V.6	Fit of 0.2, 1 and 5% radial dipoles to Z field profile	75
A.1	Noise levels for Schonstedt and Molspin designs	86
A.2	Theta Schonstedt versus theta Molspin	90

I. INTRODUCTION

The bulk of the magnetic field at the Earth's surface has its origin in the interior of the planet. Many of the methods used today to analyze the field, as well as the terms used to describe its character, have a considerable history. Thus a proper understanding of the present state of geomagnetism begins with a study of the past.

A. Geomagnetism

Some properties of magnetism are claimed by some historians to have been known in China as early as the second millenium B.C. and the Chinese are credited with the invention of the compass. After its introduction into Europe, it was noted that although the needle pointed roughly North (as defined by the pole star), it usually diverged by a small amount. This angular difference in one's local horizontal plane between true north and the compass went by various names but is today called *declination*. Sailors using the compass to navigate had to correct for this effect. When the needle was suspended through its centre of gravity and allowed to orientate itself in three dimensions, it was discovered that it also assumed an inclined position. This measure of the field is called *inclination* and is defined as the deviation of the field from the local horizontal plane. In the beginning, this property was probably a nuisance since the needle had to be weighted in order to force it to sit horizontally and give

the measure of declination which was desired for navigation. These measures of the field have remained with us to the present day, and along with a measure of the intensity, totally define the geomagnetic vector at a point of observation.

In the early stages of compass use, the origin of the force which caused the needle to orientate was unknown and surrounded by much folklore. In 1600, Sir William Gilbert, in his famous work "De Magnete", put forth the suggestion that the Earth is a great magnet, a conclusion which he had drawn from experimentation with a sphere cut from lodestone. This model was successful in predicting some of the observed characteristics of the geometry of the field, such as the increase of inclination with latitude which was subsequently confirmed by Hudson during his voyage in the Barents Sea in the early seventeenth century.

In 1634 Gellibrand discovered that the magnetic declination at London changed with time. This time-dependent behaviour of the field cast some doubt on the simple model of the Earth as a permanently magnetized body. It was later discovered that changes also occur in the inclination and intensity.

The suggestion of the dipolar nature of the Earth's field did, however, come to be verified. Gauss (1839), in his spherical harmonic expansion of the field in terms of the sum of multipoles, showed the dipole term to be dominant and in the process, verified that the field was of

predominantly internal origin. This initial work was done with the best data available at the time, which were sparse, but subsequent analyses with modern data have confirmed that the dipole term constitutes 95% of the total field as seen at the Earth's surface, while the remaining 5% represents the sum of the non-dipole terms. From this discovery naturally grew the custom of discussing the properties of the field in terms of its *dipole* and *non-dipole* parts, a practice which has continued to the present day.

The representation of the field as a sum of multipoles is simply a mathematical convenience, and warnings have been made of the potential dangers of thinking of these multipoles as having physical meaning. However, it was soon discovered that the changes which the Earth's field was undergoing manifested themselves differently in the dipole and non-dipole parts. For example, their time constants of change were found to be different. This led some authors (e.g. Barton, 1978) to suggest that there may actually be a physical basis which justifies the discussion of change in the total field in terms of its dipole and non-dipole components. As will be seen later, the most commonly invoked mechanism for change in the field is movement of field lines by circulation of fluid in the outer core, and since this process involves the main field, it is not at first glance apparent why the two parts should possess different modes of change and different time constants.

There have been several suggestions as to why these differences exist. For example, Le Mouel (1984) has calculated that the types of motions probably involved at the surface of the outer core give a time-dependent change to the non-dipole field, yet such motions are not involved in sustaining the axial dipolar part of the field and thus do not affect it significantly.

The changes in the field as recorded at magnetic observatories such as London and Paris (Figure 1-1) were observed to occur primarily as a result of changes in the non-dipole part. Such studies of the time-dependent behaviour of the field at several sites lead to the suggestion that the changes observed at these places were not only due to a time-dependent morphology change of the non-dipole field but also to a rotation of the field. This drifting phenomenon has been termed the "westward drift" because the movement is predominantly westwards. Bullard et al (1950) shifted several decades of non-dipole field data around the spin axis to the point of best match and thereby determined an average drift rate of 0.2 °/year to the west. It must, however, be emphasized that changing non-dipole features are regional, not global in their extent, and thus the above figure is an average. Not all of the field drifts in a westward sense (in fact, not only do some parts stand still, but at some locations eastward drift is observed). This behaviour has been likened to a drifting weather pattern which predominantly drifts westward but exhibits

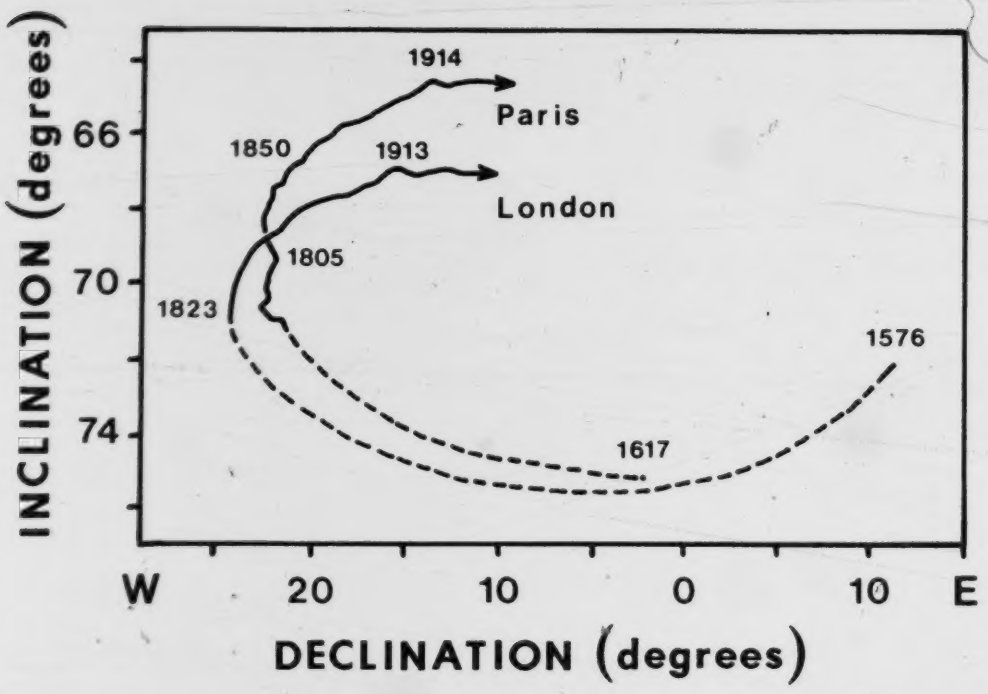

Figure 1-1: Inclination - declination variations at London and Paris (after Gaiber-Puertas, 1953).

regions in which some eastward movement occurs. A drifting feature in the non-dipole field is shown in Figure 1-2. Rates of change of the non-dipole field at the Earth's surface can be contoured as isoporic maps and reveal centres of high and low secular variation termed *isoporic foci*. Drift analysis, when applied to these foci gives a drift rate of 0.3°/year westward (Bullard et al., 1950). This higher rate results from the fact that stationary features in the non-dipole field are not present in an isoporic plot and thus do not contribute to bringing the average down. This is referred to as the *westward drift of the secular variation* whereas the former is known as the *westward drift of the non-dipole field*.

That part of the non-dipole field which does not appear to drift, exhibits regions which change their strength with time. The Mongolian positive anomaly, for instance, has strengthened with time at a linear rate of 53 nT/year over the past several hundred years while maintaining the same latitude and longitude throughout (Yukutake and Tachinaka, 1968) and is now at a level of 18,000 nT. The evolution of this anomaly with time is illustrated in Figure 1-2.

The main dipole (given by the first 3 terms in the spherical harmonic expansion) has also been observed to undergo some time-dependent behaviour. It has decreased in strength by 7% over the past 150 years (Bloxham & Gubbins, 1985). In fact, this appears to be part of a larger trend of main dipole decrease, as deduced from archeomagnetism.

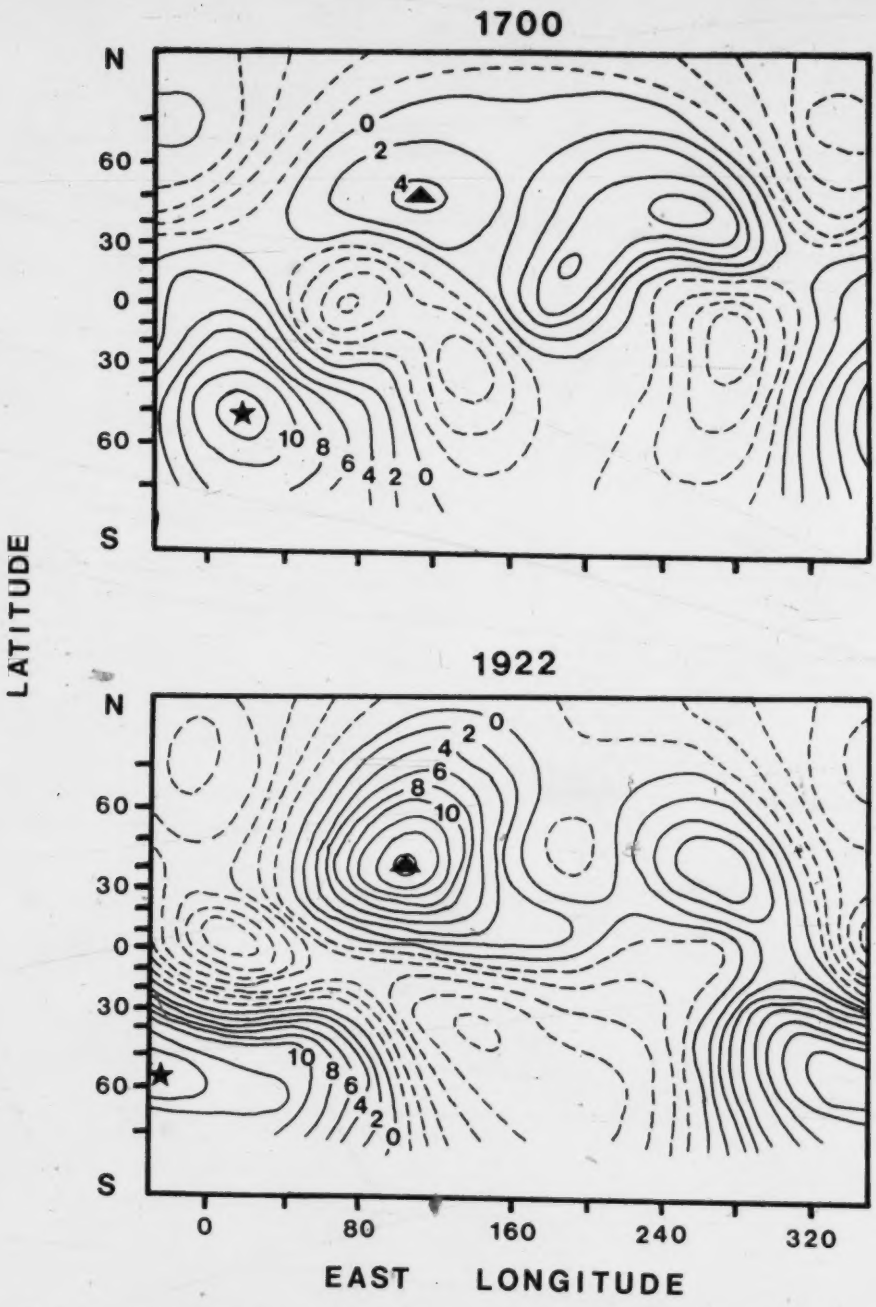

Figure 1-2: Anomalies in the vertical component of the non-dipole field at 1700 and 1922 A.D. Contour interval is 2000 nT, with solid line denoting +Z and dashed line representing -Z features. The triangle marks the position of a stationary feature which has strengthed over time (Mongolian anomaly). The star marks a westward drifting anomaly (after Yukutake and Tachinaka, 1968).

Archeological materials which are able to record the intensity of the field suggest that the main dipole moment has fluctuated in the past and has been as low as half and as high as twice its present value (Cox, 1968).

The orientation of the main dipole has not altered over the period of direct observation. At present, the axis is inclined at 11.5° to the axis of rotation and intersects the surface at 78.5° North, 70° West and 78.5° South, 110° East. This departure from the spin axis is attributed to *dipole wobble*. The nature and cause of dipole wobble is not understood but apparently involves a time scale of 10^3 years (too slow to be observed historically) with an average departure of about 10 degrees (McElhinny and Merrill, 1975).

In the modern field, we have not yet witnessed a complete cycle of change of any non-dipole or main dipole feature. For example, if the behaviour were periodic, the westward drifting features would take 1200 years (0.3°/year) to complete one revolution around the Earth and data on the modern field from direct observation go back no more than about 300 years. To extend the span of observation time, it is necessary to seek out geological material from which we might glean a chronicle of past geomagnetic field behaviour. Certain sediments may fulfil this requirement. The accumulation of detrital material, layer upon layer, yields a tape recording of the time variations of the field. Each sample collected from a section functions as a "fossil compass", providing a record of the direction of the

geomagnetic field at the time the magnetization was acquired. The record obtained is that of *paleosecular variation*. More will be said about the recording process in the next section.

Paleosecular variation records obtained from lake sediment have provided evidence of both standing sources which vary in intensity and sources which drift. Westward drift at various rates (e.g. 0.13°/year, Creer and Tucholka, 1982) has been observed, as well as some eastward drift (Denham, 1974). Features which appear to represent standing sources of varying intensity are also evident in some records (Evans, 1984; Hedlin and Evans, 1987; Latham et al., 1987). It must be emphasized, however, that the variations observed in sediments are most often of irregular period and amplitude (Creer et al., 1976; Mackereth, 1971). Typical amplitude variations for the vector at a site are usually less than 20 degrees from the position of the ambient vector.

In addition to the above, some paleosecular variation records show features which are not observed in the modern day field. The most important are polarity reversals. In such a case, the remanent magnetization vector in the material has an orientation roughly opposite to that expected from the present day dipole field. It usually remains to be established as to whether such a record represents global reversal (g¶ changes sign) or if it is a regional effect of some strong non-dipole disturbance. The

second type of field behaviour seen is an anomalously large deviation from the direction expected at a given site (greater than average paleosecular variation amplitudes, but less than a full reversal). Such behaviour is usually called an *excursion*. An excursion is defined as a movement of the dipole axis away from the spin axis with amplitude greater than 40°, but not fully reversing. "Excursions" in sediment therefore indicate a location of a paleopole (ancient geomagnetic pole) which is greater than 40° from the spin axis, however it must be established that such a signal represents a global event before such a term can be applied. The nature and cause of excursions are not understood.

B. Fossil Magnetism

In a manner akin to the alignment of a compass needle, detrital magnetic grains within a matrix of sediment are brought into alignment with the geomagnetic field. Remanent magnetization acquired in this fashion is referred to as *detrital remanent magnetism* (DRM). If this process occurs at the time of deposition, it is called *depositional detrital remanent magnetism* (dDRM), whereas any realignment taking place after deposition is termed *postdepositional* DRM (pDRM) (Verosub, 1977). The realignment takes place because the water-filled pore spaces within the sediment skeleton free the smaller magnetic grains. De-watering of the sediment

usually brings a halt to further realignment. It must be noted that there are several other forces which compete with the magnetic field in the alignment of the particles (e.g. gravity, viscous forces from water flow, etc.).

Magnetic overprinting of the DRM component can take place without physical rotation of the remanence carriers. When exposed to a field different from that which gave the DRM, the sample will sometimes pick up a component in the direction of the new field. Resistance of an individual grain to such overprinting is a function of the length of time exposed to the field and of the grain's *coercive force*. Since sediment is a collection of different magnetic grains with various coercive force values, the sample as a whole displays a *coercive force spectrum*. Such overprinting can usually be removed by alternating field (AF) demagnetization. The vector sum of all the magnetic components in a sample is referred to as the NRM (natural remanent magnetism).

The above discussion deals with the recording of direction only. The field, however, is a vector and also has a strength associated with it. How do sediments record the intensity of the geomagnetic field? The resultant magnetization results from the preferential alignment of moment vectors of individual grains. Theoretically, the stronger the field, the better the alignment and hence the higher the magnetic moment (up to a maximum attained when complete alignment is reached). This process is complicated

by variable composition. Variations in the amount of magnetic material will cause corresponding variations in intensity of magnetization. As a result, reliable paleofield intensities are rarely recovered from sediment.

C. Scope of thesis

The nature of paleosecular variation as recorded in sediment of Pleistocene age from the Old Crow Basin, Yukon Territory, Canada is examined. Two laterally equivalent vertical sections (approximately 20m and 21m in length) were sampled at stratigraphic intervals of roughly 10cm, yielding 626 samples for paleodirectional study. Fidelity of the material as a recorder of the Earth's field is established and the resultant remanent magnetization sequences are examined. Some perturbations present in this sequence of interest are modelled as sources located in the outer core, and these are compared with present day field characteristics.

II. SITE DESCRIPTION AND SAMPLING

The study area is located at latitude 67° 51' N and longitude 139° 48' W in the Old Crow Basin, Yukon Territory, Canada (Figure 2-1). The sampling sites (11 and 11N) are shown in Figure 2-2, which also shows the location of sites 15 and HH68-10 (sampled by Hedlin, 1986; Hedlin & Evans, 1987). The apparent lack of logic in the naming of these four sites is the result of the numerous investigations carried out by many different researchers over the past few decades.

The Basin itself is the product of deposition in glacial lakes formed as a result of ice damming during the Illinoian and Wisconsinan ice ages. Absence of these lakes during non-glacial periods allowed rivers to form fluvial deposits. The Old Crow and Porcupine Rivers, which presently transect the Basin, have cut down through this stratigraphy, thereby allowing it to be studied in riverbank sections. The limits of the last two ice advances (Figure 2-1) were such that the Basin was spared the effects of glaciation. Thus the NRM's recorded in the sediments potentially provide a relatively undisturbed and continuous record of the behaviour of the Earth's magnetic field during part of the Pleistocene.

A composite section of the relevant geology is given in Figure 2-3, in which Morlan and Matthews (1978) recognize nine units. This stratigraphy was compiled from several bluffs along the Old Crow valley and thus not all units are

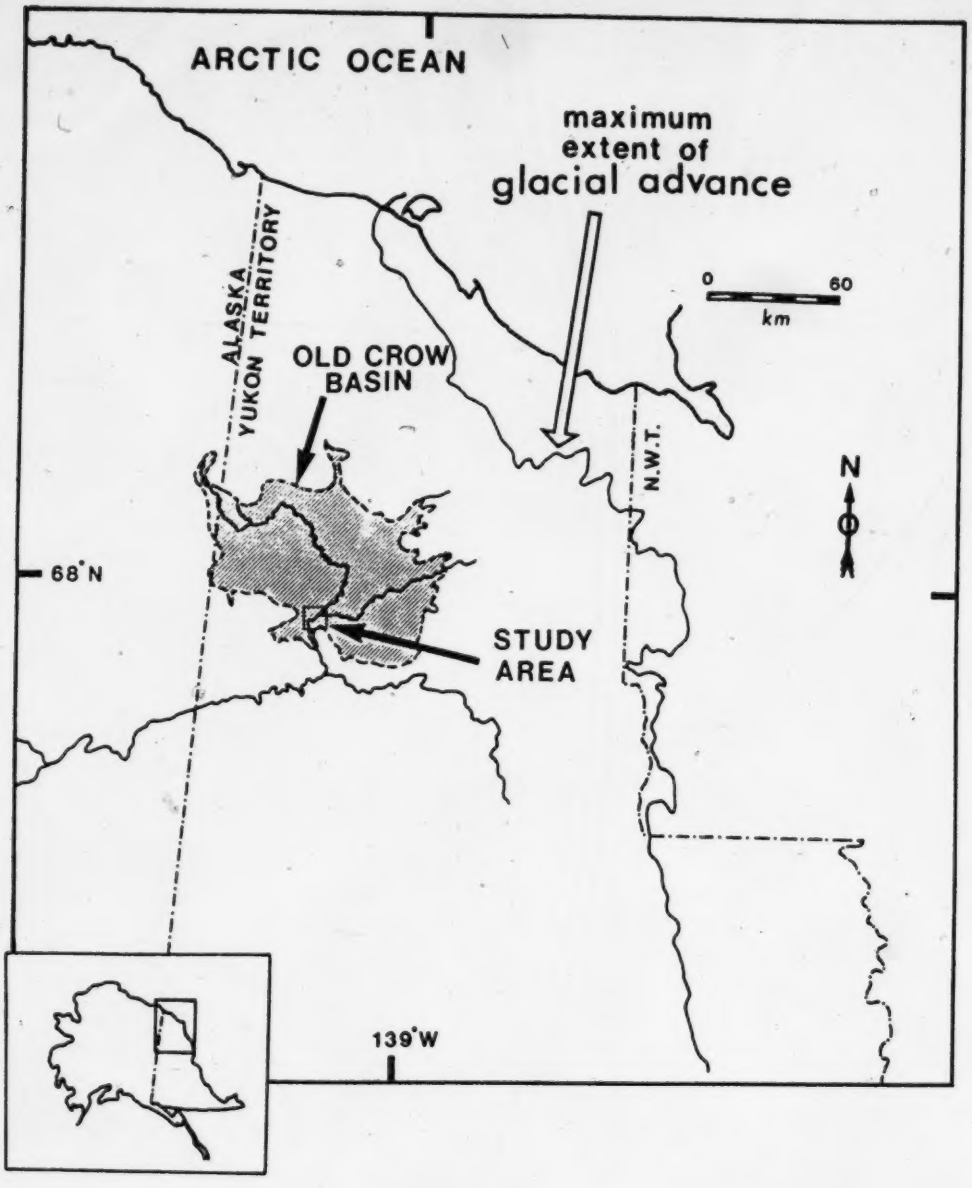

Figure 2-1: Location of the study area.

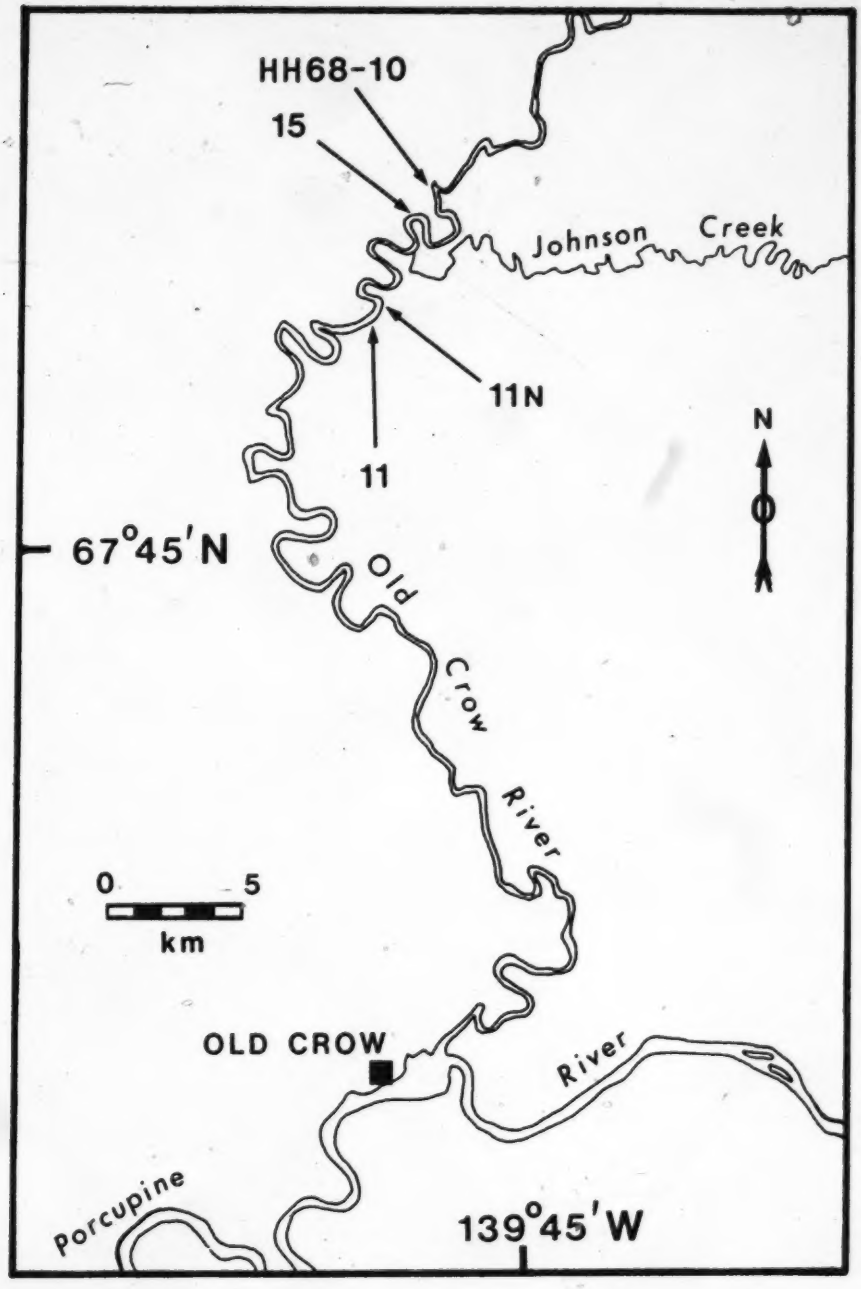

Figure 2-2: Location of sites 11 and 11N on the Old Crow River. Sites 15 and HH68-10 from Hedlin (1986) are also shown.

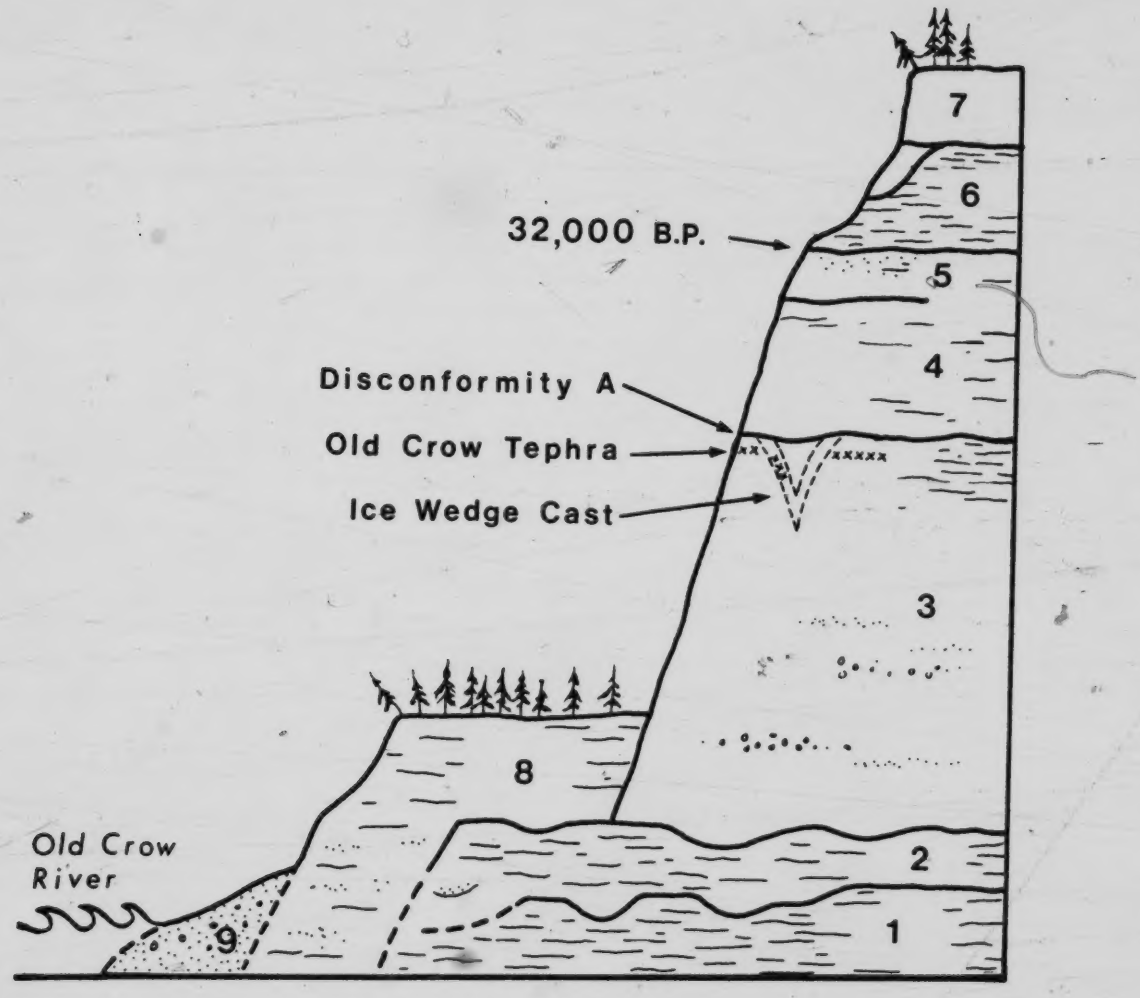

Figure 2-3: Composite stratigraphy of the Old Crow Basin. The numbers 1 through 9 denote the units as recognized by Morlan and Matthews (1978), the pertinent ones of which are described in the text.

necessarily represented at any individual site. Only four of the units (1,2,3 and 6) are present at sites 11 and 11N. The descriptions of these units by Morlan and Matthews are given below with additional detail from other pertinent studies where required.

Unit 1: Primary glacio-lacustrine clay, thought to be of Illinoian age.

Unit 2: Reworked glacio-lacustrine clay which may represent erosion and redeposition of unit 1.

Unit 3: Interbedded sands, silts and clays. In most outcrops, the upper bounding surface of this unit is disconformable and is referred to as disconformity A (Morlan, 1980). Below this level (generally a few tens of centimetres), an ash layer is sometimes found. This is the Old Crow Tephra which has a thermoluminescence age of 86,000 ± 8000 years B.P. (Westgate & Wintle, 1986). This age has inspired other researchers to look for evidence of the Blake Event (about 100,000 years B.P.) within unit 3 at various locations throughout the Basin (Hedlin & Evans, 1987; Westgate et al., 1985). The age of the Tephra is now under discussion, and is considered to be 149,000 ±13,000 years old (Westgate, 1988). The Old Crow Tephra is not present at sites 11 and 11N.

Cryoturbation features may be present near the top of this unit. At some other locations, volcanic ash is preserved in the slumped material present in ice wedge

casts.

Unit 6: Glacio-lacustrine clay, with age limit at base of 32,000 years B.P. (based on carbon 14).

Two vertical sections were sampled; one at site 11 (henceforth referred to as section KGA) and a second at 11N (section KGB). These sections are separated by a lateral distance of 500 m. Both sampled intervals start approximately 1 m below the contact between units 2 and 3 and continue upwards through the whole of unit 3. Section KGA spans a little more than 19 m of sediment and contains 318 samples for paleodirectional study and an additional 13 for susceptibility measurement and other purposes, while section KGB covers just less than 21 m, from which 308 paleodirectional samples were collected and an additional 2 for susceptibility. This makes a total of 641 samples of which 626 are for paleodirectional study.

Samples were collected using small plastic cubes (8 cc internal volume) which were inserted into the exposed sediments of the valley walls of the Old Crow River. Prior to cube insertion, slumped material was removed in order to obtain a fresh face. The bulk of the cubes were inserted by slowly pressing them into the sediment with the leverage obtained from a 2 m pole in order to minimize distortion of the samples, but in the more compacted material, the cubes were tapped in with a hammer (the direct blow of which was transmitted by a wooden block). Two samples were taken at each stratigraphic horizon, the horizontal distance between

them varying from 5 to 10 cm depending on brittleness of the sediments. Whenever possible, a 10 cm vertical spacing between sampled horizons was maintained.

Orientation was accomplished using a Brunton compass (used to measure strike) and a specially designed inclinometer, described by Hedlin (1986), which was used to measure dip and roll. Local magnetic declination was determined, from a total of 23 sun bearings, to be 033°26' azimuth with a standard error of the mean of 6'. After orientation, the cubes were removed from the face, and a lid was placed on each to minimize desiccation. Upon return to the laboratory, the samples were stored in a magnetically shielded room in which the ambient field is less than 50 nT (Reid, 1972).

III. NRM AND AF DEMAGNETIZATION RESULTS

NRM measurements were made on all samples from section KGA and KGB using a Schonstedt SSM spinner magnetometer. Magnetic moments were generally low (Figure 3-1), and consequently most samples were measured in either cart position 3 or 4 (position 4 being the closest to the sensor). The geometric mean of the NRM moments for sections KGA and KGB combined is 3.8×10^{-8} Am^2, which is low in comparison to that of most geological material measured in paleomagnetic studies (igneous rock and sedimentary rock averaging 2.8×10^{-5} Am^2 and 1.0×10^{-5} Am^2 respectively (Tarling, 1983)). The noise level quoted by the Schonstedt manufacturing company varies between 3×10^{-10} Am^2 and 1×10^{-10} Am^2 for the spin times used in this study. The quality of the NRM determinations was monitored throughout via the internal variance obtained from the spin sequence; each sample is spun around six axes, with two magnetic components measured each time, thus giving four estimates of each of the three orthogonal components (see Appendix A for details). Figures 3-2 and 3-3 show the NRM data for sections KGA and KGB respectively. In order to improve the reliability of these secular variation records, alternating field (AF) demagnetization was performed. The purpose of such treatment is to remove any secondary magnetic overprints which may be present. The presence of these overprints may be revealed by directional changes in the remanent magnetization (RM) vector during progressive

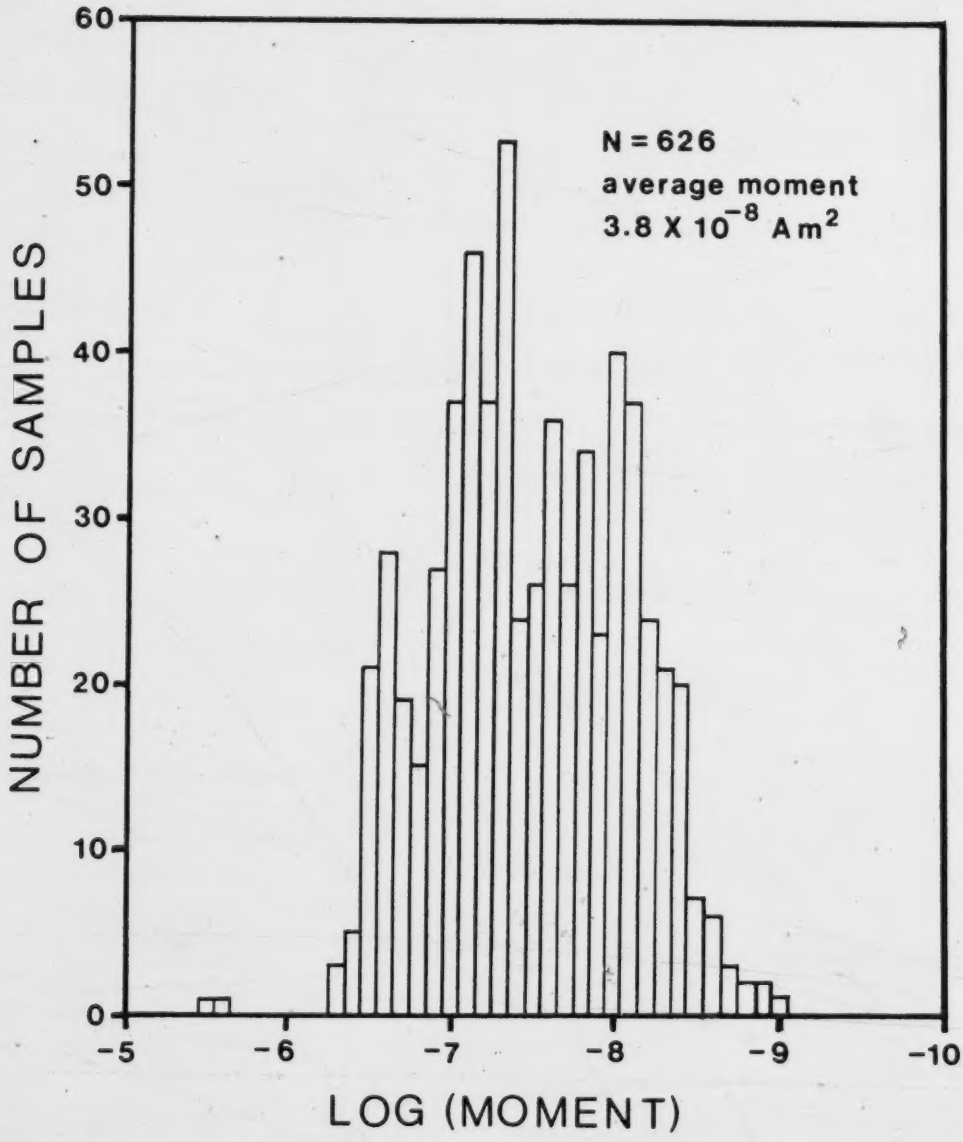

Figure 3-1: Histogram of NRM moments for sections KGA and KGB combined.

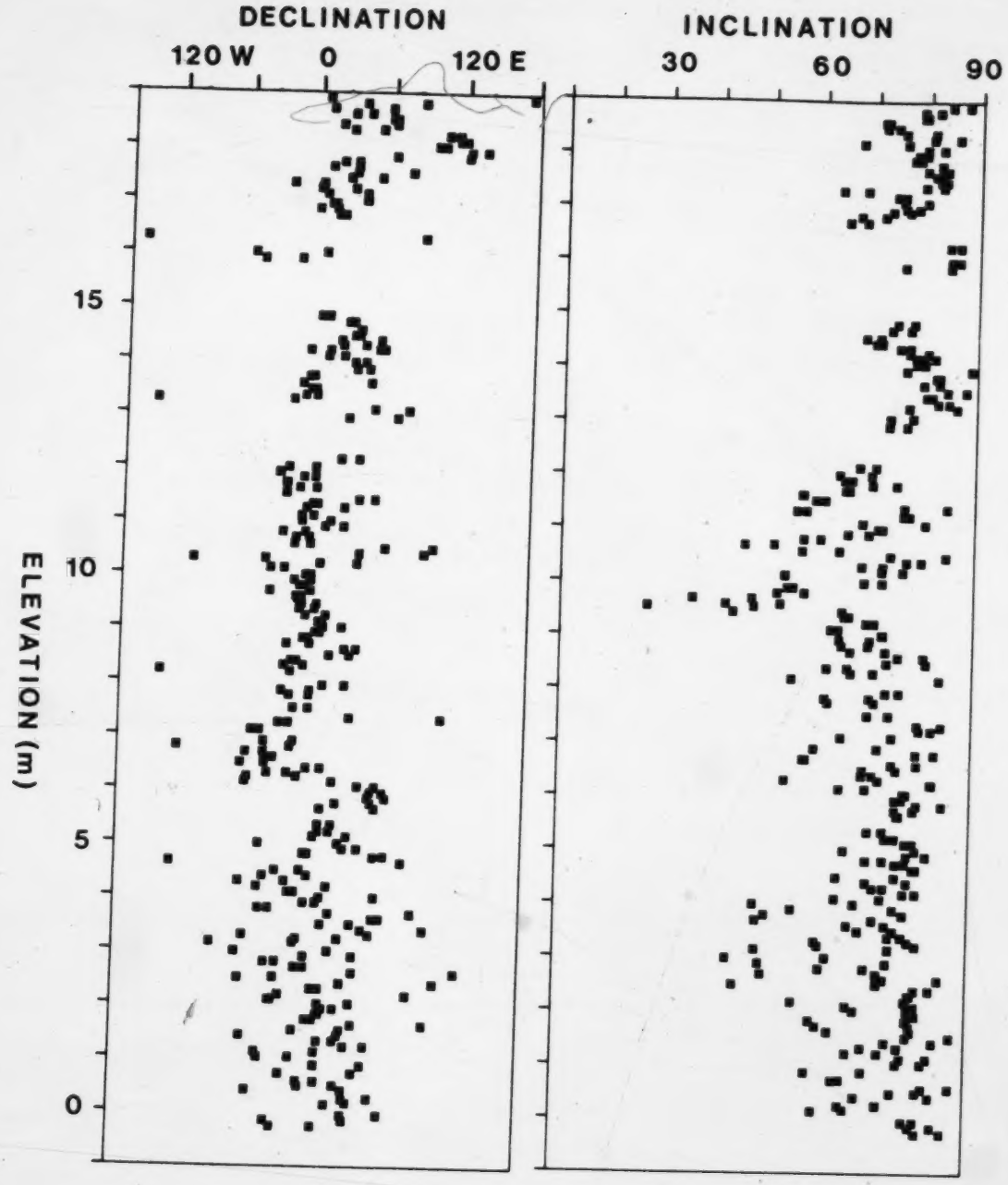

Figure 3-2: Magnetograms of NRM data for section KGA. Each square represents data from a single cube.

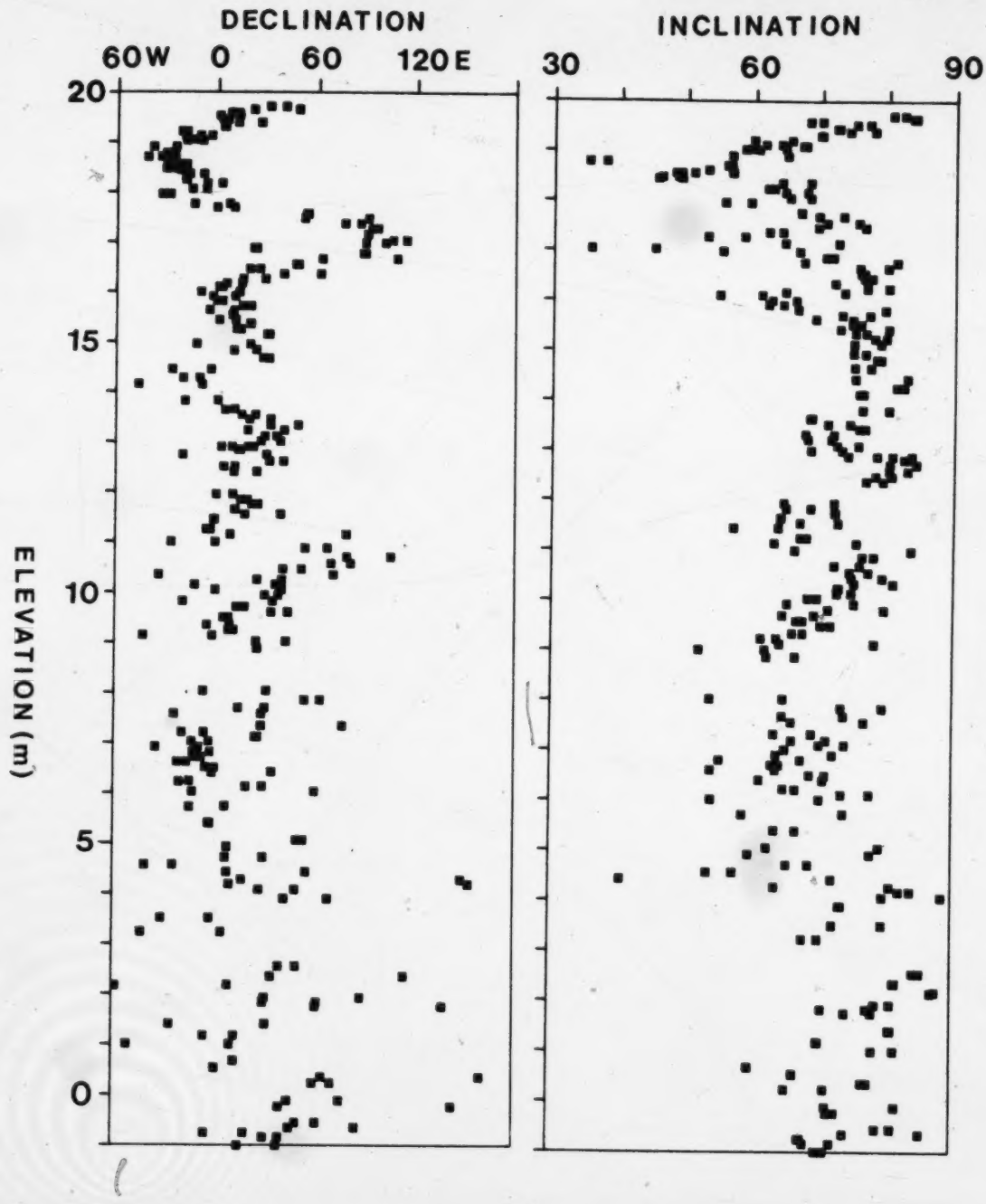

Figure 3-3: Magnetograms of NRM data for section KGB. Each square represents data from a single cube.

demagnetization. In such cases, cleaning is deemed to be complete when the angular movement of the vector has stopped (McElhinny & Gough, 1963; As & Zijderveld, 1958). Twenty pilot samples were selected from sections KGA and KGB (10 from each) and subjected to detailed AF treatment with the goal of selecting the most effective peak field level for blanket treatment of the remaining samples. The equipment used was virtually identical to that described by Murthy (1969). Demagnetization steps were 0, 2.5, 5, 10, 15, 20, 30, 40, and 50 mT. A plot of normalized moment versus peak field is shown in Figure 3-4. The median destructive field (that field at which half of the original moment is destroyed) is 24 mT.

To assess changes in direction, the results from each sample were plotted on an equal area projection. This revealed that the bulk of the samples underwent little movement (only a few degrees) during the first few steps. After this level, some samples experienced large swings and became more difficult to measure, as their moments were quite low (less than 50% of their initial value) and the internal variance became large. This behaviour is demonstrated by sample KGA278 in Figure 3-5. The amount of movement seen between demagnetization steps depends on the size of the field increment. This can, to some extent, be compensated for by dividing the angular movement by the AF increment (Figure 3-6). This reveals a broad minimum between the 5 and 30 mT steps. Since the goal of demagnetization is

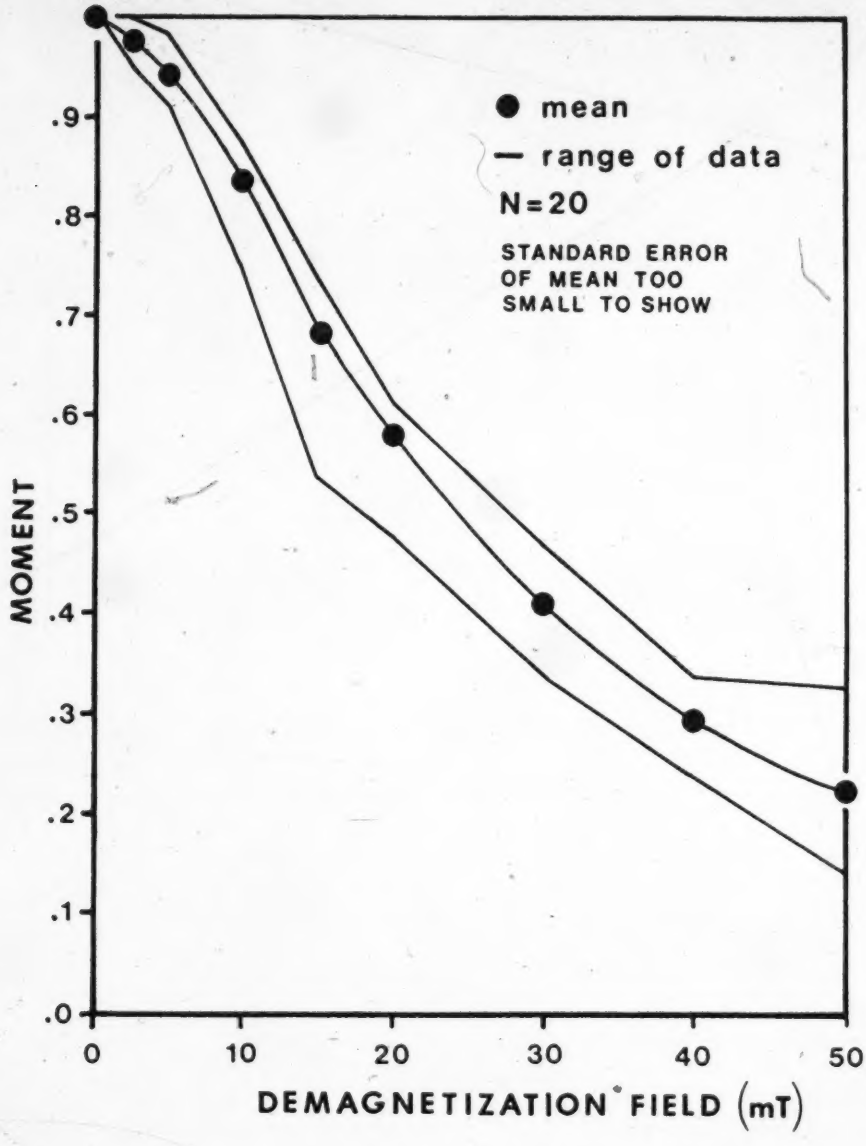

Figure 3-4: Normalized moment versus demagnetizing field (mT). Solid dots are average values of 20 data points. Solid bounding lines represent the overall range.

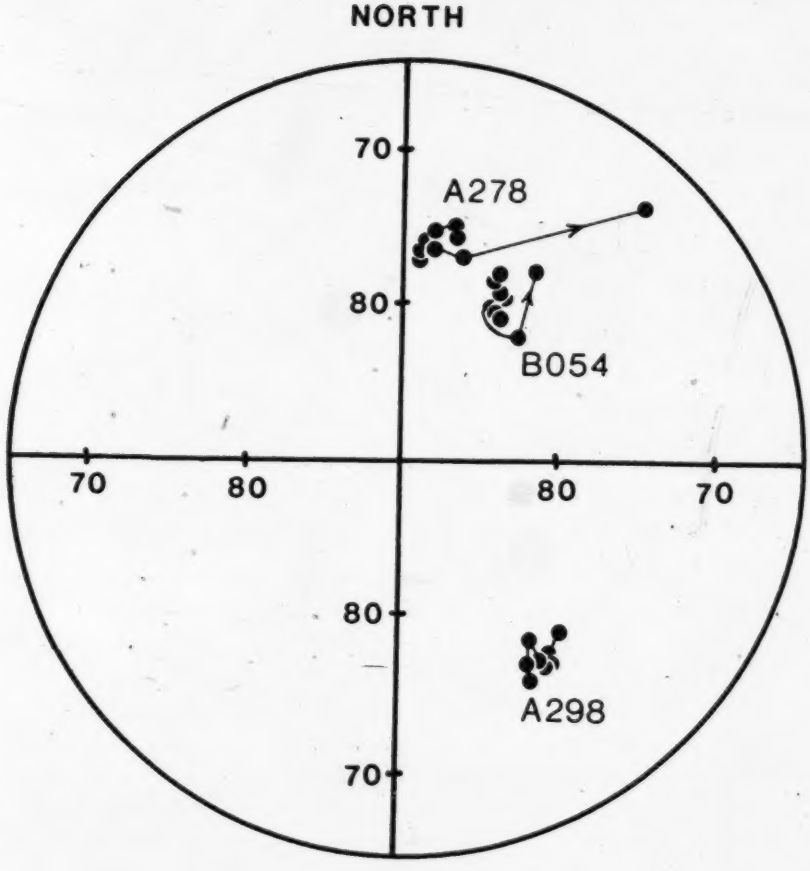

Figure 3-5: Typical pilot sample behaviour during demagnetization. (Equal area polar projection).

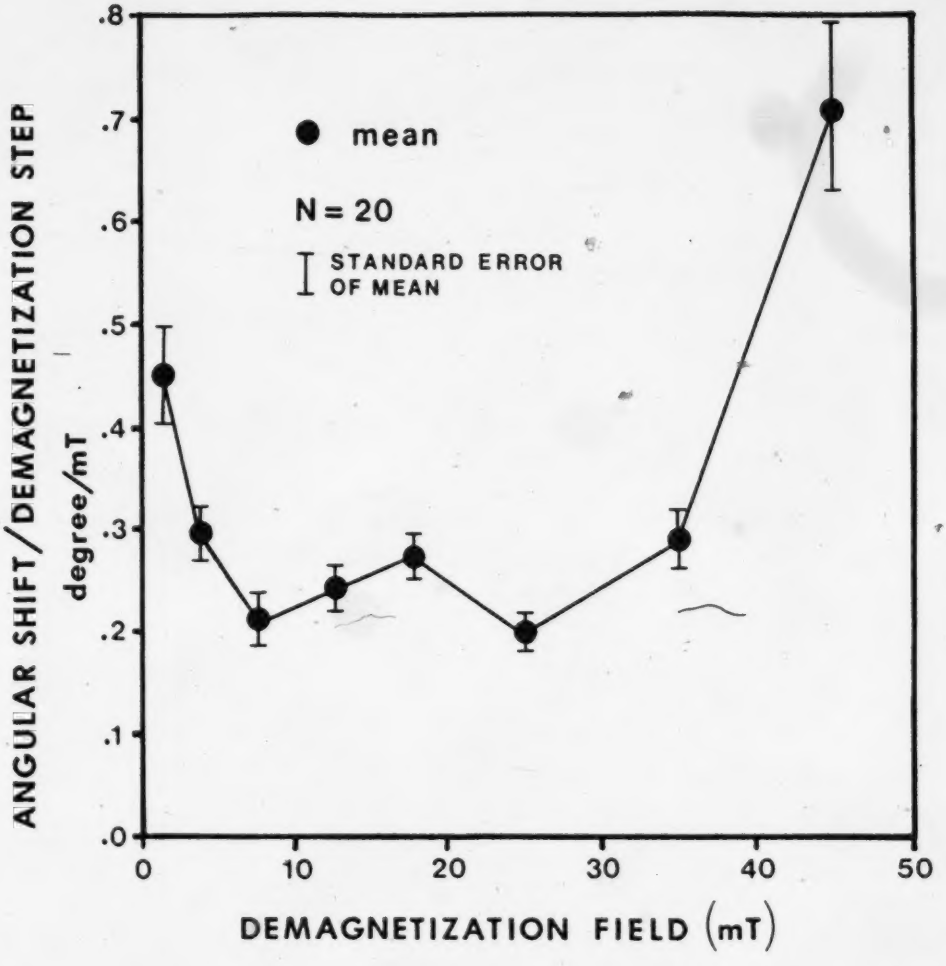

Figure 3-6: Angular shift between successive demagnetization steps normalized by increment of demagnetization field (degrees/mT). The solid dots are average values of 20 data points and are plotted at the midpoints between successive demagnetization steps.

to remove any secondary overprints with minimal degradation of the sample moment, it was decided to choose a peak value at the lower end of this broad minimum, and hence a peak field of 10 mT was selected for further blanket treatment.

During the initial stages of cleaning, it was noticed that the internal variance of most samples increased over their previous level for the NRM measurements. Large integration numbers (long spin times) were employed in an effort to bring down the internal variance of individual measurements and for some samples spin times of up to two hours were used. Even with this, many samples failed to improve, and some still got worse. It was therefore decided that some of the remaining samples were not of adequate quality to warrant this time-consuming treatment. The quality decreases towards the base of both sections, thus all samples in the zone 6 to 19 m from KGA, and those between 9 m and 21 m in KGB were demagnetized. Below these levels, only those pairs with promising initial internal variance were cleaned; this amounts to only 14 samples out of a total of 104 for KGA and 15 out of 106 for KGB.

Behaviour of the pilot samples predicted that any overprints would effectively be removed by the 10 mT alternating field and that the total movement during this treatment should be small (less than 10° as an arbitrary upper limit). The bulk of the samples behaved as expected, however the remanent magnetization (RM) vector of six specimens from KGA moved more than 10° during cleaning.

These samples were examined in detail by continuing the demagnetization process at 5 mT steps. Zijderveld plots shown in Figure 3-7 show movement towards the origin after 10 mT, suggesting that the characteristic RM has, in fact, been isolated by blanket cleaning.

The resulting declination and inclination profiles are illustrated in Figures 3-8 and 3-9. The strong similarity of these plots to their respective NRM counterparts confirms the previous assertion that the choice of 10 mT was not a critical one. Note that the data plotted are that which remained after an internal variance cutoff of 11° was applied (see Appendix A for details). Of the original 626 samples only 366 (59%) remain, 180 of the 260 rejected samples being lost at the base of both sections. This is a heavy price but worthwhile as the remaining secular variation sequences are of high quality.

The average vector removed during demagnetization may be found by examining the Fisher statistics of both the NRM and 10 mT data. In a Fisherian distribution, a group of directions is expressed as a vector mean direction with a confidence limit defined by a cone about this direction with semi-angle α. The most common level of confidence used in practice is the 95% level, hence this level is referred to as $\alpha 95$ (see Fisher, 1953; Watson, 1956).

The vector average for the 10 mT data of section KGA is declination (D) 350.5° and inclination (I) 72.3° with $\alpha 95$ of 2.1° (N=180), while the direction of the corresponding NRM

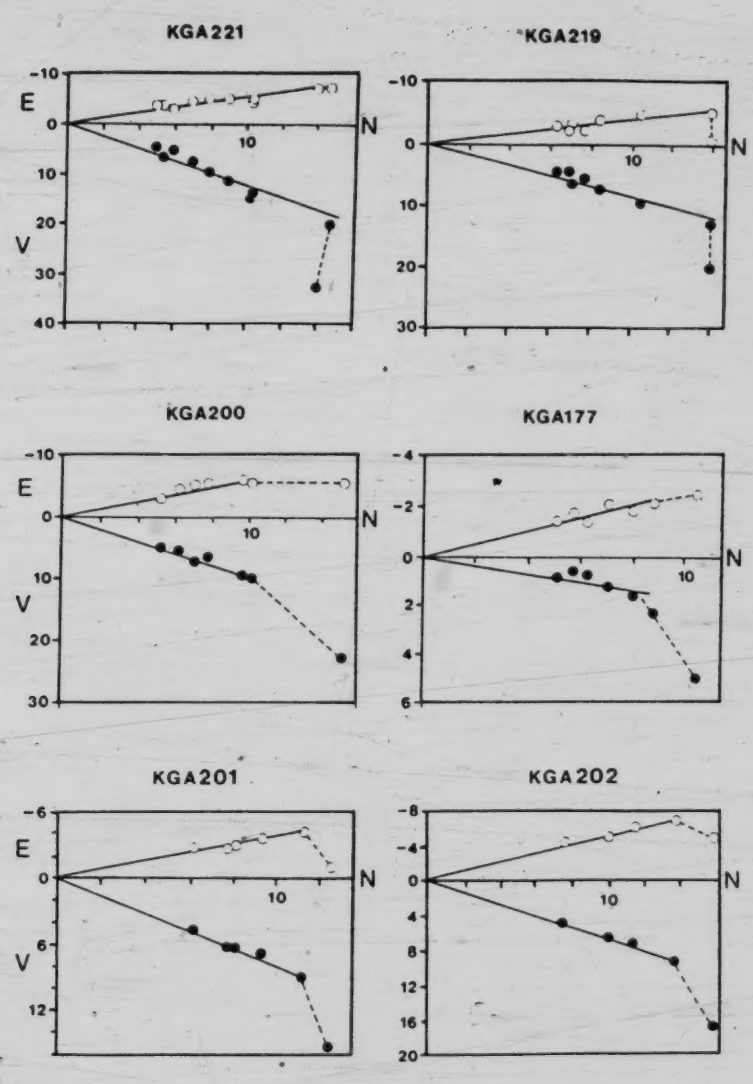

Figure 3-7: Zijderveld plots of further demagnetization performed on KGA samples the magnetizations of which moved by more than 10° during blanket cleaning of 10 mT. Points represent projections on orthogonal planes (labelled accordingly). The top box in each plot is the east-north (E-N) plane, while the bottom is the vertical-north (V-N).

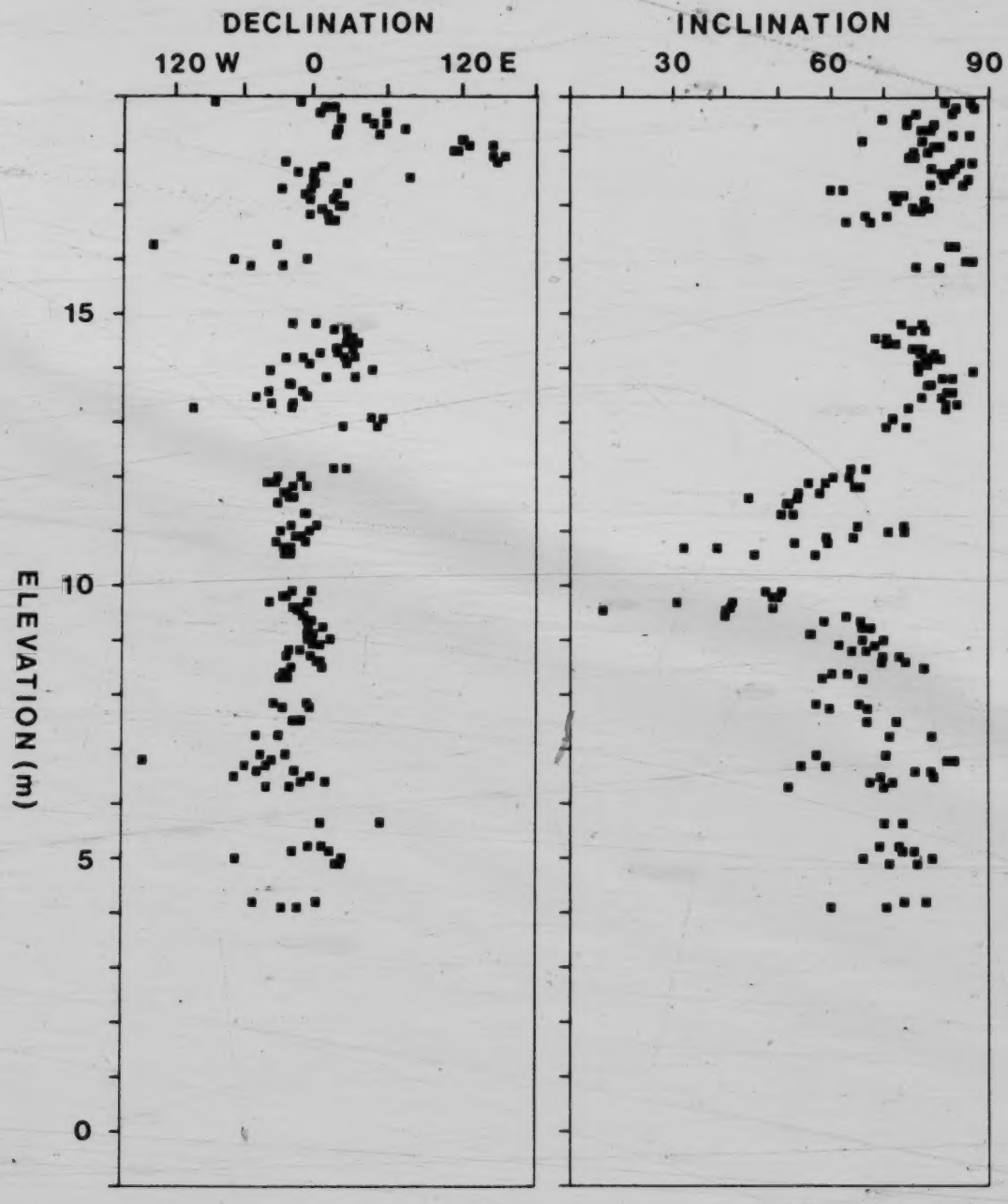

Figure 3-8: Magnetograms for 10 mT data from section KGA. Internal variance cut-off of 11.0° has been applied (see appendix A for details).

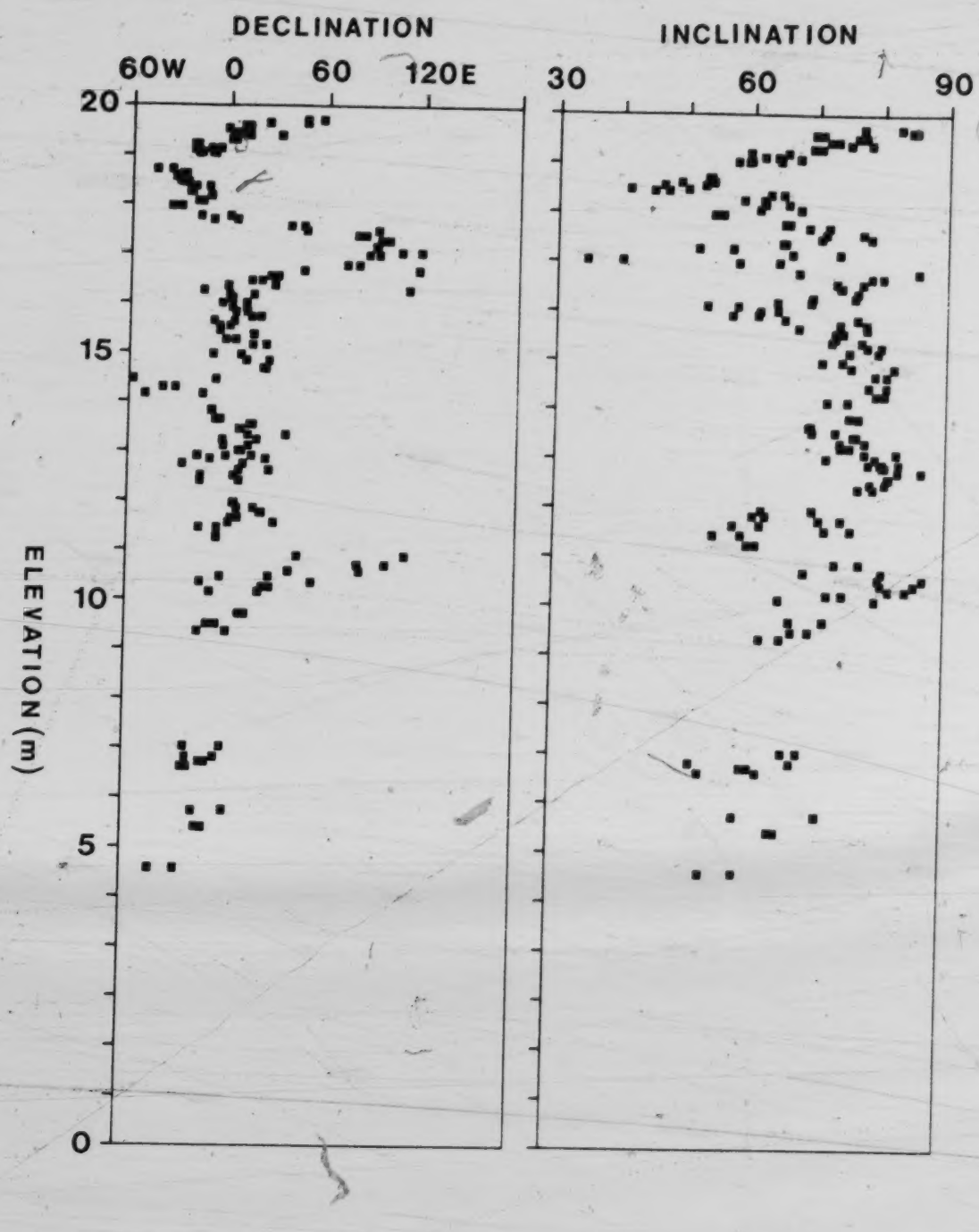

Figure 3-9: Magnetograms for 10 mT data from section KGB. Internal variance cut-off of 11.0° has been applied (see appendix A for details).

points is D=000.8° I=74.3° with $\alpha 95$ = 1.8° (N=180). This represents a general movement away from the present Earth's field (82° at 033°) of only 3.6°. This movement away from the present field suggests that this low coercivity component is a viscous overprint from the present day field at this site (Figure 3-10).

The vector average for the 10 mT data of section KGB is D=002.7° I=72.7° with $\alpha 95$ of 2.0 (N=186), whereas the corresponding NRM points give an average of D=009.5° I=73.2° ($\alpha 95$=1.9). As in the case of KGA, the movement is small (2.1°) and is generally away from the present field. Table 3-1 summarizes the statistics for KGA, KGB and both sections combined.

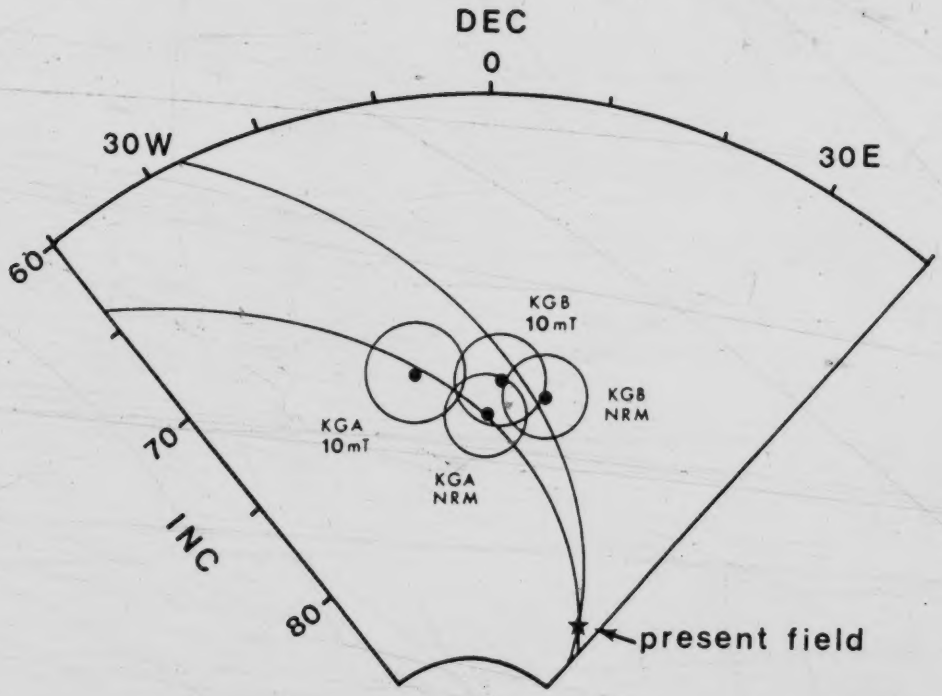

Figure 3-10: Vector averages for NRM and 10 mT data of KGA and KGB. The circles about the points are the associated $\alpha 95$, and the curves are great circles.

	DEC	INC	α_{95}	N	MOVEMENT
KGA NRM	000.8	74.3	1.8	180	3.6
KGA 10 mT	350.5	72.3	2.1	180	
KGB NRM	009.5	73.5	1.9	186	2.1
KGB 10mT	002.7	72.7	2.0	186	
KGA and KGB NRM	005.3	73.9	1.3	366	2.8
KGA and KGB 10mT	356.6	72.6	1.4	366	

Table 3-1: Table of vector statistics for NRM and 10 mT data of KGA and KGB.

IV. DECLINATION AND INCLINATION OSCILLATIONS

A. Section KGA

The sampled sequence is a function of elevation, and although it is desirable to express the results as a function of time, this is not easily done. The age of the sediment is beyond the range of carbon dating and thus the organic fragments occasionally observed in the section cannot be dated by this means. Although a general rule of thumb is that clays take longer to be deposited than coarser material such as silt and sand, a reliable estimate of the exact time represented by a given thickness of sediment is virtually impossible . There is, however, one modification which can be made to the section to bring it closer to a true time series. Sand is generally deposited so rapidly when compared to silt and clay that it can be approximated as representing zero time, and therefore removed. Between 11 and 17 m there are, in fact, four sand layers, totalling 3.0 m as indicated in Figure 4-1. Also note that between the 10.3 m and 10.7 m marks there is a sequence of finely interbedded silt and sand layers (accented with a large hollow arrow). The sand layers here represent 40% of the thickness, and this interval was therefore compressed accordingly. The effects of these modifications on the magnetograms are shown in Figure 4-2. The features of interest are labelled A1, A2, A3, A4 and A5 (in order of increasing time), the divisions being more or less

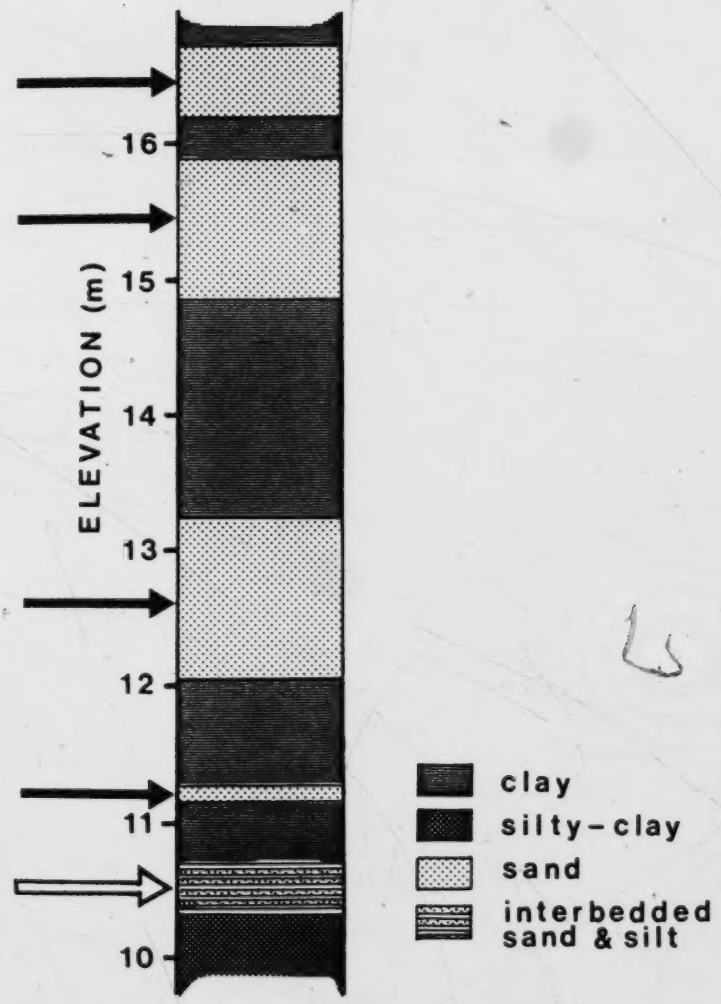

Figure 4-1: Lithology between 10 m and 17 m of section KGA. The solid arrows mark the sands to be removed. The hollow arrow highlights the zone of 40% sand.

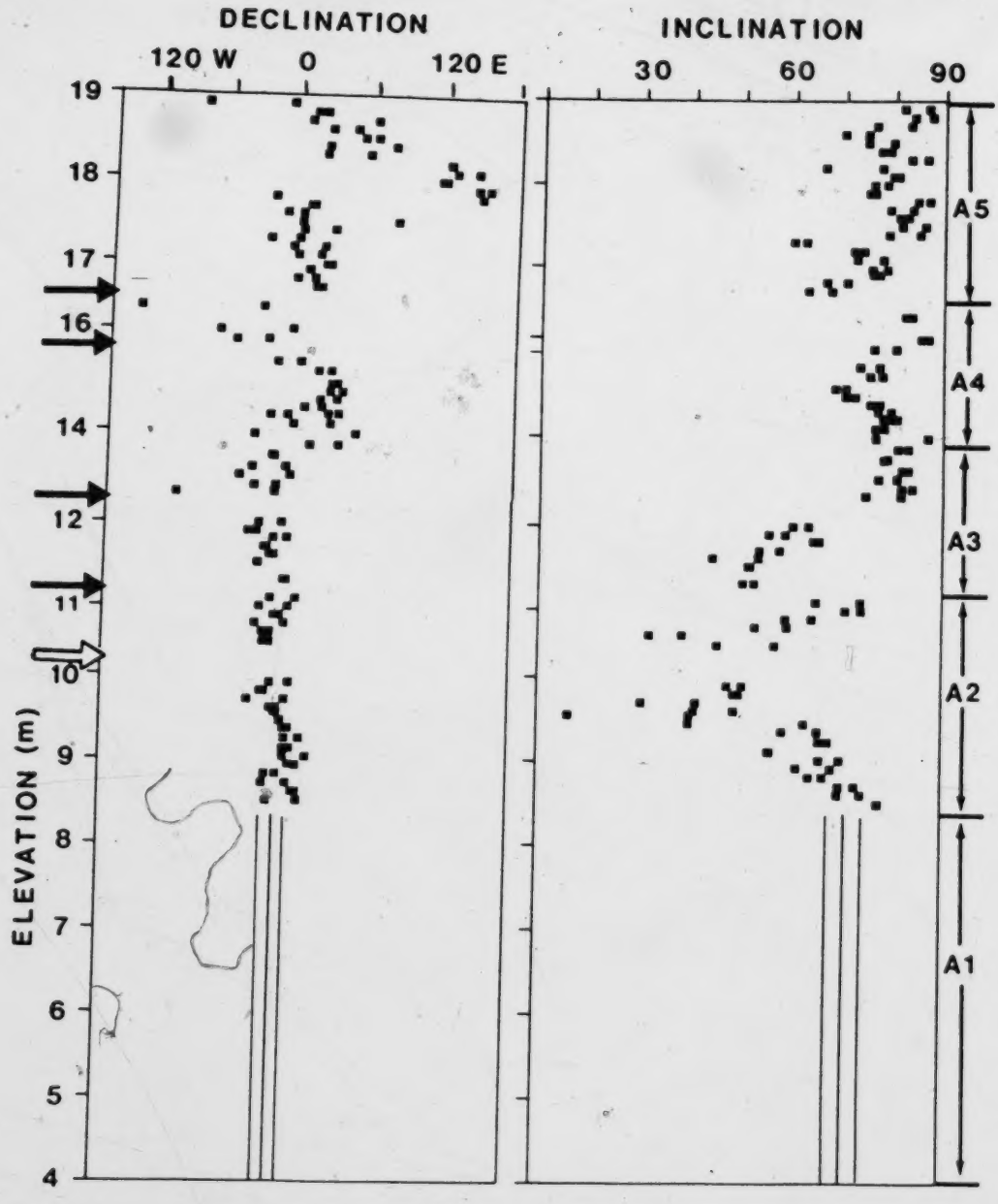

Figure 4-2: Expanded version of Figure 3-8 after removal of sand layers. The arrows of Figure 4-1 are indicated. Features of interest are labelled on the right.

arbitrary. Starting at the 4.0 m mark, we progress upwards through A1, the top of which is arbitrarily defined as the 8.4 m mark. The internal variance cutoff of 11° resulted in the rejection of 34 of the original 76 samples in this interval, leaving only 21 pairs over 4.4 m. Consequently, the resulting density of sampling is too low for investigation of secular variation and the data over this interval have simply been averaged as indicated (refer to Figure 3.8 for original data).

Feature A2 begins at the 8.4m mark and runs to 11.3m, a distance of 2.7m on this modified elevation scale. Magnetograms such as those in Figure 4-2 facilitate the recognition of individual features within the RM record, but in order to visualize the movement of the vector in three dimensions, equal area plots are more effective (Figure 4-3). Note that only those pairs in which the angular difference between individual pair members was less than 10° are plotted in Figure 4-3. The reasoning behind this need not concern us at this time and will be discussed later in this section. Suffice it to say for the present that, under enforcement of this criterion, only the highest quality data are preserved.

The character of the perturbation path for A2 (lefthand side of diagram) is a linear one, there being changes in inclination with relatively little change in declination. The shallowest direction attained is 35.3° at 22.8° west of north. This feature represents a large perturbation

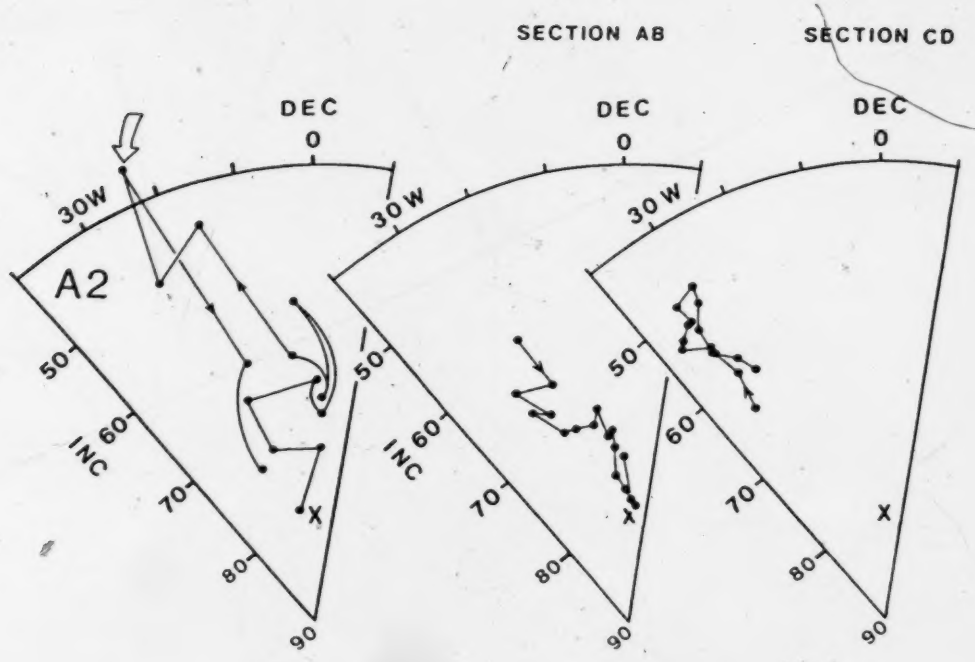

Figure 4-3: Declination-inclination equal area plots of feature A2 (unsmoothed). Internal variance of 11.0° (see Appendix A) and within-pair dispersion cut-off of 10° have been applied. The "X" marks the position of the field vector due to an axial geocentric dipole. Each point represents the average of a pair of samples. Corresponding features from previous work (Evans et al., 1988; Hedlin and Evans, 1987; Hedlin, 1986) (5 point running mean) are included. The curved hollow arrow represents the perturbation point used in modelling.

(approximately 40°) of the local field away from the direction predicted by an axial dipole field (shown by the "X"). The reality of this feature is confirmed by the presence of corresponding features (shown on right hand side of Figure) in two outcrops over 5 km away (sites 15 (AB) and HH68-10 (CD) from Evans et al (1988), sampled by Hedlin (see Figure 1-3)). As stated by Turner (1983), the supreme test of the reality of a feature in an RM sequence is reproducibility in outcrops separated by large distances. This test is rarely successful in practice and it is commonly observed that for every signal found in a single outcrop there are many outcrops in the surrounding area in which it cannot be found. For instance, Palmer et al (1979) had trouble correlating fine features in their lake sediment RM records even over 1 km. A successful correlation of the feature A2 with signals over 5 km away confirms the idea that the perturbing source is a true geomagnetic field variation and not simply a local sedimentological effect.

Next we encounter A3, which represents a return to steep inclinations from shallow values of roughly 50° (shallowest value is 49.0° at 19.2° west of north). The outward trajectory is not represented, its absence being attributed to a break between A2 and A3. There is a sudden jump in inclination of about 20° which suggests that some time is not represented here. The end of this feature is defined as the point at which the field has returned to steep inclinations and is arbitrarily taken as 14.0m. The

equal area plot of Figure 4-4 reveals that the perturbation path for A3 is also linear, and again we are able to find correlatable features at sites 15 and HH68-10.

Between 14.0 and 16.5 we find A4. This feature (Figure 4-5) can be convincingly correlated with an easterly shallowing of the geomagnetic field which occurs between -11.0 cm to +50.0 cm in section AB of Hedlin and Evans (1987). On this modified elevation scale, feature A4 spans a thickness of 1.8m which is approximately 3 times that of the corresponding feature in section AB, reflecting a difference in sedimentation rate. The Old Crow Tephra, which is present in section AB, occurs by chance at the point of maximum perturbation. Thus the point of shallowest inclination in A4 (14.6m) is taken to represent the time of deposition of tephra in the Basin as a whole, although it does not appear to have been preserved in section KGA. Susceptibility measurements were made on Hedlin's samples from sites 15 and HH68-10 and revealed that the Old Crow Tephra is present not only visually at these sites, but also as a susceptibility maximum (Evans et al., 1988). If the Tephra is present in a cryptic form it may manifest itself as a susceptibilty increase. In order to test this, low-field susceptibility measurements were made of all samples from KGA using a Conservation Instruments Susceptibility meter type M.S.1 with sensor type M.S.1.B. Calibration with eight paramagnetic salts showed that the instrument behaved linearly over the range of interest (Figure 4-6). Figure 4-7

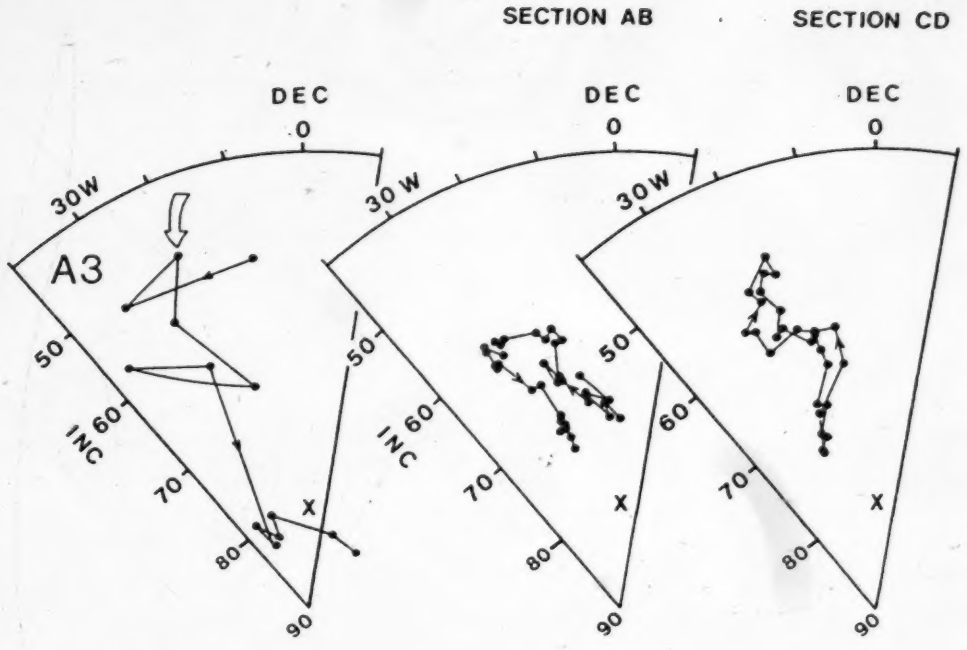

Figure 4-4: Declination - inclination equal area plot of feature A3 with corresponding features from previous work (see Figure 4-3 for full explanation).

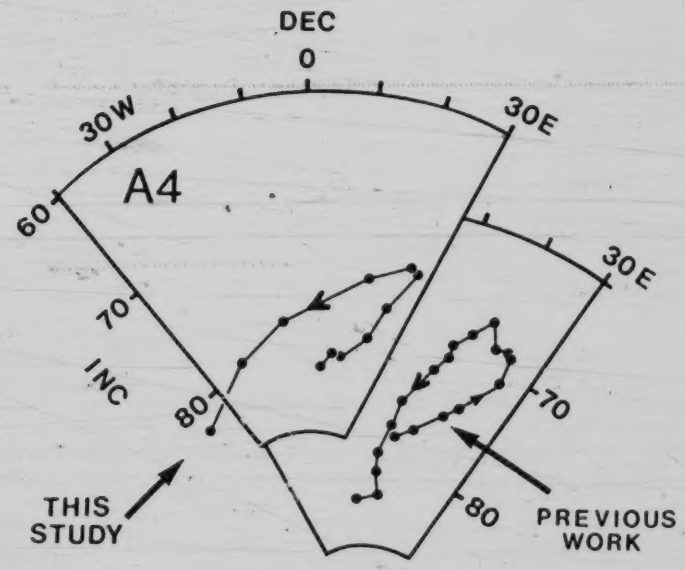

Figure 4-5: Declination-inclination equal area plots for A4 (3 point running mean) and corresponding feature from -11.0 cm to +50.0 cm mark of previous work (Evans et al., 1988; Hedlin and Evans, 1987; Hedlin, 1986) (5 point running mean).

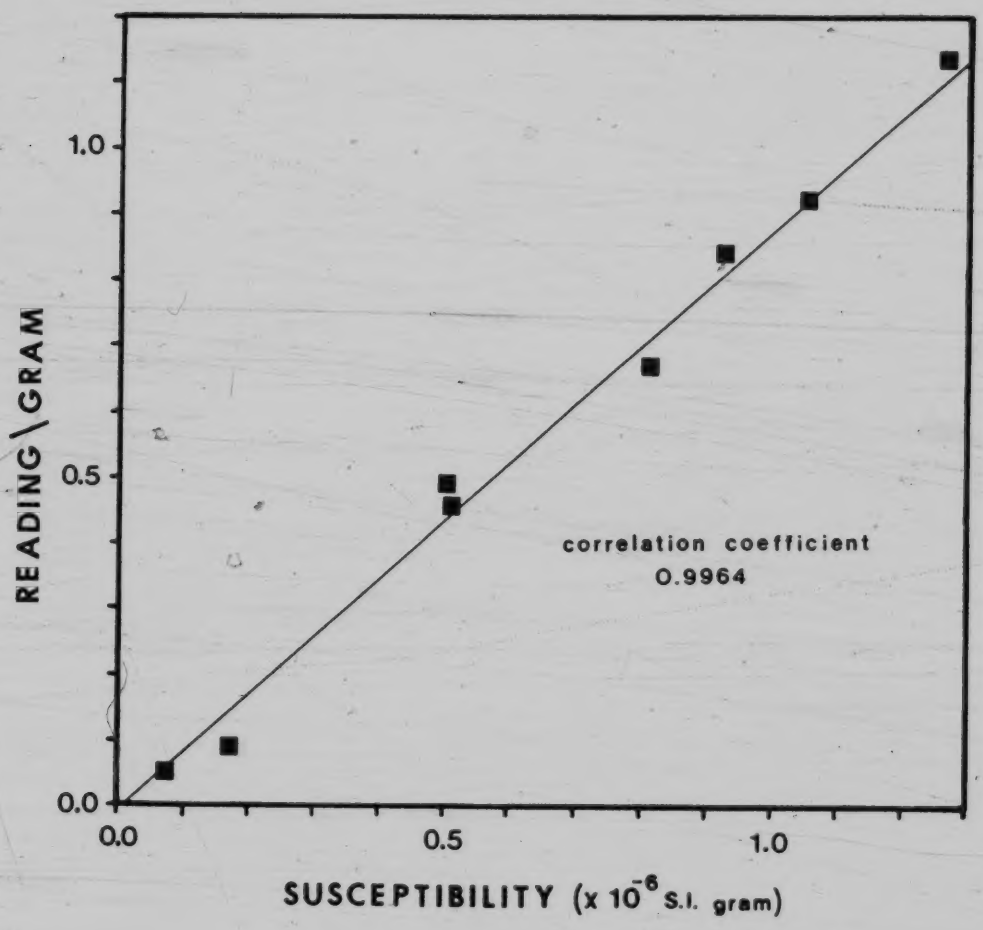

Figure 4-6: Calibration curve for Conservation Instruments M.S.1 susceptibility meter.

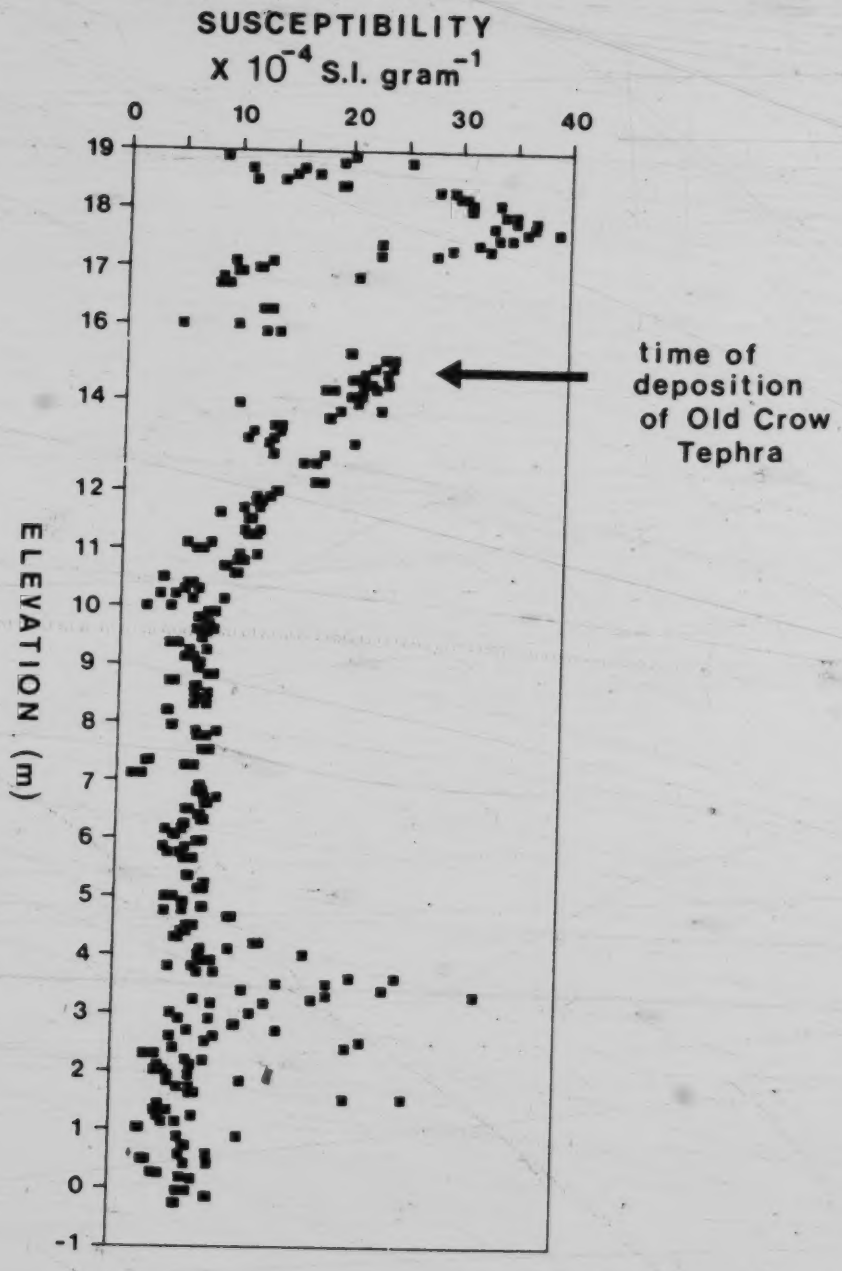

Figure 4-7: Susceptibility versus elevation for section KGA. The elevation thought to represent the time of deposition of the Old Crow Tephra in the Basin is indicated.

shows the results plotted against elevation, with the presumed time of deposition of the Old Crow Tephra indicated. There is indeed a significant increase in the susceptibility around this point, but further work involving a search for chemical evidence would be required to verify its existence.

The reality of A2, A3 and A4 is confirmed by the fact that corresponding features exist in the records recovered from sites 15 and HH68-10 by Evans et al (1988), and also by the fact that all correlatable features occur in the same order in each record. Furthermore, these cannot be perturbations introduced by the method of sampling. Sampling of soft sediment with plastic cubes using the method described in chapter II has been shown to produce a "push error" in some cases, i.e., a magnetic component seems to be added in the direction of cube insertion (Lovlie, pers. comm., 1988). Such a mechanism could not have produced the shallowing seen here since the declination of these features in roughly north, while the direction of push is predominantly east. In addition, the corresponding features in section AB were recovered from cubes which were pushed to the west, the opposite direction of that involved in collecting section KGA, yet the declination of all features is virtually identical. These facts attest to the fidelity of the sediments in this region as good recorders of geomagnetic field variations.

Feature A5, which overlies A4, is a perturbation of the RM vector to the east of south. The most extreme value attained is 149.2° declination and 75.4° inclination. This feature is illustrated in the equal area plot of Figure 4-8. Unfortunately, a great deal of faith cannot be placed in the orientation of this feature in space since these beds may have been distorted. The sediments containing this feature are divided from the horizontal beds below it by a sharp high angle plane of discontinuity. Although the beds containing A5 are massive clay and contain no indications of horizontal, the beds immediately above this zone are deformed and tilted to the south-east in what appears to be an ancient slump. This massive clay may have been involved in the deformation and thus may be responsible for the south-east orientation of A5.

At this point we return to the reasoning behind the plotting of only those pairs in which the angular difference between the two RM vectors of individual members of sample pairs was less than 10°. If members of a pair represent the same point in time, their directions of magnetization should agree. This is referred to as the within-pair dispersion, and was applied by rejecting any pairs for which the angular separation in space between members exceeded 10°. Hedlin and Evans (1987) arbitrarily used a value of 10°, noting that this is a very strict criterion (the angle between a pair of vectors must exceed 26° before they can statistically be considered at the 95% level to be from a random population).

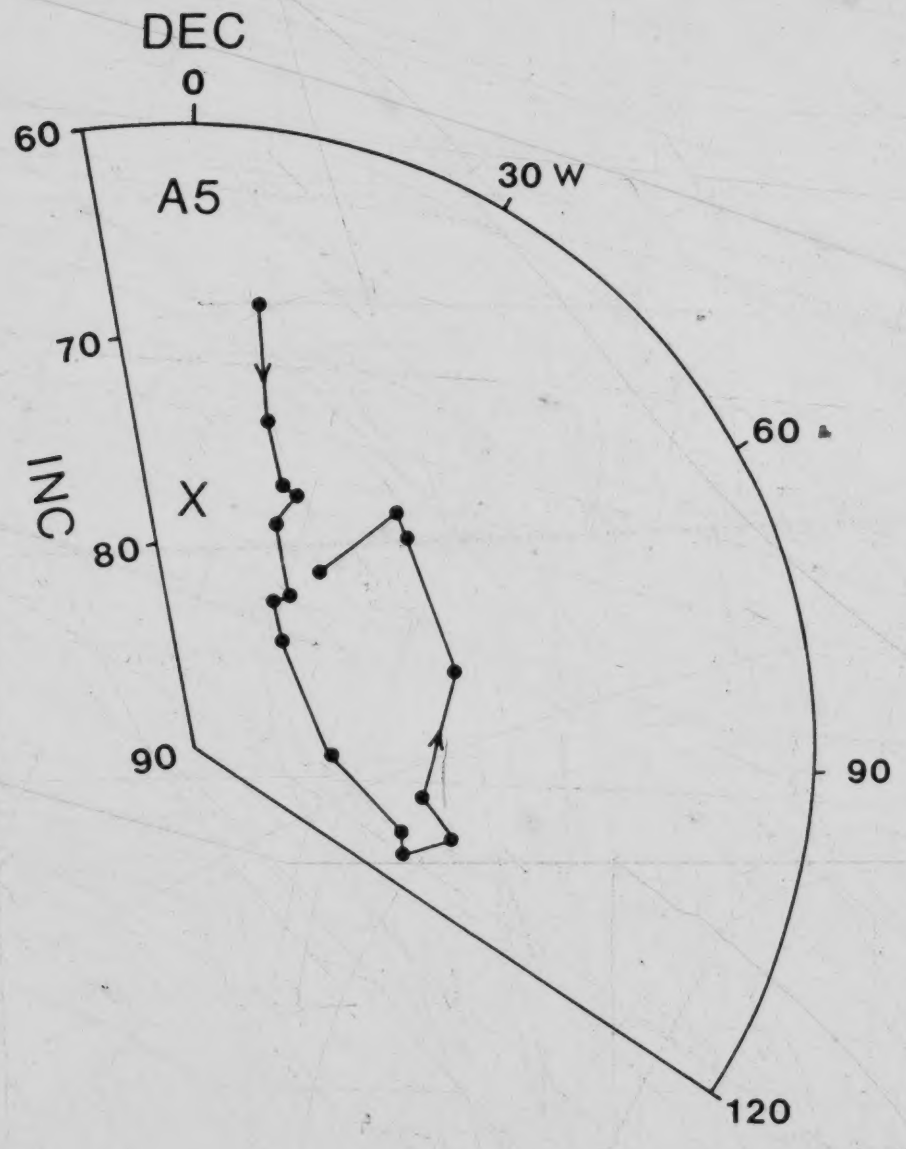

Figure 4-8: Declination - inclination equal area plot of feature A5 (3-point running mean). The "X" marks the position of the field vector due to an axial geocentric dipole.

Application of this filter to A3 resulted in rejection of only a single pair (for which the angular separation was 16.5°), thus in this case, we need not consider further the ramifications of this quality criterion on the character of that feature. Similarly, A4 loses only 2 of its original 13 pairs (within-pair separations of 13.5° and 16.5°) and A5 loses 4 of 23 of which no pair rejected showed a within-pair separation exceeding 11.6°.

By contrast, A2 lost 7 of its original 21 pairs. Consequently, we examine in greater detail the effect of the within-pair dispersion cut-off of 10° on this feature. The pairs rejected have angular separations varying from 10.7° to 27.1°. If the basic assumption that the members of a sample pair represent the same point in time is violated, this criterion is no longer applicable. In such a case, angular discrepancies may very well be due to secular variation processes, not error in recorded field direction. Slight misalignments in elevation are possible, since the measured elevation is only accurate to ± 0.5 cm at best. High temporal 1st derivatives of the geomagnetic field direction and/or slow deposition rates will yield zones of high spatial 1st derivative in the remanence signal. In such intervals, it may be necessary to relax the within-pair dispersion criterion. The question of how much to relax is a difficult one. It is best approached by totally lifting the filter and observing the consequences. Figure 4-9 shows the outcome. The important point is that the essential

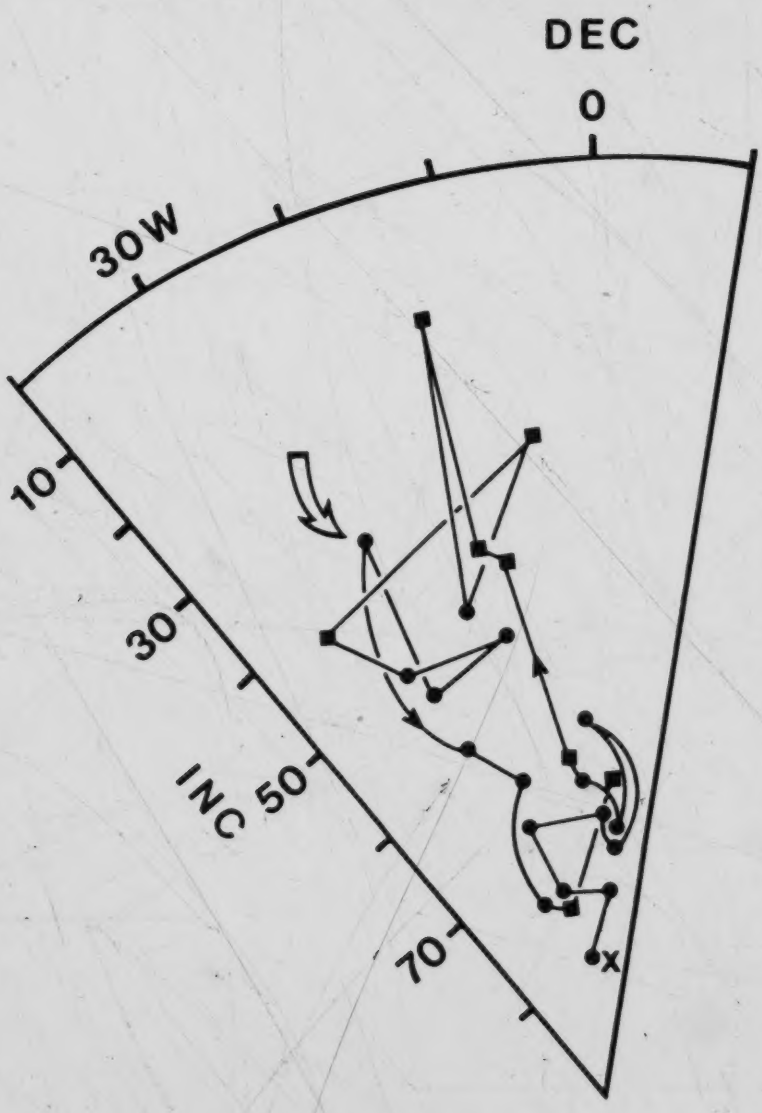

Figure 4-9: Declination-inclination equal area plot for A2 with in-pair dispersion criterion removed. Individual members of pairs with angular separations of greater than 20° are plotted as squares. The new points with angular separations of greater than 10° but less than 20° are averaged and plotted as circles for the sake of clarity. The squares are joined with the lines which represent the minimum path length. The curved arrow marks the position of the previous minimum in inclination from figure 4-3.

characteristics with respect to the pattern of movement of the geomagnetic vector remains unaltered, but the feature is reinforced by the added points. The only change which results is the extension of the signal to shallower inclinations (16.5° at 12.5° west of north). For comparison the position of the previous extreme is indicated.

Feature A1 also suffers under the within-pair cutoff of 10°, losing 12 of its original 21 pairs. The average of all vectors is declination 340.1° and inclination 71.1° with $\alpha 95$ = 3.3°. Removal of all pairs which do not meet the within-pair cutoff yields an average of declination 346.5° and inclination 71.5° with $\alpha 95$ of 3.6° which is not statistically different from the average of all samples in A1 at the 95% level. Thus the final result remains the same.

B. Section KGB

Adjustments to elevation for two sand layers between the 8 and 10 m marks (total thickness 1.3 m) were made as was done for section KGA. The resulting sequence is shown in Figure 4-10, with the arrows on the left marking the positions of the removed sands and the features of interest indicated to the right. In section KGA features A2, A3 and A4 could be confidently correlated with signals reported by Evans et al., (1988). A similar sequence of three features can be identified in section KGB. B1 (from 4.0 m to 11.0 m, a thickness of 5.7 m on this modified elevation scale), B2

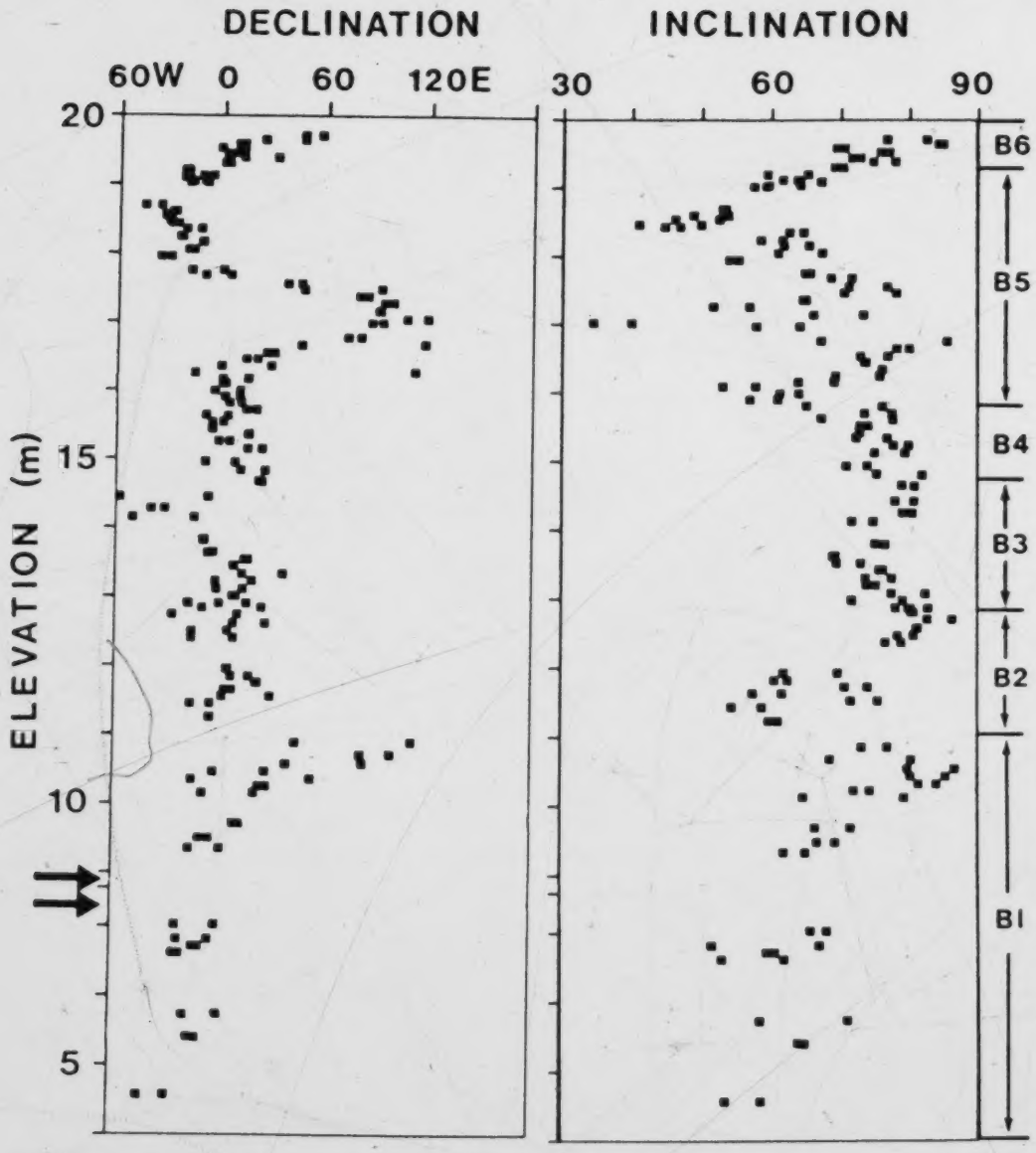

Figure 4-10: Expanded version of Figure 3-9 after removal of two sand layers (indicated by the horizontal arrows). Features of interest are labelled to the right.

(11.0 m to 12.87 m) and B3 (12.87 m to 14.5 m) are replotted on the equal area plots of Figure 4-11, with the corresponding signals from the sequence reported by Evans et al. Note that the increased noise level requires that some smoothing be done; the 3 horizon (6 samples) running mean is plotted here. Admittedly, at first glance the correlation is not as strong as it is for A2 to A4. The similarity of any individual signal with its counterpart is not as good here, as for example the case of B2 where the shallowing of the vector trends northward rather than west of north. In addition, only the return trajectories from positions of shallow to steeper inclinations are represented here by B1 and B2. However, the fact that three similar features in KGB appear in the same order and at approximately the same elevations as those in KGA makes the correlation more convincing. Section KGB thus provides useful supporting evidence for the reality of the geomagnetic features evident in KGA and in the work of Hedlin (1986).

Features B1, B2 and B3 are taken from a zone of horizontal bedding. Above B3 we encounter two intervals of tilted strata. The first of these is labelled B4 and runs from 14.5 m to 15.8 m. The dip of the strata is 29° west with a strike of 162° azimuth. Figure 4-12 shows the pattern of movement on an equal area plot with no tilt correction applied. There is no interesting pattern of movement to this signal and as a consequence, it is not discussed further.

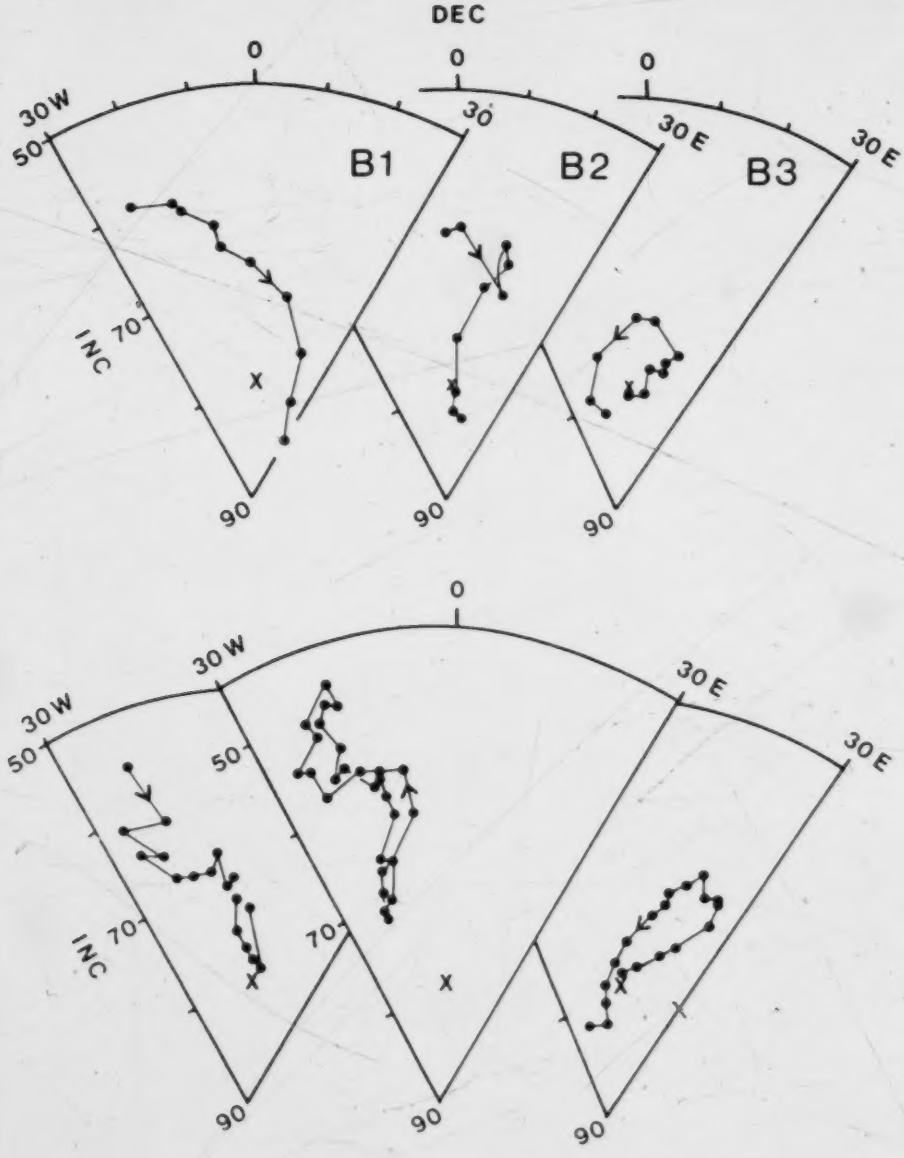

Figure 4-11: Declination-Inclination equal area plots for features (a) B1, B2 and B3 (three horizon (i.e., 6 sample) running mean). Internal variance of 11.0° (see Appendix A) and within-pair dispersion cut-off of 10° have been applied. The "X" marks the position of the field vector due to an axial geocentric dipole. Similar features from previous work (Evans et al., 1988; Hedlin and Evans, 1987; Hedlin, 1986) (5 horizon running mean) are included.

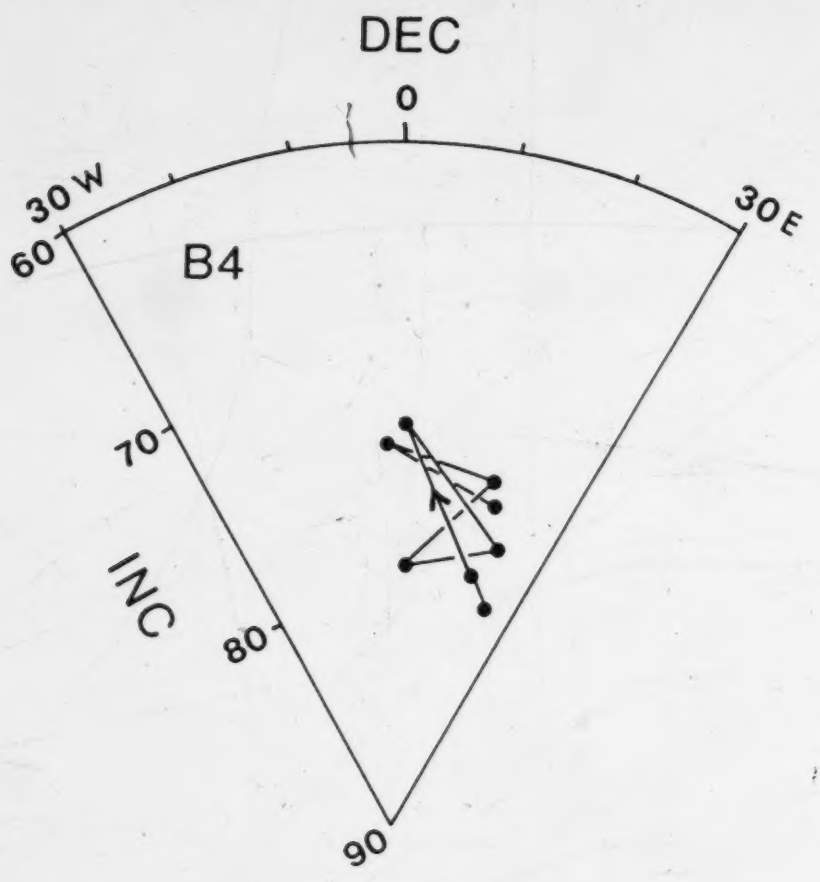

Figure 4-12: Feature B4 with no tilt correction.

Above B4 the bedding tilts in the opposite direction, dipping between 20° East and 26.5° East with strike varying from 010.0° to 017.0° azimuth. The end of the feature in this interval (B5) is designated as the 19.4m mark, as the bedding suddenly returns to horizontal at this point. An equal area plot of the data before and after correction to the tilted zone is presented in Figure 4-13 (the signal B6 from the horizontal beds above this zone contains only 6 pairs of which the pattern on an equal angle plot is not interesting enough to warrant further discussion, but is included in the Figure for completeness). The zone containing B5 is separated from the sediments below it by a steep plane of discontinuity, above which the package of sediments is undeformed internally and is tilted as a block, the general character being reminicent of an ancient slump feature. If the sediment layers were originally deposited horizontally then the correction made to rotate tilted beds back to the horizontal assumes that the rotation has taken place about the existing line of strike. If this is not the case, declination will be in error, thus one must view the resulting declinations with caution, but the inclination will be correct. With or without rotation, two remarkable characteristics of this feature remain clear; it is linear and large. The RM vector moves in a definite linear fashion for an angular distance of 70.5°. This angle is based on the points indicated in Figure 4-13. All solid triangles and circles have had an arbitrary within-pair cut-off of 10°

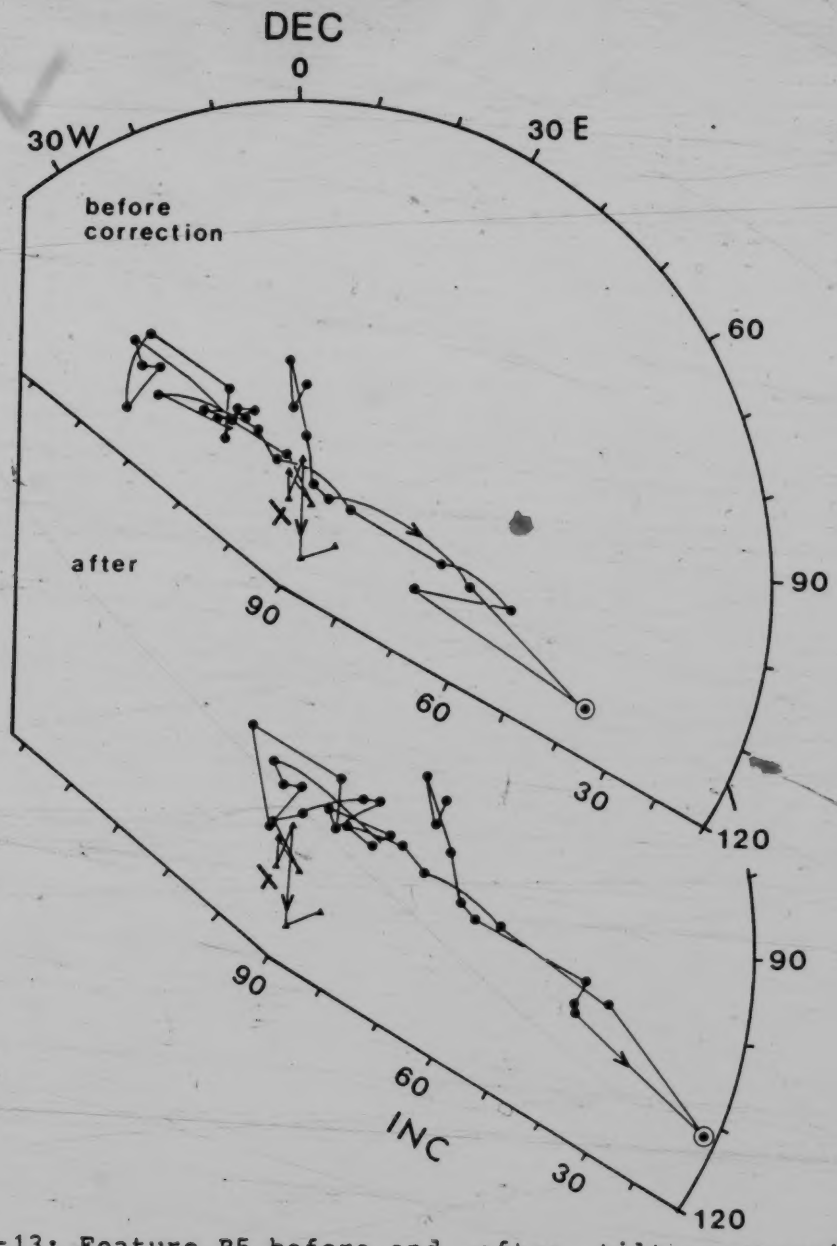

Figure 4-13: Feature B5 before and after tilt correction. The solid triangles are feature B6 (horizontally bedded sediment) and have had internal variance cut-off of 11° and within-pair dipersion cut-off of 10° applied. The solid circles are feature B5 (strata tilted to the east), with the same cut-off criteria as above. The solid circle with the ring around it represents the new minimum in inclination when the within-pair cut-off is removed. Before correction plot shows B5 with no tilt adjustment, while the lower plot shows B5 after correction for tilt. The "X" marks the position of the field due to an axial geocentric dipole.

applied. Under this cut-off B5 lost only 7 out of 42 pairs, of which all but one fall inside the linear track defined by the remaining points. The single pair which falls outside this range is plotted in the figure as a circled dot (see figure caption) and has a within-pair separation of only 11.1°. Using this point in the previous calculation gives a total angular movement of 90.8°. Therefore, although the true orientation of this feature is not known, it nevertheless presents evidence of a third linear perturbation in these sediments.

V. ANALYSIS OF GEOMAGNETIC SECULAR VARIATION

When plotted on an equal area plot, the track of typical paleosecular variation records generally resembles a "plate of spaghetti" (Constable and McElhinny, 1985, p. 117). Features A2 (=B1) and A3 (=B2), however, display perturbations of the geomagnetic field with remarkably linear trajectories and hence are of great geophysical interest. These signals are the type to be expected from stationary sources of secular variation (Evans, 1984) as opposed to the commonly observed westerly drifting sources described in Chapter I. They have therefore been selected for a more detailed analysis with a view to determining their likely origin.

A. Modelling of features A2 and A3

In this section the goal is to develop the simplest physical model capable of explaining the observations. We therefore start by calculating the minimum perturbing field necessary at the site to generate the observed features. The minimum perturbing vector (Pmin) is perpendicular to the resultant vector (R) (Figure 5-1). In vectorial terms this is equivalent to the subtraction of the background field vector (F - due to a geocentric axial dipole) from its projection on the perturbed one.

The directions and magnitudes of Pmin for the shallowest inclinations in A2 and A3 are listed in Table 5-1. Since the magnitudes of F and R are unknown, Pmin is

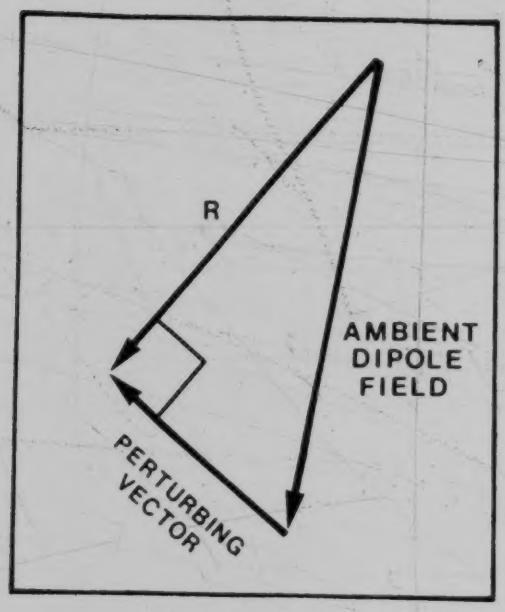

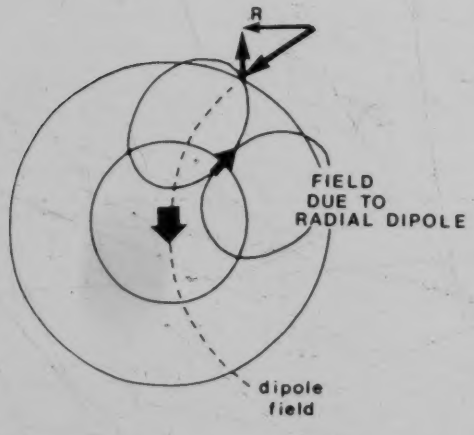

Figure 5-1: The top box illustrates the relationship between the minimum perturbing vector and the ambient and resultant fields. The bottom cartoon demonstrates how this vector relationship applies to the model used herein.

Table 5-1: Modelling data and results for A2 and A3.

feature	perturbation		elevation (m)	P_{min}				radial dipole solution					
								outward			inward		
	dec	inc		dec	inc	mag*	angle+	$M_{rd}/M\%$	lat	long E	M_{rd} M%	lat	long E
A2 within-pair cut	337.2	35.3	11.3 – 14.0	326.3	-54.2	69.9	44.3	7.4	64.7	230.1	69.8	66.0	87.3
A2 no within-pair cut	347.5	16.5	11.3 – 14.0	337.8	-73.3	88.6	62.4	8.4	66.2	224.3	131.4	56.0	62.0
A3	340.9	49.0	8.4 – 11.3	331.1	-40.6	50.7	30.4	6.1	62.3	230.6	35.4	73.0	91.5

* magnitude as a % of background field

+ angle between background and perturbing field

expressed as a percentage of F. The smallest perturbing field necessary to explain A3 (the smaller perturbation of the two) is 51% of the ambient field (geocentric axial dipole). This amounts to a field at the Earth's surface of 29,600 nT (for a main dipole moment of 8 x 10^{22} Am^2, the present-day value) directed at 29° west of north and 41° upwards. Not only is this anomalous field intense, but it points in the wrong direction to that expected in the northern hemisphere (the Z component of which is expected to point towards the geocentre). In the case of the greatest shallowing of the field (A2) the perturbing field is 89% of the intensity of the main field and corresponds to 52,000 nT directed 22° west and 74° upwards. This is a very intense anomalous field directed almost radially away from the geocentre.

The source of the perturbing field can be modelled as a radial dipole (r.d.) at the Core-Mantle Boundary (CMB). Representation as a dipole source is only a convenience. It has long been argued that the sources of secular variation are, in fact, electric currents flowing in the outer skin (approximately 40 km) of the liquid outer core (Lowes and Runcorn, 1951), while the contribution of deeper current systems to rapidly varying B is suppressed by electromagnetic shielding. This skin depth is a rough calculation based on a plane wave and solid conductor possessing typical values of pertinent core parameters. A more recent detailed calculation by Le Mouel and Courtillot

(1982) using a different technique gives estimates of 100 to 200 km for the thickness of the outer portion of the outer core that gives rise to secular variation (SV). The horizontal dimensions of typical SV foci are on the order of 1000 km. Since the moment perpendicular to a given cross-section is proportional to the current density times the area of that cross-section, the section with the greatest area will contribute most to the total moment (assuming constant current density). Since the SV foci have approximately a 10:1 ratio of horizontal to vertical dimensions, the product of current density and horizontal area will dominate. The equivalent dipole moment vector for such a situation will have a radial orientation. This is a physical justification for the use of a radial dipole suggested previously. Indeed, radial dipoles have provided good fits to both the present day non-dipole and SV fields (Alldredge and Hurwitz, 1964; Lowes and Runcorn, 1951; Alldredge and Stearns, 1969).

The perturbed and unperturbed directions at the site can be used to provide the locations of possible r.d.'s which are able to explain the observations. R and F define a plane in which such a source must lie. The assumption that the source must lie on the CMB further constrains it to a locus of points, and the final position of the minimum r.d. can be found by iteration as was done by Hedlin and Evans (1987) for their Old Crow results. This process can be repeated with a series of possible perturbing vectors (other

than the minimum) to produce the graph shown in Figure 5-2. Point 5 represents the position of closest approach to the site and it is from this point that the angular distances in Figure 5-2b are measured. Points 2 and 6 represent the minima for the inwardly and outwardly directed moment r.d. solutions respectively. The gap between the two curves results from the fact that the geometry does not allow any r.d. solution in this interval.

Inspection of Table 5-1 reveals that for all three inclination minima modelled, the minimum perturbing vector is directed away from the geocentre (negative inclination). This can result either from an r.d. close to the site with an outwardly directed moment, or from an r.d. located somewhat further away with an inwardly directed dipole moment. Obviously the latter will have greater moment than the former due to its greater distance from the site. The minimum r.d.'s required to produce the observed perturbations are given in Table 5-1 and vary from 5% to 9% of the strength of the main dipole. The corresponding inwardly directed r.d.'s for the same perturbations are much higher (35% to 131%) leaving outward moment r.d.'s as a much more attractive model. The fact that moments of only a few percent are required in order to explain these results underscores the robustness of this model (i.e. stationary eccentric radial dipoles which pulse in strength). Malin and Bullard (1981) were able to explain the looping behaviour of the field at London over the past several hundred years by

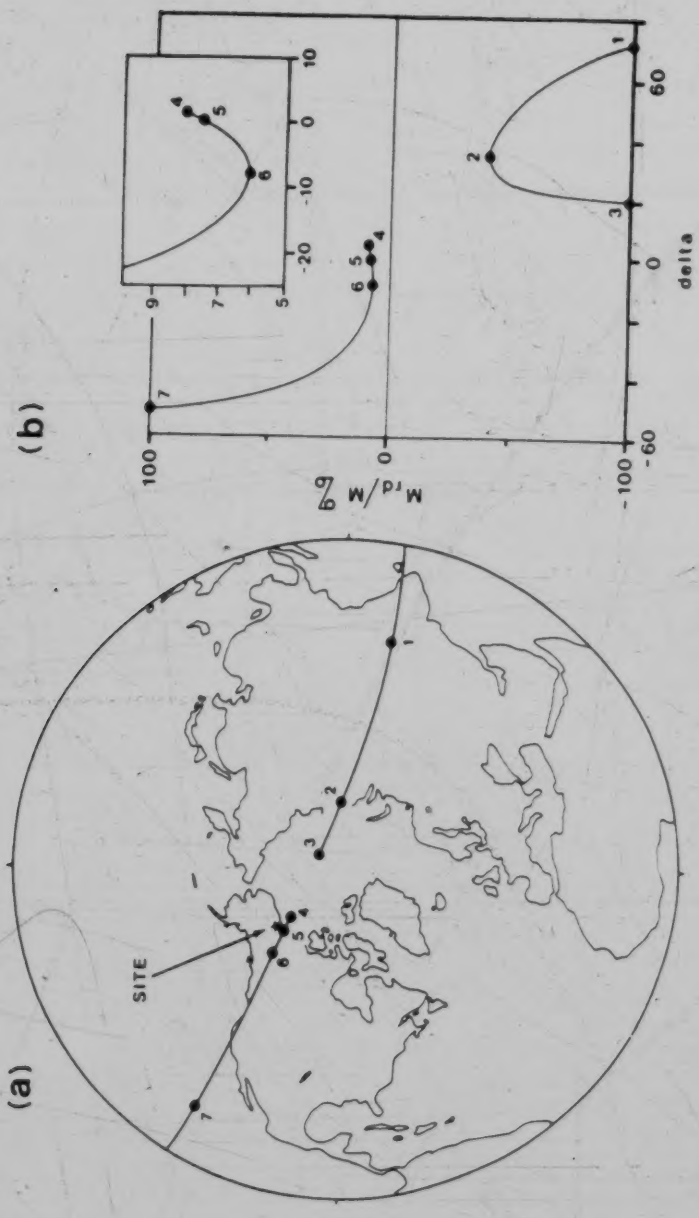

Figure 5-2: The possible locations on the CMB (a) and magnitude (b) of radial dipoles capable of explaining the shallowest inclination for feature A3. Magnitude is expressed as a percentage of the main dipole. Delta refers to the angle from the position of closest approach to the site (point 5). Points 2 and 6 represent the two minima. Points 1,3 and 7 denote the locations where the ratio is 100%.

drifting an r.d. of 3% past that site in a westward direction. The fact that other secular variation features of the geomagnetic field, such as the ones being examined in this study, are likewise explainable by r.d.'s of only a few percent makes the outwardly directed moment solutions very credible.

These results represent the lowest possible value that the r.d. can assume since they are placed at the CMB. There are, however, physical reasons why they should be placed deeper. The equivalent dipole for a spherical cap of current would be at some distance below the CMB, but the appropriate depth is not known. Lowes and Runcorn (1951) fitted dipoles to the SV field and found the majority of them to be radial and at a distance from the geocentre of from 0.35 (1,200 km below CMB) to 0.55 Re (roughly on the CMB). Much greater depth, corresponding to a distance from the geocentre of 0.28 Re (1780 km below the CMB), was determined by Alldredge and Hurwitz (1964) using best fit r.d.'s to represent the present global non-dipole field. In order to assess the effects of depth variation on the results for A2 and A3, the change in the minimum moment of the inwardly directed r.d. with increasing depth below the CMB is illustrated in Figure 5-3. As an upper limit we may examine the effect of placing the r.d. used to explain the most extreme value of A3 (declination 347.5, inclination 16.5) at a depth of 1780 km (the maximum depth given by Alldredge and Hurwitz). The Figure shows that an outward moment r.d. of 35% will explain

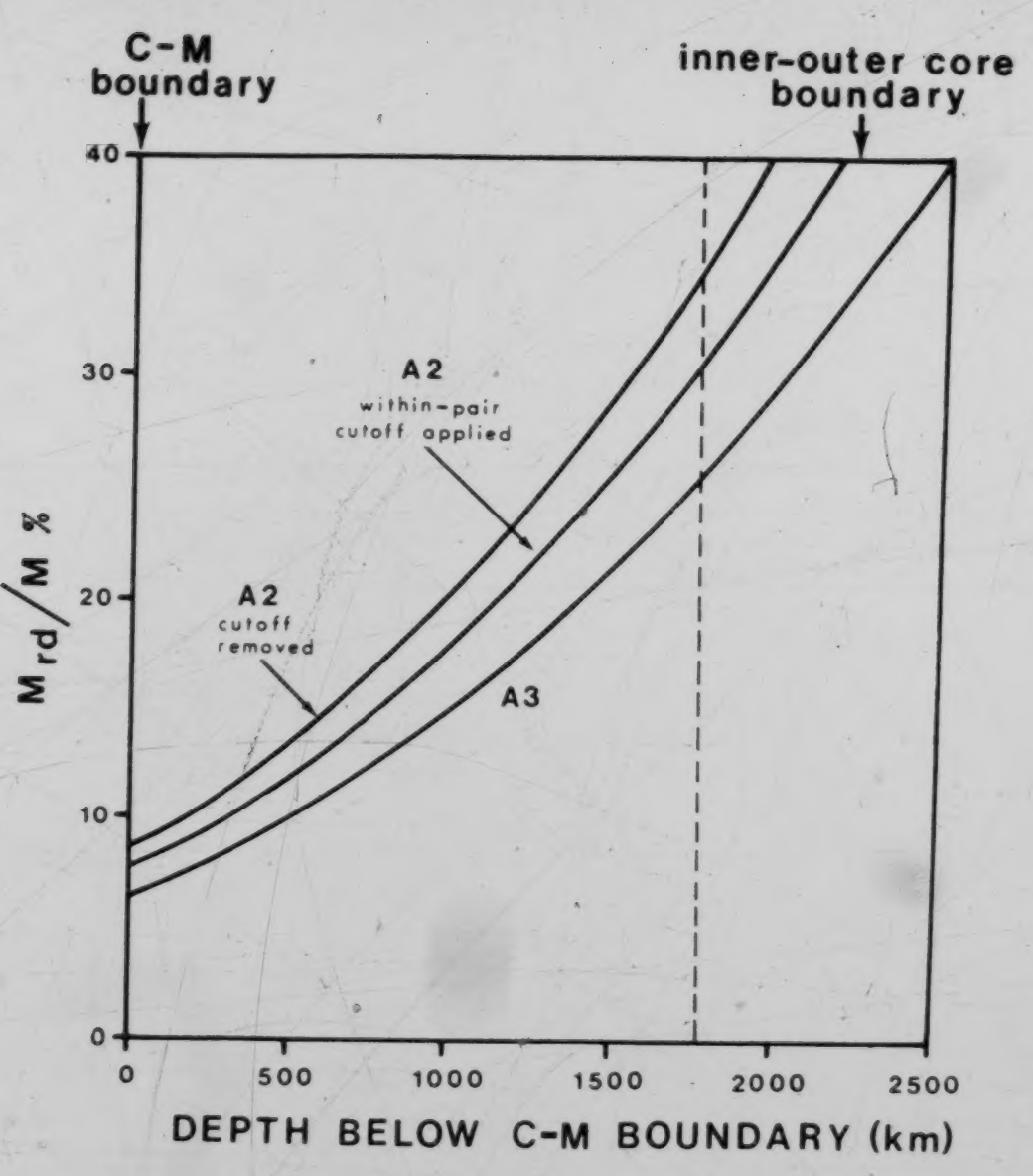

Figure 5-3: Variation of the moment of the radial dipole used to explain features A2 and A3 with depth below the Core-Mantle interface. Magnitude is expressed as a percentage of the main dipole. The vertical broken line refers to the maximum depth used by Alldredge and Hurwitz (1964) and is discussed in the text.

this feature and lesser values are obviously required to explain the other shallow inclinations listed in Table 5-1. It is not known how strong such r.d.'s may get, however it is probably reasonable to be suspicious of solutions which require moments in excess of that of the main dipole. This result emphasizes the fact that we need not invoke moments of much greater than one third the main dipole moment even in this extreme case. In contrast to this, the inward moment r.d. solution for even the smallest perturbation value of the three listed in Table 5-1 (declination 340.9, inclination 49.0) must exceed the main dipole (108%) when placed at these depths, once again showing the outward solution to be the more attractive solution.

B. Comparison with the modern field

The next question to be addressed is that of the existence of similar sources in the present field. As pointed out previously, modern field observations extend back only a fraction of the postulated period of change for non-dipole features. In addition, the Earth's field has had a long history of change of which we presently see only one of many possible configurations. Hence it should not greatly disturb us if a perfect analogy to the modelled perturbing source cannot be found in the present field.

As distance from the sources increases, the characteristics of an individual anomaly may be obscured by its neighbours. It is therefore more desirable to have an

expression for the geomagnetic field at the CMB rather than at the surface if one is to hypothesize about possible sources for paleofield results by studying modern day analogues. Downwardly continued maps of the field have been produced by Bloxam and Gubbins (1985) from various data of the Earth's field spanning several decades.

The modelling of features A2 and A3 revealed that an r.d. with moment vector directed away from the geocentre is the most plausible perturbing source. Such an r.d. would produce a patch of concentrated reversely directed flux vertically above itself, i.e., contoured values of the Z component of the field would reveal a circular patch of flux directed away from the geocentre in the northern hemisphere where flux is normally directed inwards. Such patches do in fact, exist today, the most prominent being in the southern hemisphere (Figure 5-4a). The reversely directed flux (inward for the southern hemisphere) of these features is claimed by Gubbins (1987) to be responsible for the 7% drop in the main dipole over the last 150 years. Over this period, both anomalies have intensified. This rapid intensification makes them attractive analogues to the r.d. model used to explain A2 and A3. As Gubbins points out, we have not yet seen a complete cycle of growth and decay of these features, so we have no idea of the time scale and hence our understanding of these features is incomplete. Over the period of observation, these anomalies have exhibited some westward drift and consequently do not

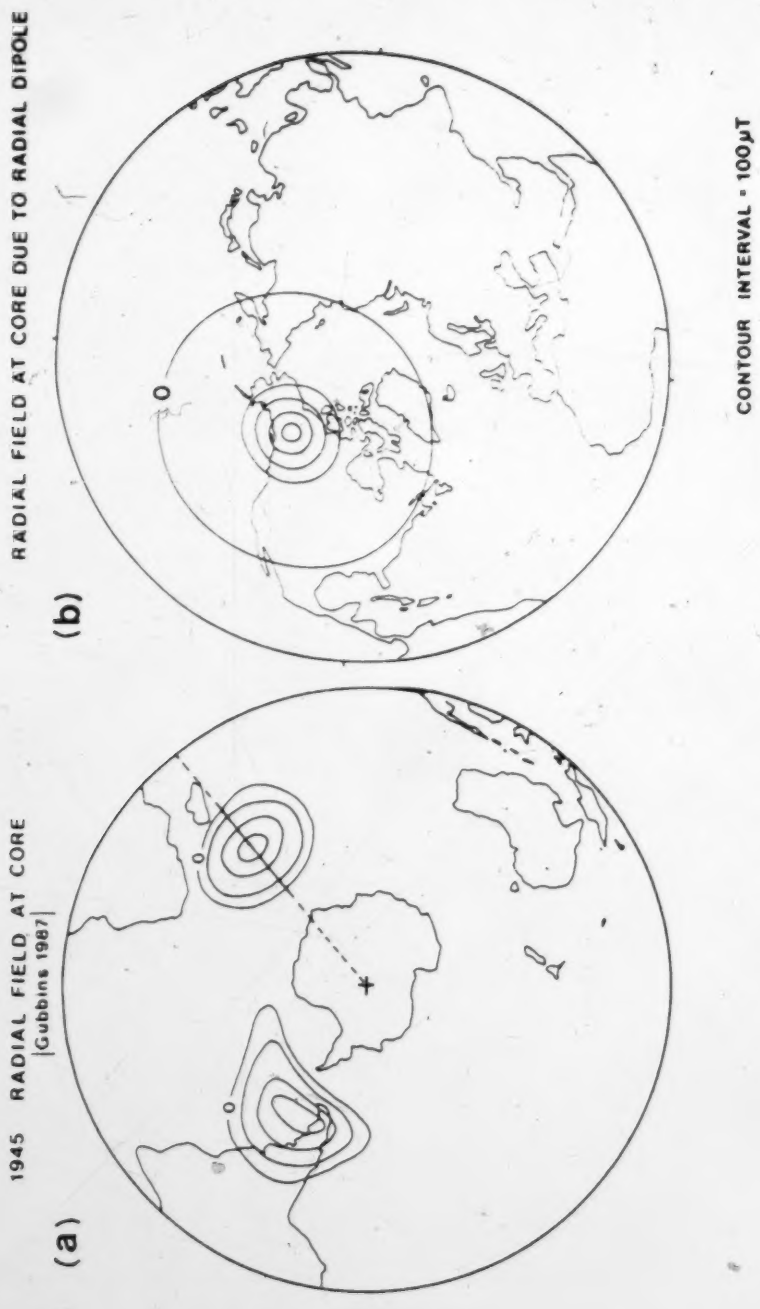

Figure 5-4: (a) Reverse flux patches at the Core-Mantle interface in the 1945 radial field component. Contour interval is in 100 microtesla. (adapted from Gubbins, 1987). Profile line used in Figure 5-6 is indicated. (b) Radial field at the CMB due to a radial dipole of moment 1% placed at 700km below interface with outwardly directed moment.

strictly comply with the requirement that the source be stationary. However, the movement has slowed somewhat in more recent times. Despite this movement, the characteristics of reverse flux and rapid intensification make further analysis worthwhile.

The anomalies in Figure 5-4a are roughly circular in plan and suggest sources which can be modelled as radial dipoles. We can therefore obtain minimum estimates for the moments of the paleosources in the following manner. On the original plots (Gubbins, 1987) there are no values of $Z\cos(\theta)$ greater than 300 microTesla. For the colatitude at which these anomalies occur (θ approximately 50° S) this corresponds to approximately 460 microTesla as a maximum that the radial field (Z) may attain. Since we seek a minimum for the ratio of the moment of the paleosources to the moment of the present-day sources (Mrd/Mpd), we must find the largest value of Mpd and the smallest value of Mrd. As we have just seen, the present-day source may have a <u>maximum</u> of 460 microTesla at the CMB, which for a given depth fixes the upper limit of Mpd. The lower limit for Mrd is obtained by using the minimum outward solution (Table 5-1). To be conservative, we approach the problem by using the linear feature with the smallest perturbation (i.e. A3). Calculating Mpd values for various depths below the CMB using the 460 microTesla limit on Z, and dividing these by the Mrd of A3 obtained from Figure 5-3 for corresponding depths gives the curve of Figure 5-5, which represents the

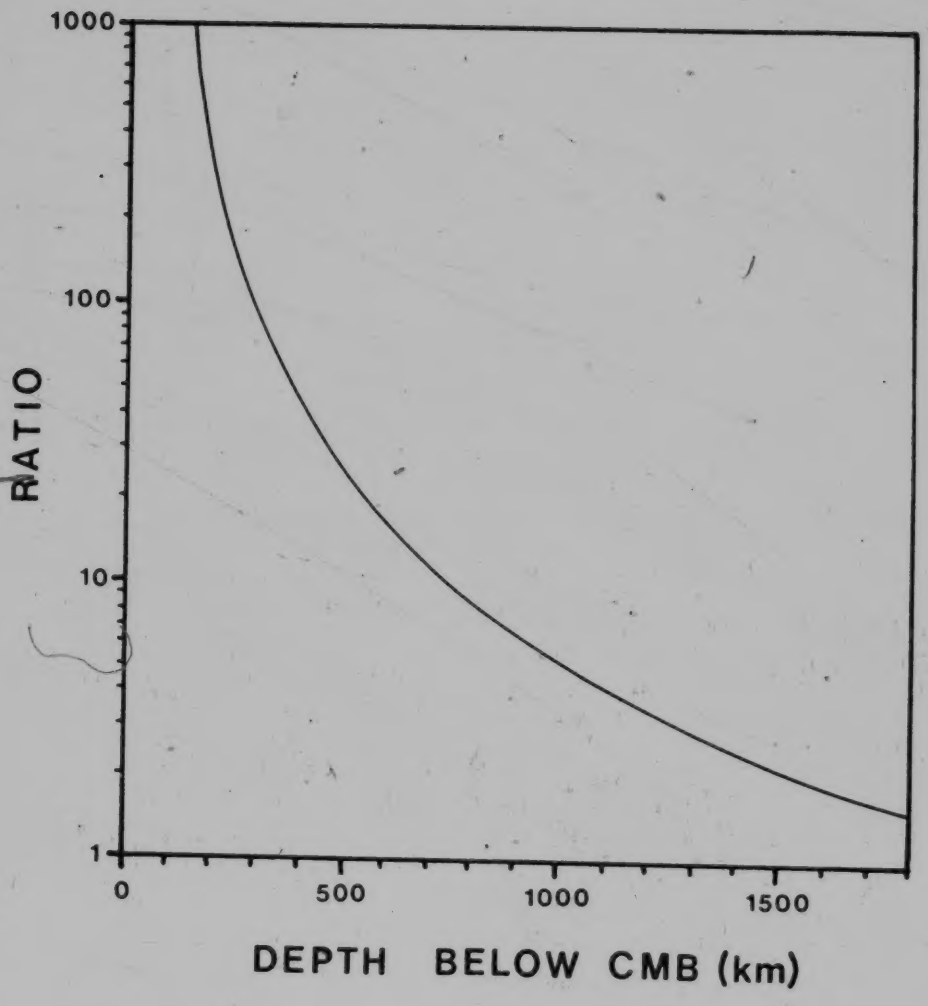

Figure 5-5: Minimum values of ratio of moments of paleosources to present-day sources with depth below the CMB.

minimum values of Mrd/Mpd. This value decreases monotonically with increasing depth and therefore we must identify the maximum depth at which we may place the r.d. in order to find the minimum ratio. This is determined by taking a profile across the feature of interest in Figure 5-4a, placing r.d.'s of various strengths at different depths below the anomaly centre and examining the fit. Since the starting point in this procedure was a small published diagram, a rigorous fitting procedure is not justified, and given that we seek only an order of magnitude comparison, a fit by eye is adequate. Figures 5-6a through 5-6c show the procedure for r.d.'s of moments 1% (Figure 5-6b), 5% (5 times greater - Figure 5-6c) and 0.2% (5 times less - Figure 5-6a). The best-fitting curve of Figure 5-6a (depth = 410km) underestimates most of the values on the flanks. A better fit is provided by the 1% r.d. at 700 km (Figure 5-6b) which also has the advantage that it slightly overestimates the values of Z and hence gives a maximum depth. Figure 5-6c shows that once a value of 5% is reached, a good fit cannot be found. We select the 700km 1% solution, and reference to Figure 5-5 then gives a ratio of at least 12 to 1. The same procedure using perturbation A2 without the within-pair cutoff gives a ratio of 16 to 1. Therefore it appears that the paleosources required to explain the observed perturbations are at least an order of magnitude higher than present-day reverse flux features.

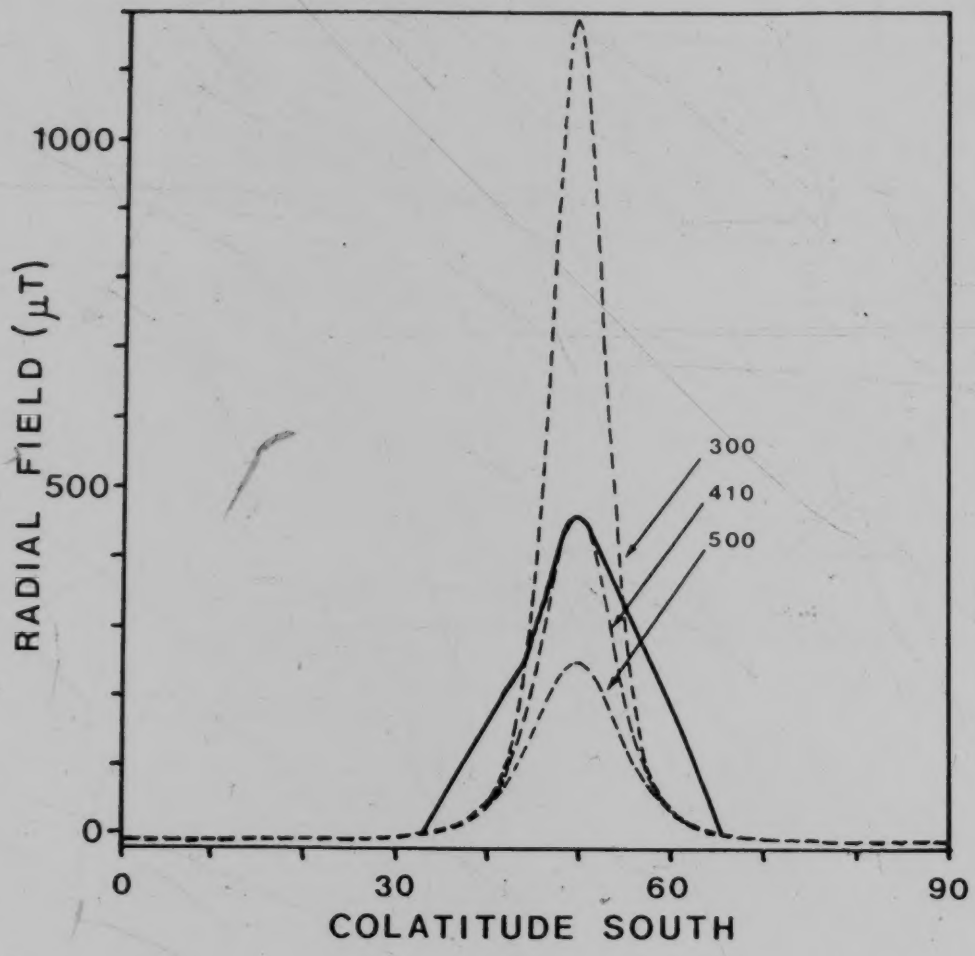

Figure 5-6: Comparison of profile of Z field feature of Figure 5-4 with Z profiles (broken curves) generated by radial dipoles of arbitraty strengths (a) 0.2%, (b) 1%, and (c) 5%, placed at indicated depths below the CMB.

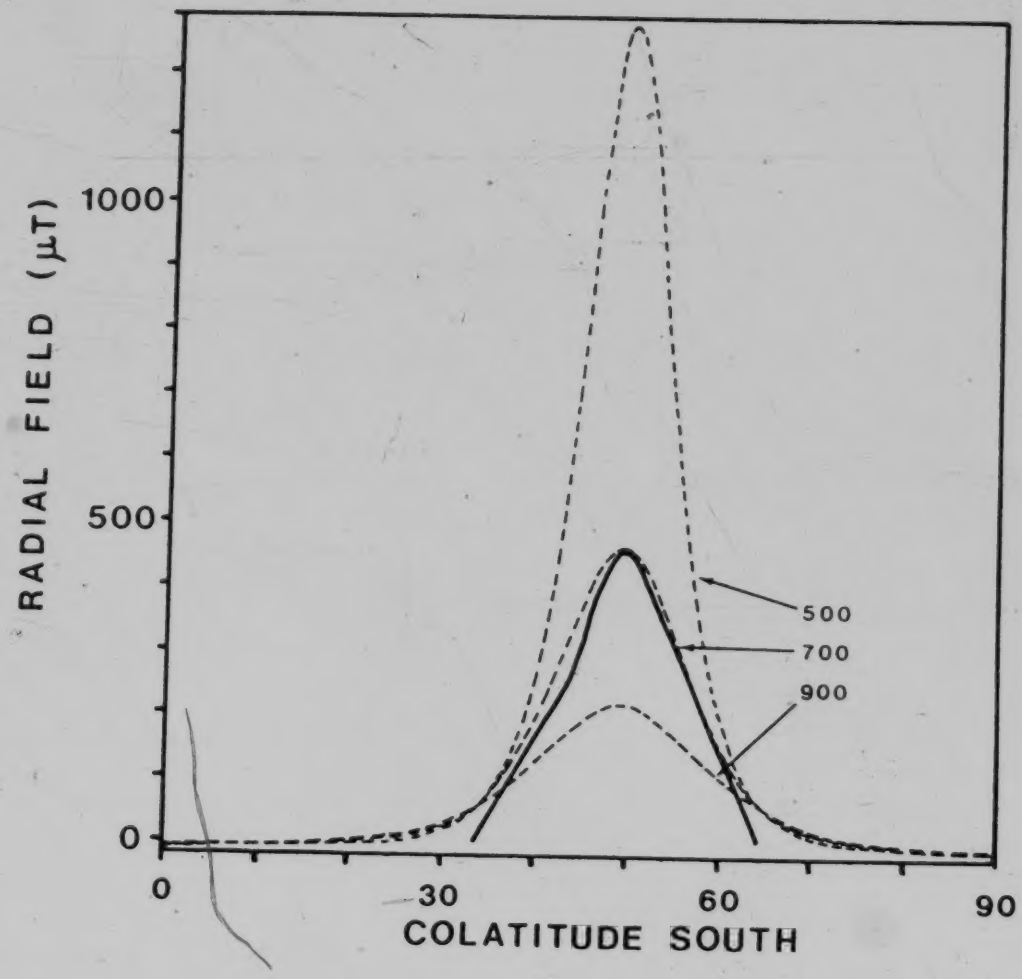
RADIAL FIELD (μT)
1000
500
0
0
30
60
90
COLATITUDE SOUTH
500
700
900

Figure 5-6(b)

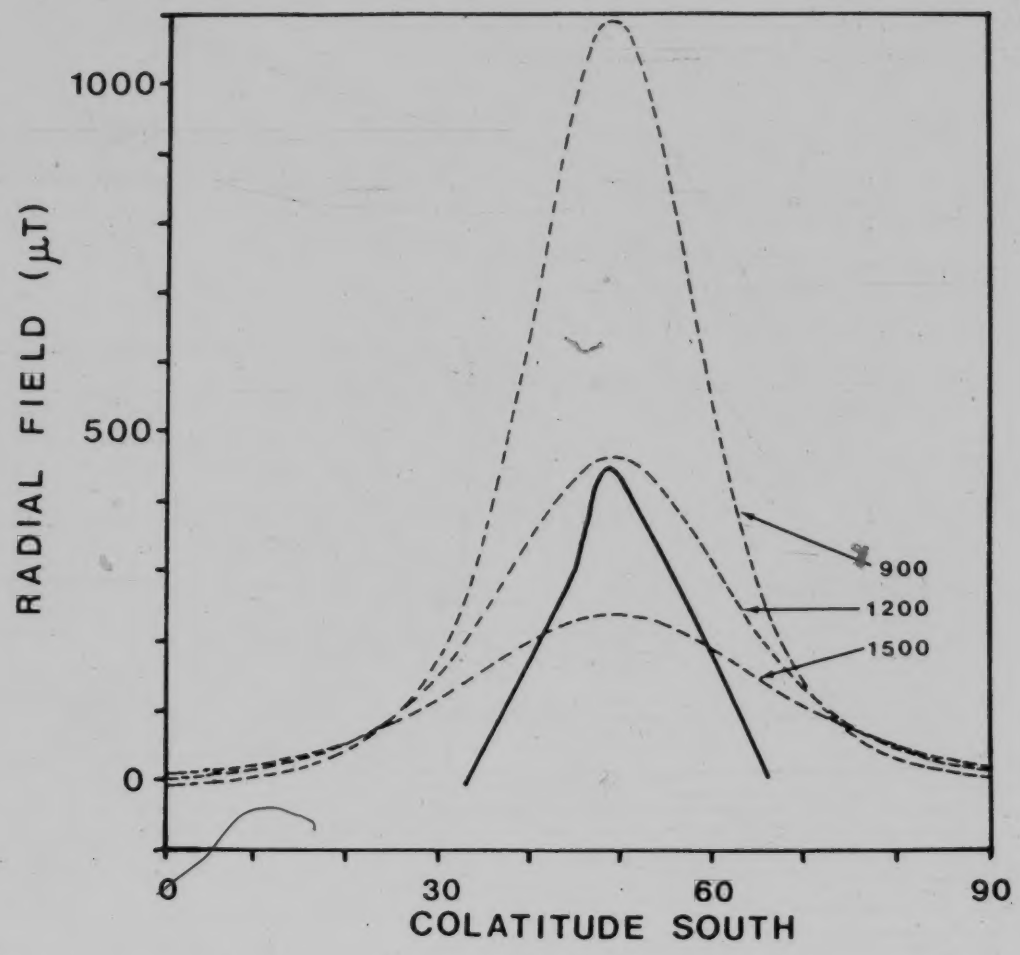
1000
500
0
RADIAL FIELD (μT)
900
1200
1500
0
30
60
90
COLATITUDE SOUTH

Figure 5-6(c)

VI. SUMMARY AND CONCLUSIONS

The remanent magnetization records recovered from two sections of Pleistocene sediments (each approximately 20 m in vertical extent) exposed in the valley walls of the Old Crow River display features of both geological and geophysical interest. The fact that a sequence of three features (A2, A3 and A4) can be correlated with previous findings from other sections upstream supports their reality, and the fact that these and the previously sampled sections are separated by over 5 km favours a geomagnetic perturbing mechanism over a sedimentological one. This remarkable correlation of three features allows a date to be established for these sediments by paleomagnetic means. A volcanic ash (the Old Crow Tephra) present at the outcrop at which Hedlin and Evans (1987) recovered their records showed a distinctive paleomagnetic signature. The age of this tephra is currently believed to be 149,000 ±13,000 years (Westgate, 1988) and thus sediments at the 14.6m level in KGA which display this characteristic paleomagnetic signal are believed to represent this age, i.e. the time of deposition of the Old Crow Tephra in the Basin. The same RM signal is suggested at the 13.3m mark in section KGB, although the quality is not as good.

The paleosecular variation sequences recovered also display behaviour consistent with the existence of several cycles of growth and decay of stationary sources at the CMB. These involve perturbations of the RM vector in linear

trajectories up to 62.4° from the ambient position dictated by an axial geocentric dipole field. Such features can be easily modelled by elementary magnetostatic theory by placing an eccentric radial dipole at the CMB. The strength for an r.d., the moment vector of which is directed outwards (away from the geocentre) need only be a few percent of the dipole, even in the most extremely perturbed case (declination 347.5, inclination 16.5). The results for the corresponding inwardly directed moment r.d.'s are always much higher and in the case of the above perturbation, exceed the strength of the main dipole itself. This leaves the outward solution as a much more attractive explanation. Such r.d's would produce patches of concentrated reversely directed flux at the CMB (i.e., outwards in the northern hemisphere where flux should be inwards). No perfect analogue can be found in the modern field, but patches of rapidly intensifying reversely directed flux do exist. Simple magnetostatic modelling of such a patch currently existing in the southern hemisphere demonstrates that a radial dipole with moment approximately 1% of that of the main dipole produces an excellent fit when placed under these anomalies at a depth of 700 km below the CMB. At this same depth, r.d.'s ranging from 12% to 16% are required to explain the features A2 and A3, thus suggesting an order of magnitude difference.

As Bloxham and Gubbins (1985) mention, the pattern of fluid flow in the outer core is unlikely to remain

stationary with respect to the mantle, so the existence of static features implies that this flow must be coupled to the lower mantle in some regions. The coupling mechanism could be thermal, electromagnetic, topographical or some combination of these. Topographic coupling seems plausible insofar as recent seismic tomography results suggest that topography exists today at the CMB and thus there is no reason to believe that it would not have existed in the past. Hide and Malin (1971) demonstrated that even small scale vertical relief (small on the planetary scale) of only a few kilometres at the CMB could cause fluid flow perturbations which could penetrate to great depths within the core. The general idea is that fluid flow encountering local topography on the CMB is induced to flow in what is loosely termed an "eddy", and whatever the exact motion is, it is sufficient to generate magnetic flux by virtue of the velocity and magnetic field interaction. Certainly the regular appearance of several linear perturbation features in these paleosecular variation records (and the lack of such features in most other RM records from around the world) suggests that there was some property of the CMB which was in the past inducing these sources to form and/or causing them to be localized in the general vicinity of this site.

REFERENCES

Alldredge, L.D. and Stearns, C.O., 1969, Dipole model as the sources of the earth's main magnetic field, *J. Geophys. Res.*, 74, 6583-6593.

Alldredge,L.D. and Hurwitz,L., 1964, Radial dipoles as sources of the Earth's main magnetic field, *J. Geophys. Res.*, *69*, 2631-2640.

As, J.A., and Zijderveld, J.D.A., 1958, Magnetic cleaning of rocks in paleomagnetic research, *Geophys. J.*, *1*, 308-319

Barton, C.E., 1978, *Magnetic studies of some Australian lake sediments*, Unpub. Ph.D. thesis, Australian National Univ.

Bloxham,J. and Gubbins,D., 1985, The secular variation of the Earth's magnetic field, *Nature*, *317*, 777-781.

Bullard,E.C., Freedman,C., Gellman,H., Nixon,J. 1950, The westward drift of the Earth's magnetic field, *Phil. Trans. Roy. Soc. London*, *A243*, 67-92.

Constable, C.G. and McElhinny, M.W., 1985, Holocene geomagnetic secular variation records from north-eastern Australian lake sediments, *Geophys. J. R. astr. Soc.*, 81, 103-120.

Cox, A.V., 1968, Lengths of Geomagnetic Polarity Intervals, *J. Geophys.*, *73*, 3247-3260.

Creer, K.M., and Tucholka, P., 1982, Secular variation as recorded in lake sediments: a discussion of North American and European results, *Phil. Trans. R. Soc., Lond.*, *A306*, 87-102.

Creer, K.M., D.L. Grosss and J.A. Lineback, 1976, Origin of regional geomagnetic variations recorded by Wisconsinan and Holocene sediments from Lake Michigan, USA, and Lake Windermere England, *Geol Soc. Amer. Bull*, 87, 531-540.

Denham, C.R., 1974, Counter-clockwise motion of paleomagnetic directions 2400 years ago at Mono Lake, California, *J. Geomag. Geoelect.*, *26*, 487-498.

Evans, M.E., Gillen, K.P., and Hedlin, M.A.H., (in press), Further paleomagnetic results from northern Canada.

Evans,M.E., 1984, Paleomagnetic evidence for stationary sources of geomagnetic secular variation, *Phys. Earth Planet. Interiors*, *35*, 223-226.

Fisher,R.A., 1953, Dispersion on a sphere, *Proc. Roy. Soc.*, *A217*, 295-305.

Gaiber-Puertas, C., 1953, *Variacion secular del campo geomagnetico*, Obser. del Elso, Memo no 11 (4).

Gubbins, D., 1987, Mechanism for Geomagnetic polarity reversals, *Nature*, 326, 167-169.

Hedlin, M.A.H., 1986, *A Pleistocene high-latitude geomagnetic study*, Unpub. M.Sc. thesis, Univ. of Alberta.

Hedlin, M.A.H., and Evans, M.E., 1987, A paleomagnetic study of some Pleistocene sediments in northern Canada and its bearing on the secular variation of the geomagnetic field. *Geophys. J. R. astr. Soc.*, *90*, 693-703.

Hide, R.and Malin, S.R.C., 1971, *Bumps on the Core Mantle Boundary*, Comments on Earth Sciences: Geophysics 1-13.

Le Mouel, J.L., 1984, Outer-core geostrophic flow and secular variation of Earth's geomagnetic field, *Nature*, *311*, 734-735.

Le Mouel, J.L., and V. Courtillot, 1982, On the outer layers of the core and geomagnetic secular variation, *J. Geophys. Res.*, *87*, 4103-4108.

Lowes, F.J. and Runcorn, S.K., 1951, The analysis of the geomagnetic secular variation, *Phil. Trans. R. Soc., Lond., A243*, 525-546.

Mackereth, F.J.H., 1971, On the variation in direction of the horizontal component of remanent magnetization in lake sediments, *Earth Plan. Sci. Let.*, 12, 332-338.

Malin,S.R.C. and Bullard,E.C., 1981, The direction of the Earth's magnetic field at London, 1570-1975, *Philos. Trans. R. Soc. London, Ser A, 299* 357-423.

McElhinny, M.W., and Gough, D.I., 1963, The paleomagnetism of the Great Dyke of Southern Rhodesia, *Geophys., J., 7*, 287-303.

Merrill, R.T. and McElhinny, M.W., 1983, *The Earth's Magnetic Field*, 401 p., Academic Press, International Geophysics Series, 32.

Molyneux,L., 1971, A complete result magnetometer for measuring the remanent magnetization of rocks, *Geophys. J. Roy. Astr. Soc., 24*, 429-433.

Morlan,R.E., 1980, *Taphonomy and Archaeology in the Upper Pleistocene of northern Yukon Territory: A glimpse of the peopling of the New World*, National Museum of Man (Mercury Series), Archaeological Survey of Canada, Paper 94.

Morlan, R.E., and Matthews, J., 1978, New dates for early Man, *GEOS*, Winter, 2-5.

Murthy,G.S., 1969, *Paleomagnetic Studies in the Canadian Shield*, Unpub. Ph.D. thesis, Univ. of Alberta.

Palmer, D.F., Henyey, T.L., and Dodson, R.E., 1979, Paleomagnetic and sedimentological studies at Lake Tahoe, California Nevada, *Earth Planet Sci. Letters*, 46, 125-137.

Reid, A.B., 1972, A paleomagnetic study at 1800 million years in Canada, Unpub. M.Sc. thesis, Univ. of Alberta.

Tarling, D.H., 1983, *Paleomagnetism: principles and applications in geology, geophysics and archaeology*, 379 pp., Chapman and Hill Ltd., London.

Turner, G.M., 1983, Comment on "A paleomagnetic record from Tangle lakes, Alaska: large amplitude secular variation at high latitudes" by K.L. Verosub, *Geophys. Res. Lett.*, 10, 185.

Verosub, K.L., 1977, Depositional and postdepositional processes in the magnetization of sediments., *Revs Geophys. Space Phys.*, *15*, 129-143.

Watson, G.S., 1956, Analysis of dispersion on a sphere, *Mon. Not. Roy. Ast. Soc., Geophys Supp.*, *7*, 153-159.

Westgate, J., 1988, Isothermal plateau fission-track age of the late Pleistocene Old Crow Tephra, Alaska, *Geophys. Res. Lett.*, 15, 376-379.

Westgate, J., and Wintle, 1986, Thermoluminescence age of Old Crow tephra in Alaska, preprint.

Westgate, J., R.C. Walter, G.W. Pearce, and M.P. Gorton, 1985, Distribution, stratigraphy, petrochemistry, and paleomagnetism of the late Pleistocene Old Crow tephra in Alaska and the Yukon, *C.J. Earth Sci.*, 22, 893-906.

Yukutake,T. and Tachinaka,H., 1968, The non-dipole part of the Earth's magnetic field, *Bull. Earthq. Res. Inst., Tokyo*, *46*, 1027-1074.

APPENDIX A - Theta

The purpose of the work herein is to establish a relationship between "theta" values obtained from the Schonstedt SSM-2 and Molspin (Molyneux, 1971) magnetometers. Theta is a measure of the internal variance of a measurement and is defined as:

$$\text{theta} = \sin^{-1}\left(\frac{\sqrt{(\text{disX}^2 + \text{disY}^2 + \text{disZ}^2)}}{\text{moment}}\right)$$

$$\text{where disX} = \frac{1}{4}\sqrt{\Sigma(\bar{X}-X)^2}$$

and similarly for disY and disZ.

The value obtained from a sample is a function of (a) magnetometer noise and (b) inhomogeneity of magnetization.

(a) In order to assess the effects of noise only, we require a perfectly homogeneous specimen. For most cities, air will suffice for this purpose, and thus the magnetometers were operated with the sample holders empty. Theoretically, noise will be reduced by the act of stacking together repeated measurements on a single sample. This process is refered to as "integration" and the number of determinations stacked in called the integration number. The noise level at different integration numbers for both the Schonstedt and Molspin are shown in Figure A-1.

The Molspin has a tendency to drift and consequently at long integration numbers (long spin times) it is unable to attain the low noise levels possible in the Schonstedt. The lowest levels attainable for the Molspin and Schonstedt are of the order of 1×10^{-9} and 1×10^{-10} respectively. Note that although the Schonstedt approaches 1×10^{-11} for

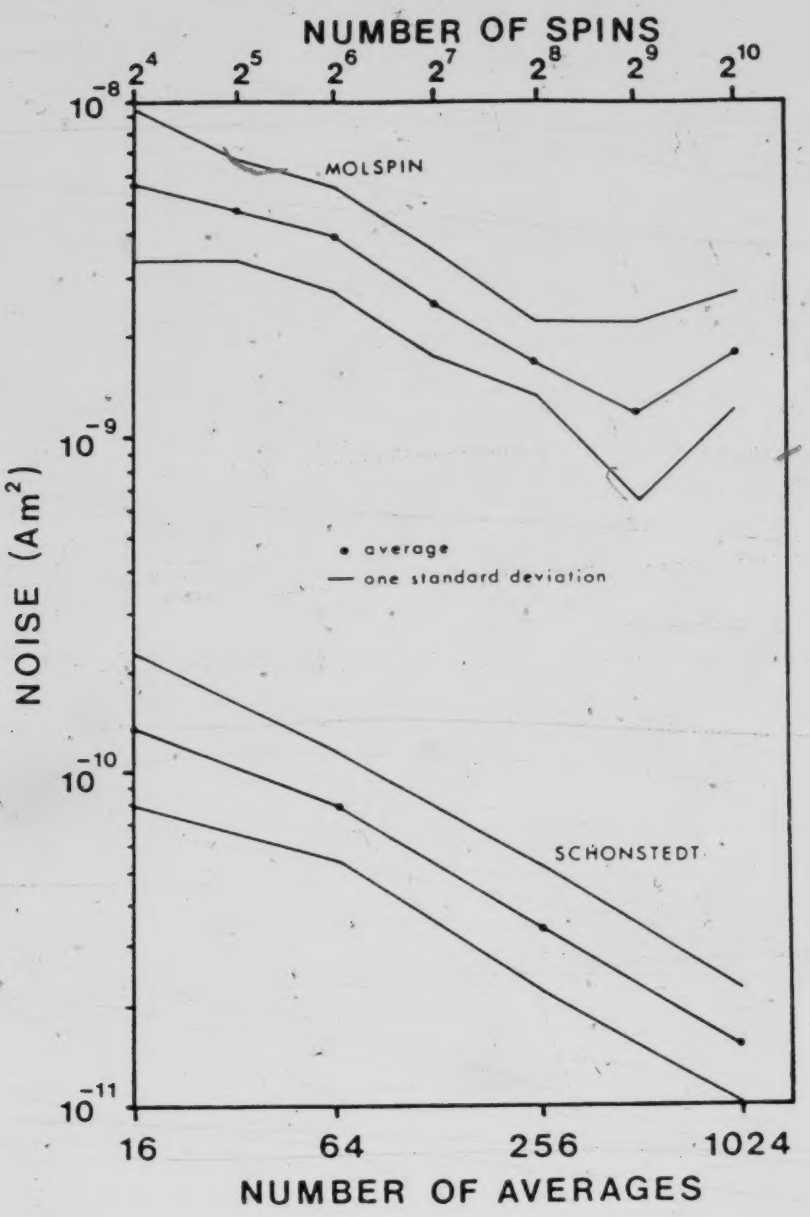

Figure A-1 Comparison of noise for Molspin and Schonstedt system designs.

averages 2⁸ and 2¹⁰, these excessively long spin times were only used in cases where inhomogeneous samples were measured in cart position 3, and in this position, the sample moment as seen by the sensor is reduced by a factor of ten, thus effectively increasing system noise by a factor of ten. Therefore the figure of 1 x 10-¹⁰ is still applicable. This allows us to calculate the lowest moment level for a homogeneous sample at which it will exceed a theta of 5°.

$5° = \arcsin(1 \times 10^{-9}/Mmol)$

$5° = \arcsin(1 \times 10^{-10}/Msch)$

therefore,

$Mmol = 1 \times 10^{-8}$

$Msch = 1 \times 10^{-9}$

This explains why Hedlin could not measure his weakest samples (less than 1 x 10-⁸ Am²) with enough precision (theta less than 5°). For moments less than 1 x 10-⁸ Am², even a perfectly homogeneous sample will give theta greater than 5° on the Molspin.

(b) Determination of the effect of sample inhomogeneity requires samples with sufficiently high moments to render noise insignificant. In addition, the specimen cannot have low theta, since it is not inhomogeneous in this case. Unfortunately, most samples with high moments also had low theta and consequently only 5 specimens were judged suitable. These were measured on both magnetometers. For the Schonstedt, the position of the sample from the sensor is adjustable (4 possible "cart positions", 1 being furthest

and 4 being closest) with the effect that increasing distance reduces the apparent degree of inhomogeneity. Since all measurements were made using cart position 3 or 4, the comparison between device designs was made using cart position 3 (the further). Table A-1 summarizes the results.

A plot of theta from columns 2 and 3 is shown in Figure A-2. The slope of the best fit line through the origin is 2.4, thus showing that a theta of 5° on the Molspin (used by Hedlin) corresponds to 12° on the Schonstedt (used in the present study). To be conservative, the actual value selected was 11°, but the actual value chosen is not critical to the form of the magnetograms for both sections. Plots made with theta cut-offs of 10°,11°,12°, and 13° simply affects the number of points in the plots, but the geophysical interpretation is unaffected.

	Theta		
sample	Molspin	Schonstedt	Ratio(Sch/Mol)
KGA067	3.1	6.1	2.0
KGA073	4.7	11.9	2.5
KGA050	4.5	13.2	2.9
KGA053	3.9	8.9	2.3
KGA059	3.4	8.5	2.5

Table A-1: Table of theta values used to construct Figure A-2.

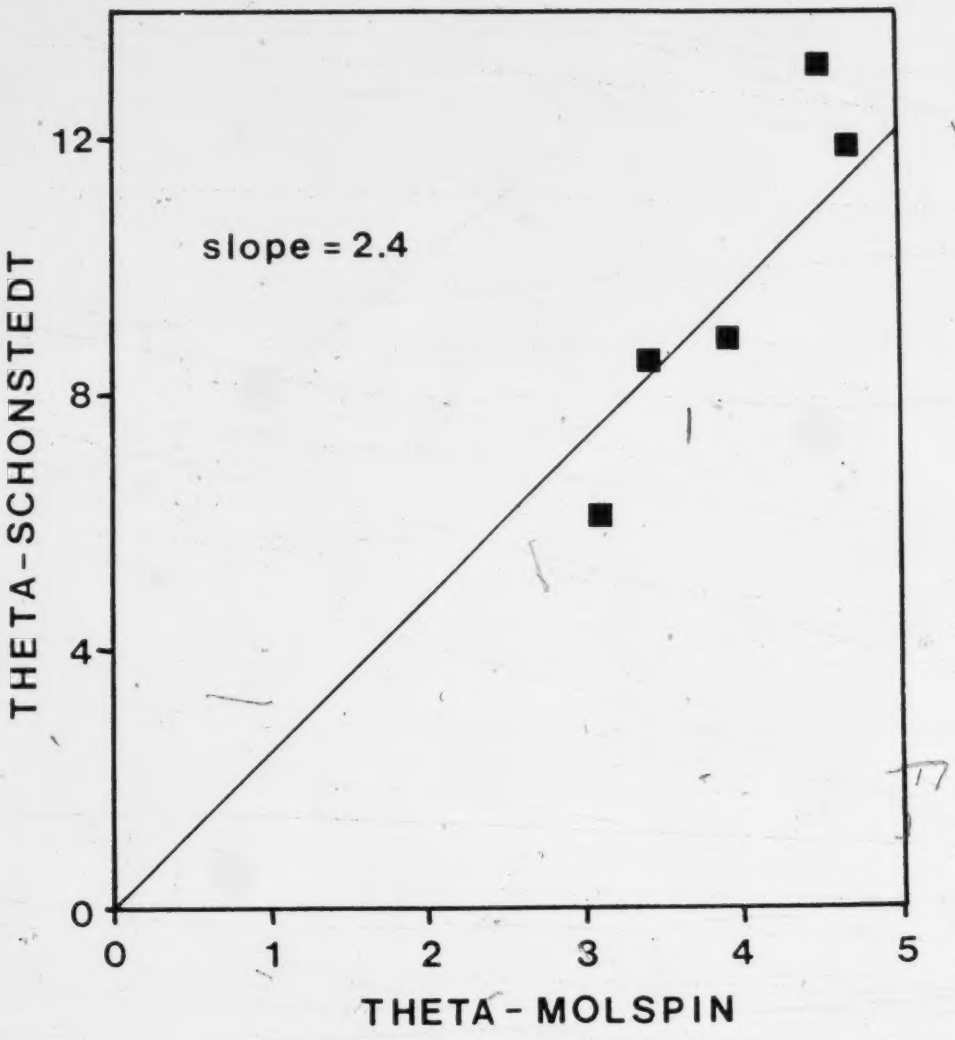

Figure A-2: Comparison of theta for Molspin and Schonstedt system designs using the best measurements obtained from selected specimens.

APPENDIX B - Data

The data used to produce this thesis are contained herein.

THIS FILE CONTAINS ALL DATA USED IN THE PRODUCTION OF KEVIN GILLEN'S
M.Sc. THESIS

****

COLUMN 1 ..... SAMPLE NUMBER
COLUMN 2 ..... ELEVATION
COLUMN 3 ..... DECLINATION
COLUMN 4 ..... INCLINATION
COLUMN 5 ..... DEC (CORRECTED FOR BEDDING)
COLUMN 6 ..... INC (CORRECTED FOR BEDDING)
COLUMN 7 ..... INTERNAL VARIANCE
COLUMN 8 ..... MOMENT (CGS)
COLUMN 9 ..... PERCENT ERROR IN MOMENT
COLUMN 10 ..... A F TREATMENT

****

A 1	-0 260	11 50	80 80	0 0	0 0	4 70	0 331E-02	8 3	0
A 2	-0 260	336 70	85 70	0 0	0 0	4 10	0 313E-02	7 2	0
A 3	-0 150	331 30	83 80	0 0	0 0	8 20	0 319E-03	14 3	0
A 4	-0 150	37 30	79 60	0 0	0 0	3 40	0 191E-02	5 9	0
A 5	-0 050	66 70	78 30	0 0	0 0	3 90	0 613E-04	6 8	0
A 6	-0 050	35 90	80 40	0 0	0 0	3 90	0 184E-03	6 8	0
A 7	0 150	22 20	60 90	0 0	0 0	18 00	0 411E-04	30 8	0
A 8	0 180	40 10	67 10	0 0	0 0	8 90	0 370E-04	15 5	0
A 9	0 250	36 70	66 10	0 0	0 0	33 20	0 661E-04	54 7	0
A 10	0 260	58 20	73 30	0 0	0 0	13 60	0 277E-04	23 6	0
A 11	0 410	35 90	83 30	0 0	0 0	12 30	0 630E-04	21 3	0
A 12	0 410	314 80	69 10	0 0	0 0	24 80	0 102E-03	42 0	0
A 13	0 500	28 80	80 80	0 0	0 0	13 20	0 270E-04	22 8	0
A 14	0 490	359 60	76 00	0 0	0 0	11 70	0 330E-04	20 3	0
A 15	0 580	358 10	87 10	0 0	0 0	10 70	0 799E-04	18 6	0
A 16	0 570	12 70	81 90	0 0	0 0	12 30	0 349E-04	21 4	0
A 17	0 730	44 10	66 20	0 0	0 0	10 80	0 586E-04	18 7	0
A 18	0 720	342 90	64 70	0 0	0 0	21 20	0 630E-04	36 2	0
A 19	0 880	12 40	70 40	0 0	0 0	18 90	0 142E-03	32 4	0
A 20	0 870	51 30	59 40	0 0	0 0	19 40	0 909E-04	33 3	0
A 21	1 030	324 10	81 70	0 0	0 0	9 90	0 348E-04	17 2	0
A 22	1 030	350 80	77 00	0 0	0 0	8 60	0 383E-04	14 9	0
A 23	1 130	12 30	82 70	0 0	0 0	12 20	0 723E-04	21 1	0
A 24	1 130	322 00	77 70	0 0	0 0	17 20	0 690E-04	29 6	0
A 25	1 230	36 50	67 30	0 0	0 0	9 20	0 227E-04	16 0	0
A 26	1 230	53 60	73 40	0 0	0 0	9 20	0 863E-04	16 1	0
A 27	1 330	27 40	70 20	0 0	0 0	15 00	0 307E-04	25 9	0
A 28	1 330	14 40	77 10	0 0	0 0	9 50	0 517E-04	16 4	0
A 29	1 430	308 50	83 80	0 0	0 0	12 70	0 455E-04	22 0	0
A 30	1 430	30 90	74 70	0 0	0 0	16 90	0 452E-04	29 1	0
A 31	1 530	353 10	78 70	0 0	0 0	10 70	0 333E-03	18 5	0
A 32	1 530	32 80	87 10	0 0	0 0	7 90	0 391E-03	13 8	0
A 33	1 630	42 30	79 50	0 0	0 0	4 80	0 567E-04	8 3	0
A 34	1 630	102 00	63 70	0 0	0 0	29 40	0 691E-04	49 1	0
A 35	1 730	9 80	79 30	0 0	0 0	10 00	0 352E-04	17 4	0
A 36	1 730	3 90	61 30	0 0	0 0	15 00	0 516E-04	25 9	0
A 37	1 830	15 00	78 60	0 0	0 0	9 00	0 377E-04	15 7	0
A 38	1 830	13 00	60 00	0 0	0 0	13 70	0 148E-03	23 7	0
A 39	1 930	17 30	79 90	0 0	0 0	9 30	0 116E-03	16 2	0
A 40	1 930	26 70	80 30	0 0	0 0	9 30	0 598E-04	16 2	0
A 41	2 020	14 10	68 60	0 0	0 0	8 60	0 416E-04	15 0	0
A 42	2 020	40 00	78 80	0 0	0 0	6 30	0 509E-04	10 9	0
A 43	2 100	334 40	67 10	0 0	0 0	19 60	0 627E-04	33 5	0
A 44	2 100	332 20	80 10	0 0	0 0	6 50	0 349E-04	11 4	0
A 45	2 180	87 70	56 50	0 0	0 0	25 80	0 443E-04	43 5	0
A 46	2 190	340 40	78 30	0 0	0 0	8 60	0 509E-04	15 0	0
A 47	2 300	7 60	79 00	0 0	0 0	5 90	0 281E-04	10 4	0
A 48	2 300	13 80	79 30	0 0	0 0	9 50	0 260E-04	16 5	0
A 49	2 400	31 60	80 10	0 0	0 0	13 30	0 331E-04	23 0	0
A 50	2 400	109 90	82 90	0 0	0 0	13 20	0 202E-03	22 8	0
A 51	2 510	335 80	72 90	0 0	0 0	22 90	0 267E-03	38 9	0
A 52	2 500	305 70	45 00	0 0	0 0	26 90	0 943E-03	45 2	0
A 53	2 600	127 20	74 10	0 0	0 0	8 90	0 117E-03	15 4	0
A 54	2 600	41 80	84 60	0 0	0 0	4 50	0 397E-04	7 9	0
A 55	2 700	1 00	72 80	0 0	0 0	13 30	0 316E-04	23 0	0
A 56	2 700	353 40	50 40	0 0	0 0	14 60	0 243E-03	25 2	0
A 57	2 800	327 40	70 40	0 0	0 0	23 10	0 149E-03	38 2	0
A 58	2 800	336 90	61 70	0 0	0 0	13 60	0 133E-03	23 4	0
A 59	2 900	41 30	74 60	0 0	0 0	9 80	0 400E-04	17 0	0
A 60	2 900	0 90	49 90	0 0	0 0	19 50	0 885E-04	33 4	0
A 61	2 990	302 20	43 50	0 0	0 0	30 90	0 289E-03	51 4	0
A 62	3 000	20 80	62 90	0 0	0 0	7 00	0 219E-04	12 2	0
A 63	3 160	281 40	49 10	0 0	0 0	19 90	0 177E-03	34 1	0
A 64	3 160	351 40	75 00	0 0	0 0	13 00	0 681E-04	22 5	0
A 65	3 230	28 60	61 40	0 0	0 0	16 90	0 683E-04	29 1	0
A 66	3 230	354 10	80 10	0 0	0 0	16 90	0 250E-03	29 0	0
A 67	3 300	308 10	78 60	0 0	0 0	6 10	0 517E-03	10 7	0
A 68	3 300	54 70	60 70	0 0	0 0	14 50	0 428E-03	25 0	0
A 69	3 390	100 00	74 90	0 0	0 0	9 40	0 283E-03	16 3	0
A 70	3 390	48 10	77 40	0 0	0 0	15 80	0 491E-03	27 2	0
A 71	3 500	14 00	75 80	0 0	0 0	26 70	0 159E-03	44 9	0
A 72	3 500	38 70	69 10	0 0	0 0	13 80	0 217E-03	23 8	0
A 73	3 600	57 20	67 00	0 0	0 0	11 90	0 348E-03	20 6	0
A 74	3 600	63 10	74 20	0 0	0 0	9 30	0 278E-03	16 1	0
A 75	3 700	89 40	49 10	0 0	0 0	33 60	0 104E-03	55 3	0
A 76	3 700	20 50	71 80	0 0	0 0	8 50	0 853E-04	14 8	0
A 77	3 800	329 90	77 60	0 0	0 0	7 50	0 340E-04	13 1	0
A 78	3 800	321 20	50 80	0 0	0 0	14 60	0 828E-04	25 2	0
A 79	3 900	359 60	75 70	0 0	0 0	7 80	0 778E-04	13 6	0
A 80	3 900	9 50	56 00	0 0	0 0	12 90	0 572E-04	22 4	0
A 81	4 000	12 60	68 20	0 0	0 0	5 50	0 555E-04	9 6	0
A 82	4 000	58 40	48 60	0 0	0 0	14 70	0 214E-03	25 3	0
A 83	4 100	351 10	64 50	0 0	0 0	7 50	0 414E-04	13 1	0
A 83	4 100	346 40	60 00	0 0	0 0	8 90	0 286E-04	15 4	10
A 84	4 100	345 90	73 20	0 0	0 0	4 30	0 948E-04	7 4	0
A 84	4 100	333 60	70 60	0 0	0 0	3 90	0 469E-04	6 8	10
A 85	4 200	319 50	77 60	0 0	0 0	4 00	0 135E-03	6 9	0
A 85	4 200	309 90	73 90	0 0	0 0	3 90	0 915E-04	6 9	10
A 86	4 200	18 10	79 90	0 0	0 0	9 60	0 104E-03	16 6	0
A 86	4 200	1 80	78 00	0 0	0 0	9 80	0 631E-04	17 1	10
A 87	4 300	342 80	71 70	0 0	0 0	14 30	0 160E-04	24 7	0
A 88	4 300	303 70	73 70	0 0	0 0	12 70	0 133E-04	21 9	0
A 89	4 400	324 30	78 20	0 0	0 0	11 30	0 143E-04	19 6	0
A 90	4 400	1 70	70 40	0 0	0 0	9 90	0 120E-04	17 2	0
A 91	4 500	355 40	64 70	0 0	0 0	11 70	0 129E-04	20 3	0
A 92	4 500	334 60	75 90	0 0	0 0	12 90	0 101E-04	22 3	0
A 93	4 650	245 90	79 90	0 0	0 0	20 40	0 534E-05	34 9	0
A 94	4 650	80 40	79 30	0 0	0 0	25 30	0 438E-05	42 7	0
A 95	4 760	65 30	77 70	0 0	0 0	7 70	0 137E-04	13 4	0
A 96	4 750	56 80	75 90	0 0	0 0	15 20	0 109E-04	26 3	0
A 97	4 810	358 10	73 50	0 0	0 0	20 10	0 101E-04	34 3	0
A 98	4 810	1 60	70 30	0 0	0 0	5 50	0 171E-04	9 5	0
A 99	4 900	42 80	81 70	0 0	0 0	9 50	0 125E-04	16 6	0
A 99	4 900	20 90	76 40	0 0	0 0	9 50	0 762E-05	16 5	10
A100	4 900	30 80	78 10	0 0	0 0	4 30	0 128E-04	7 5	0
A100	4 900	17 10	77 20	0 0	0 0	3 50	0 972E-05	6 1	10
A101	5 000	319 60	79 70	0 0	0 0	9 60	0 120E-04	16 6	0
A101	5 000	294 70	79 20	0 0	0 0	9 40	0 806E-05	16 4	10
A102	5 000	26 50	66 00	0 0	0 0	5 70	0 124E-04	9 9	0
A102	5 000	22 30	66 20	0 0	0 0	7 30	0 851E-05	12 8	10
A103	5 130	33 70	79 10	0 0	0 0	5 70	0 170E-04	10 0	0
A103	5 130	12 40	75 80	0 0	0 0	4 40	0 112E-04	7 7	10
A104	5 130	5 80	77 80	0 0	0 0	7 00	0 170E-04	12 3	0
A104	5 130	342 10	73 70	0 0	0 0	5 20	0 106E-04	9 0	10
A105	5 220	9 90	75 70	0 0	0 0	6 10	0 165E-04	10 7	0
A105	5 220	355 20	73 00	0 0	0 0	8 60	0 117E-04	14 9	10
A106	5 220	18 60	73 90	0 0	0 0	6 10	0 164E-04	10 7	0
A106	5 220	6 10	69 30	0 0	0 0	4 90	0 113E-04	8 5	10
A107	5 350	20 30	73 30	0 0	0 0	7 60	0 188E-04	13 2	0
A108	5 350	9 50	70 50	0 0	0 0	8 40	0 208E-04	14 6	0
A109	5 650	56 50	76 10	0 0	0 0	6 50	0 157E-04	11 2	0
A109	5 650	53 50	73 70	0 0	0 0	7 80	0 106E-04	13 7	10
A110	5 650	10 80	76 40	0 0	0 0	5 60	0 180E-04	9 7	0

A110	5 650	4 90	70 20	0 0	0 0	8 10	0 123E-04	14 0	10
A111	5 750	52 90	75 60	0 0	0 0	8 20	0 157E-04	14 3	0
A112	5 750	23 30	79 10	0 0	0 0	18 00	0 116E-04	31 0	0
A113	5 850	50 30	79 70	0 0	0 0	7 20	0 103E-04	12 6	0
A114	5 840	65 30	84 60	0 0	0 0	10 20	0 124E-04	17 7	0
A115	5 950	52 50	76 90	0 0	0 0	9 30	0 109E-04	16 2	0
A116	5 940	62 70	75 60	0 0	0 0	11 40	0 131E-04	18 8	0
A117	6 060	41 60	77 20	0 0	0 0	15 20	0 114E-04	26 2	0
A118	6 050	56 20	77 70	0 0	0 0	7 80	0 133E-04	13 5	0
A119	6 150	306 70	64 90	0 0	0 0	11 80	0 306E-04	20 6	0
A120	6 150	20 20	69 90	0 0	0 0	10 00	0 195E-04	17 4	0
A121	6 240	308 30	82 60	0 0	0 0	6 60	0 326E-04	11 5	0
A122	6 240	350 20	82 30	0 0	0 0	22 60	0 293E-04	38 5	0
A123	6 310	325 30	72 30	0 0	0 0	6 00	0 583E-04	10 4	0
A123	6 310	320 70	70 10	0 0	0 0	2 90	0 429E-04	5 0	10
A124	6 310	342 00	54 20	0 0	0 0	5 30	0 609E-04	9 3	0
A124	6 310	339 90	51 90	0 0	0 0	3 80	0 447E-04	6 6	10
A125	6 400	358 10	71 10	0 0	0 0	7 60	0 355E-04	13 2	0
A125	6 400	349 20	71 80	0 0	0 0	6 00	0 275E-04	10 4	10
A126	6 400	10 00	69 10	0 0	0 0	4 60	0 413E-04	8 0	0
A126	6 400	9 00	67 50	0 0	0 0	4 20	0 304E-04	7 3	10
A127	6 500	322 80	75 70	0 0	0 0	7 70	0 182E-04	13 5	0
A127	6 500	356 80	79 50	0 0	0 0	7 60	0 124E-04	13 2	10
A128	6 500	302 50	69 30	0 0	0 0	5 70	0 421E-04	9 9	0
A128	6 500	293 50	69 50	0 0	0 0	8 40	0 308E-04	14 6	10
A129	6 600	329 90	74 80	0 0	0 0	5 60	0 490E-04	9 8	0
A129	6 600	343 70	76 00	0 0	0 0	4 80	0 355E-04	8 4	10
A130	6 600	322 80	79 60	0 0	0 0	2 80	0 416E-04	4 8	0
A130	6 600	312 80	79 00	0 0	0 0	3 30	0 288E-04	5 7	10
A131	6 700	321 60	57 70	0 0	0 0	8 20	0 315E-04	14 2	0
A131	6 700	320 60	54 30	0 0	0 0	6 90	0 237E-04	12 0	10
A132	6 700	306 60	58 20	0 0	0 0	8 30	0 614E-04	14 5	0
A132	6 700	302 30	59 00	0 0	0 0	4 80	0 481E-04	8 3	10
A133	6 800	343 90	79 40	0 0	0 0	5 60	0 400E-04	9 8	0
A133	6 800	325 30	82 00	0 0	0 0	4 30	0 295E-04	7 4	10
A134	6 800	249 20	82 90	0 0	0 0	6 20	0 429E-04	10 9	0
A134	6 800	217 30	83 50	0 0	0 0	6 50	0 313E-04	11 3	10
A135	6 900	321 70	59 80	0 0	0 0	3 70	0 343E-04	6 4	0
A135	6 900	315 90	57 20	0 0	0 0	5 80	0 243E-04	10 2	10
A136	6 900	346 30	72 00	0 0	0 0	4 60	0 309E-04	8 1	0
A136	6 900	336 60	70 50	0 0	0 0	6 50	0 207E-04	11 2	10
A137	7 110	310 80	65 00	0 0	0 0	19 80	0 377E-05	33 8	0
A138	7 110	317 80	74 70	0 0	0 0	20 30	0 466E-05	34 7	0
A139	7 250	342 10	82 20	0 0	0 0	8 00	0 121E-04	13 9	0
A139	7 250	311 90	79 10	0 0	0 0	10 60	0 827E-05	18 5	10
A140	7 250	333 80	79 90	0 0	0 0	10 30	0 216E-04	17 9	0
A140	7 250	330 80	71 20	0 0	0 0	7 30	0 145E-04	12 8	10
A141	7 340	33 00	79 50	0 0	0 0	6 10	0 776E-05	10 6	0
A142	7 330	109 80	84 10	0 0	0 0	8 60	0 632E-05	15 0	0
A143	7 520	358 50	74 00	0 0	0 0	4 70	0 352E-04	8 2	0
A143	7 520	348 80	72 50	0 0	0 0	5 40	0 271E-04	9 3	10
A144	7 520	345 80	70 00	0 0	0 0	5 40	0 291E-04	9 5	0
A144	7 520	342 30	66 90	0 0	0 0	5 40	0 228E-04	9 4	10
A145	7 760	358 80	62 30	0 0	0 0	4 60	0 240E-04	8 0	0
A145	7 760	356 00	59 70	0 0	0 0	4 20	0 192E-04	7 4	10
A146	7 760	342 10	71 20	0 0	0 0	7 90	0 162E-04	13 7	0
A146	7 760	334 00	67 00	0 0	0 0	6 30	0 111E-04	10 9	10
A147	7 840	359 40	70 30	0 0	0 0	6 50	0 239E-04	11 3	0
A147	7 840	353 60	65 40	0 0	0 0	7 30	0 167E-04	12 7	10
A148	7 840	335 60	61 70	0 0	0 0	10 00	0 227E-04	17 4	0
A148	7 840	326 50	57 10	0 0	0 0	6 40	0 176E-04	11 1	10
A149	7 940	28 50	75 90	0 0	0 0	7 00	0 682E-05	12 1	0
A149	7 940	23 50	78 80	0 0	0 0	10 30	0 403E-05	17 8	10
A150	7 940	10 30	73 40	0 0	0 0	10 30	0 607E-05	17 9	0
A150	7 940	357 40	67 40	0 0	0 0	11 50	0 430E-05	19 9	10
A151	8 200	233 50	55 20	0 0	0 0	47 70	0 611E-05	74 0	0
A152	8 200	342 50	83 60	0 0	0 0	7 80	0 534E-05	13 5	0
A153	8 310	336 80	66 70	0 0	0 0	9 20	0 937E-05	15 9	0
A153	8 310	331 60	58 30	0 0	0 0	10 60	0 672E-05	18 5	10

A154	8 310	353 40	71 00	0 0	0 0	7 20	0 989E-05	12 5	0
A154	8 310	338 20	66 10	0 0	0 0	6 30	0 672E-05	11 0	10
A155	8 400	347 50	66 00	0 0	0 0	4 30	0 174E-04	7 6	0
A155	8 400	334 60	63 20	0 0	0 0	6 60	0 110E-04	11 4	10
A156	8 400	342 90	62 00	0 0	0 0	4 00	0 190E-04	6 9	0
A156	8 400	336 10	60 20	0 0	0 0	8 60	0 116E-04	15 0	10
A157	8 500	31 70	73 50	0 0	0 0	10 60	0 848E-05	18 3	0
A157	8 500	6 00	77 60	0 0	0 0	8 50	0 538E-05	14 7	10
A158	8 500	14 90	81 00	0 0	0 0	4 40	0 825E-05	7 7	0
A158	8 500	340 80	77 70	0 0	0 0	4 70	0 550E-05	8 2	10
A159	8 610	27 40	75 60	0 0	0 0	6 20	0 862E-05	10 8	0
A159	8 610	1 70	69 70	0 0	0 0	6 10	0 535E-05	10 6	10
A160	8 610	37 10	80 50	0 0	0 0	6 40	0 798E-05	11 1	0
A160	8 610	4 50	74 20	0 0	0 0	7 80	0 520E-05	13 6	10
A161	8 710	339 00	66 50	0 0	0 0	5 30	0 981E-05	9 2	0
A161	8 710	337 00	69 90	0 0	0 0	8 00	0 678E-05	13 8	10
A162	8 710	358 30	73 20	0 0	0 0	8 50	0 830E-05	14 8	0
A162	8 710	356 70	73 00	0 0	0 0	10 40	0 538E-05	18 1	10
A163	8 820	352 60	64 80	0 0	0 0	8 40	0 180E-04	14 6	0
A163	8 820	339 10	66 70	0 0	0 0	7 40	0 112E-04	12 9	10
A164	8 820	356 60	69 90	0 0	0 0	5 30	0 144E-04	9 2	0
A164	8 820	348 00	64 00	0 0	0 0	7 40	0 916E-05	12 9	10
A165	8 930	2 50	64 30	0 0	0 0	6 20	0 375E-04	10 8	0
A165	8 930	358 20	61 50	0 0	0 0	6 80	0 292E-04	11 9	10
A166	8 920	6 60	70 20	0 0	0 0	4 90	0 336E-04	8 6	0
A166	8 920	4 20	68 30	0 0	0 0	4 10	0 237E-04	7 2	10
A167	9 020	24 80	72 70	0 0	0 0	6 60	0 152E-04	11 5	0
A167	9 020	12 50	70 00	0 0	0 0	6 70	0 897E-05	11 7	10
A168	9 020	9 30	72 50	0 0	0 0	7 00	0 119E-04	12 2	0
A168	9 020	354 10	66 00	0 0	0 0	9 80	0 727E-05	17 2	10
A169	9 120	5 10	62 70	0 0	0 0	15 70	0 112E-04	27 1	0
A169	9 120	353 80	55 90	0 0	0 0	7 80	0 841E-05	13 6	10
A170	9 120	8 20	64 10	0 0	0 0	10 00	0 108E-04	17 4	0
A170	9 120	358 90	56 20	0 0	0 0	10 80	0 671E-05	18 7	10
A171	9 240	10 90	71 00	0 0	0 0	5 60	0 182E-04	9 8	0
A171	9 240	6 60	67 60	0 0	0 0	7 50	0 134E-04	13 0	10
A172	9 240	354 00	69 50	0 0	0 0	8 30	0 230E-04	14 4	0
A172	9 240	354 70	65 90	0 0	0 0	6 90	0 167E-04	12 0	10
A173	9 360	348 70	65 30	0 0	0 0	13 50	0 880E-05	23 3	0
A173	9 360	357 40	65 60	0 0	0 0	10 50	0 646E-05	18 3	10
A174	9 360	1 70	66 20	0 0	0 0	10 20	0 110E-04	17 7	0
A174	9 360	353 60	58 60	0 0	0 0	10 80	0 765E-05	18 8	10
A175	9 450	3 20	64 80	0 0	0 0	8 20	0 138E-04	14 3	0
A175	9 450	351 10	62 90	0 0	0 0	6 60	0 959E-05	11 4	10
A176	9 450	350 80	43 60	0 0	0 0	11 70	0 182E-04	20 3	0
A176	9 450	350 10	40 00	0 0	0 0	10 80	0 146E-04	18 7	10
A177	9 550	347 40	26 90	0 0	0 0	5 90	0 116E-04	10 2	0
A177	9 550	347 50	16 20	0 0	0 0	5 80	0 899E-05	10 1	10
A178	9 550	347 50	47 60	0 0	0 0	9 00	0 118E-04	15 6	0
A178	9 550	346 00	40 10	0 0	0 0	4 10	0 773E-05	7 2	10
A179	9 600	350 30	42 10	0 0	0 0	16 90	0 237E-04	28 1	0
A179	9 600	347 30	49 00	0 0	0 0	2 90	0 165E-04	5 1	10
A180	9 600	345 70	52 70	0 0	0 0	18 40	0 200E-04	31 6	0
A180	9 600	342 10	41 00	0 0	0 0	10 10	0 148E-04	17 5	10
A181	9 700	323 70	47 20	0 0	0 0	7 10	0 360E-04	12 3	0
A181	9 700	323 00	41 40	0 0	0 0	6 30	0 292E-04	11 0	10
A182	9 700	357 80	35 70	0 0	0 0	5 30	0 213E-04	9 3	0
A182	9 700	354 00	30 60	0 0	0 0	4 40	0 154E-04	7 7	10
A183	9 800	353 00	52 10	0 0	0 0	7 20	0 175E-04	12 5	0
A183	9 800	333 90	48 90	0 0	0 0	2 00	0 123E-04	3 5	10
A184	9 800	348 80	57 40	0 0	0 0	3 60	0 188E-04	6 3	0
A184	9 800	336 80	49 90	0 0	0 0	3 70	0 125E-04	6 5	10
A185	9 900	358 30	55 20	0 0	0 0	6 60	0 205E-04	11 5	0
A185	9 900	357 30	50 60	0 0	0 0	6 30	0 139E-04	11 0	10
A186	9 900	344 10	54 00	0 0	0 0	4 80	0 201E-04	8 4	0
A186	9 900	341 60	47 60	0 0	0 0	4 00	0 143E-04	7 0	10
A187	10 000	358 00	72 40	0 0	0 0	10 70	0 741E-05	18 9	0
A187	10 000	325 30	54 70	0 0	0 0	16 20	0 333E-05	27 8	10
A188	10 000	353 70	69 00	0 0	0 0	7 00	0 750E-06	12 1	0

A188	10 000	336 80	59 00	0 0	0 0	11 30	0 449E-05	19 5	10
A189	10 130	335 30	53 50	0 0	0 0	28 50	0 146E-04	47 7	0
A189	10 130	331 50	44 40	0 0	0 0	36 80	0 936E-05	60 0	10
A190	10 130	323 70	53 60	0 0	0 0	17 50	0 246E-04	30 1	0
A190	10 130	318 00	49 40	0 0	0 0	20 30	0 174E-04	34 6	10
A191	10 210	5 30	72 30	0 0	0 0	18 00	0 588E-05	30 9	0
A191	10 210	356 00	66 30	0 0	0 0	23 90	0 339E-05	40 5	10
A192	10 210	36 10	76 30	0 0	0 0	11 80	0 637E-05	20 5	0
A192	10 210	97 20	78 90	0 0	0 0	26 70	0 359E-05	45 0	10
A193	10 300	319 20	72 50	0 0	0 0	17 70	0 622E-05	30 4	0
A193	10 300	308 20	75 80	0 0	0 0	43 30	0 315E-05	68 5	10
A194	10 300	258 90	68 50	0 0	0 0	9 50	0 649E-05	16 6	0
A194	10 300	285 30	58 30	0 0	0 0	25 00	0 285E-05	42 2	10
A195	10 400	37 80	77 00	0 0	0 0	13 10	0 629E-05	22 6	0
A195	10 400	39 70	74 50	0 0	0 0	33 20	0 229E-05	54 7	10
A196	10 400	92 30	79 80	0 0	0 0	9 60	0 824E-05	16 6	0
A197	10 500	59 50	73 90	0 0	0 0	11 90	0 907E-05	20 6	0
A198	10 500	99 50	84 50	0 0	0 0	5 70	0 108E-04	9 9	0
A199	10 580	356 80	64 10	0 0	0 0	10 30	0 245E-04	17 9	0
A199	10 580	340 30	56 90	0 0	0 0	6 80	0 146E-04	11 9	10
A200	10 580	343 40	56 90	0 0	0 0	7 50	0 284E-04	13 0	0
A200	10 580	335 10	48 50	0 0	0 0	8 30	0 155E-04	14 5	10
A201	10 700	355 80	51 40	0 0	0 0	9 80	0 199E-04	17 1	0
A201	10 700	340 30	38 50	0 0	0 0	10 00	0 153E-04	17 3	10
A202	10 700	344 50	45 70	0 0	0 0	7 00	0 236E-04	12 1	0
A202	10 700	334 30	32 00	0 0	0 0	10 90	0 182E-04	18 9	10
A203	10 800	352 20	60 40	0 0	0 0	8 40	0 303E-04	14 7	0
A203	10 800	352 20	59 30	0 0	0 0	5 00	0 238E-04	8 7	10
A204	10 800	333 30	57 10	0 0	0 0	5 60	0 414E-04	9 8	0
A204	10 800	328 10	53 00	0 0	0 0	9 00	0 289E-04	15 6	10
A205	10 900	8 80	65 70	0 0	0 0	2 70	0 298E-04	4 6	0
A205	"	347 70	61 40	0 0	0 0	4 50	0 243E-04	7 8	2
A205	"	351 30	59 90	0 0	0 0	4 20	0 233E-04	7 3	5
A205	10 900	348 30	59 00	0 0	0 0	3 70	0 189E-04	6 5	10
A205	"	350 80	59 70	0 0	0 0	5 20	0 156E-04	9 1	15
A205	"	344 50	58 20	0 0	0 0	4 00	0 136E-04	7 0	20
A205	"	338 30	59 10	0 0	0 0	6 70	0 104E-04	11 6	30
A205	"	358 70	54 40	0 0	0 0	9 60	0 826E-05	16 7	40
A205	"	356 50	46 80	0 0	0 0	9 10	0 723E-05	15 8	50
A206	10 900	24 20	69 70	0 0	0 0	4 00	0 246E-04	7 0	0
A206	"	350 30	69 90	0 0	0 0	3 90	0 188E-04	6 7	2
A206	"	349 50	68 60	0 0	0 0	4 10	0 177E-04	7 2	5
A206	10 900	343 80	64 20	0 0	0 0	5 40	0 149E-04	9 5	10
A206	"	335 40	66 00	0 0	0 0	6 20	0 105E-04	10 9	15
A206	"	341 80	67 70	0 0	0 0	9 80	0 935E-05	17 0	20
A206	"	359 90	67 90	0 0	0 0	11 30	0 659E-05	19 5	30
A206	"	353 30	64 20	0 0	0 0	10 90	0 660E-05	19 0	40
A206	"	20 90	66 50	0 0	0 0	14 00	0 406E-05	24 2	50
A207	11 000	349 30	71 50	0 0	0 0	6 00	0 200E-04	10 4	0
A207	11 000	331 70	70 80	0 0	0 0	7 70	0 135E-04	13 4	10
A208	11 000	13 20	72 30	0 0	0 0	7 30	0 170E-04	12 7	0
A208	11 000	355 20	73 90	0 0	0 0	6 40	0 108E-04	11 1	10
A209	11 100	358 70	68 50	0 0	0 0	6 30	0 185E-04	10 9	0
A209	11 100	1 20	65 00	0 0	0 0	5 80	0 132E-04	10 1	10
A210	11 100	348 80	80 40	0 0	0 0	4 50	0 186E-04	7 8	0
A210	11 100	340 30	73 80	0 0	0 0	5 50	0 125E-04	9 6	10
A211	11 250	352 70	76 30	0 0	0 0	4 40	0 187E-04	7 6	0
A211	11 250	337 40	66 00	0 0	0 0	14 00	0 879E-05	24 1	10
A212	11 250	24 30	77 40	0 0	0 0	14 10	0 178E-04	24 4	0
A212	11 250	30 00	81 00	0 0	0 0	15 40	0 103E-04	26 6	10
A213	11 320	357 70	57 60	0 0	0 0	4 40	0 262E-04	7 8	0
A213	11 320	353 00	52 70	0 0	0 0	7 10	0 168E-04	12 4	0
A214	11 320	2 00	55 70	0 0	0 0	6 10	0 291E-04	10 6	0
A214	11 320	351 10	50 50	0 0	0 0	6 80	0 195E-04	11 9	0
A215	11 400	36 60	76 40	0 0	0 0	7 90	0 193E-04	13 7	0
A216	11 400	49 90	84 60	0 0	0 0	8 00	0 189E-04	14 0	0
A217	11 520	335 20	59 40	0 0	0 0	9 00	0 329E-04	15 6	0
A217	11 520	329 20	51 50	0 0	0 0	10 60	0 219E-04	18 3	10
A218	11 520	335 70	61 20	0 0	0 0	9 40	0 348E-04	16 3	0
A218	11 520	329 60	51 90	0 0	0 0	10 90	0 222E-04	19 0	10
A219	11 620	0 90	56 70	0 0	0 0	6 20	0 251E-04	10 8	0
A219	11 620	349 50	44 40	0 0	0 0	6 00	0 201E-04	10 4	10
A220	11 620	346 70	57 00	0 0	0 0	7 40	0 314E-04	12 8	0
A220	11 620	338 90	53 50	0 0	0 0	8 50	0 242E-04	14 9	10
A221	11 710	335 10	65 90	0 0	0 0	6 10	0 372E-04	10 6	0
A221	11 710	336 50	53 70	0 0	0 0	3 80	0 266E-04	6 6	10
A222	11 710	336 20	65 10	0 0	0 0	6 60	0 381E-04	11 6	0
A222	11 710	334 30	57 70	0 0	0 0	8 00	0 269E-04	13 9	10
A223	11 820	349 90	70 30	0 0	0 0	6 30	0 261E-04	11 0	0
A223	11 820	341 70	65 50	0 0	0 0	9 90	0 179E-04	17 1	10
A224	11 820	359 60	74 90	0 0	0 0	11 20	0 264E-04	19 4	0
A224	11 820	353 10	64 40	0 0	0 0	8 10	0 185E-04	14 0	10
A225	11 900	329 30	66 40	0 0	0 0	8 80	0 400E-04	15 3	0
A225	11 900	320 60	58 80	0 0	0 0	5 80	0 281E-04	10 2	10
A226	11 900	330 10	64 90	0 0	0 0	8 00	0 424E-04	13 8	0
A226	11 900	327 70	55 60	0 0	0 0	8 30	0 315E-04	14 4	10
A227	12 000	359 70	70 10	0 0	0 0	6 00	0 511E-04	10 4	0
A227	12 000	348 40	63 40	0 0	0 0	3 60	0 354E-04	6 2	10
A228	12 000	337 00	63 90	0 0	0 0	5 70	0 492E-04	9 8	0
A228	12 000	329 50	60 30	0 0	0 0	4 60	0 373E-04	8 0	10
A229	12 150	35 60	70 90	0 0	0 0	2 40	0 551E-04	4 2	0
A229	12 150	24 90	66 60	0 0	0 0	5 10	0 394E-04	8 9	10
A230	12 150	20 60	67 80	0 0	0 0	8 20	0 480E-04	14 2	0
A230	12 150	14 70	63 70	0 0	0 0	8 10	0 329E-04	14 1	10
A231	12 920	26 00	73 20	0 0	0 0	6 60	0 810E-04	11 4	0
A231	12 920	22 20	70 40	0 0	0 0	6 50	0 446E-04	11 3	10
A232	12 920	67 30	76 60	0 0	0 0	3 30	0 851E-04	5 8	0
A232	12 920	50 40	74 20	0 0	0 0	5 00	0 468E-04	8 8	10
A233	13 060	76 70	73 40	0 0	0 0	4 90	0 719E-04	8 5	0
A233	13 060	55 00	71 70	0 0	0 0	4 60	0 455E-04	8 0	10
A234	13 080	47 70	77 70	0 0	0 0	5 90	0 678E-04	10 2	0
A234	13 080	45 40	71 60	0 0	0 0	5 40	0 473E-04	9 3	10
A235	13 260	225 40	86 10	0 0	0 0	4 50	0 603E-04	7 8	0
A235	13 260	258 20	81 60	0 0	0 0	4 00	0 392E-04	6 8	10
A236	13 270	339 60	76 90	0 0	0 0	6 60	0 595E-04	11 5	0
A236	13 270	340 80	74 60	0 0	0 0	2 90	0 405E-04	5 1	10
A237	13 350	358 80	82 40	0 0	0 0	3 40	0 826E-04	6 0	0
A237	13 350	341 80	81 70	0 0	0 0	4 20	0 613E-04	7 3	10
A238	13 350	349 30	84 50	0 0	0 0	4 60	0 738E-04	8 0	0
A238	13 350	324 00	83 80	0 0	0 0	4 90	0 528E-04	8 5	10
A239	13 470	358 10	80 20	0 0	0 0	6 50	0 630E-04	11 3	0
A239	13 470	353 40	80 80	0 0	0 0	4 80	0 389E-04	8 4	10
A240	13 470	354 00	81 30	0 0	0 0	2 70	0 634E-04	4 6	0
A240	13 470	311 20	77 10	0 0	0 0	4 90	0 410E-04	8 6	10
A241	13 570	44 20	87 80	0 0	0 0	6 90	0 657E-04	12 1	0
A241	13 570	349 80	81 80	0 0	0 0	5 20	0 471E-04	9 0	10
A242	13 570	346 60	84 20	0 0	0 0	5 00	0 574E-04	8 8	0
A242	13 570	321 80	83 00	0 0	0 0	5 30	0 395E-04	9 3	10
A243	13 710	356 20	82 60	0 0	0 0	5 10	0 734E-04	8 8	0
A243	13 710	338 60	78 90	0 0	0 0	4 80	0 479E-04	8 3	10
A244	13 700	352 40	79 60	0 0	0 0	7 60	0 756E-04	13 2	0
A244	13 700	340 00	78 20	0 0	0 0	4 40	0 520E-04	7 5	10
A245	13 830	42 60	82 00	0 0	0 0	5 40	0 668E-04	9 4	0
A245	13 830	32 10	83 00	0 0	0 0	4 00	0 451E-04	6 9	10
A246	13 830	31 70	82 70	0 0	0 0	6 20	0 821E-04	10 8	0
A246	13 830	8 80	81 00	0 0	0 0	4 30	0 574E-04	7 6	10
A247	13 960	29 90	76 30	0 0	0 0	7 10	0 693E-04	12 4	0
A247	13 960	46 20	76 50	0 0	0 0	5 60	0 475E-04	9 8	10
A248	13 960	39 10	88 80	0 0	0 0	11 60	0 800E-04	20 1	0
A248	13 960	323 00	86 90	0 0	0 0	4 90	0 564E-04	8 5	10
A249	14 080	20 70	78 20	0 0	0 0	9 90	0 946E-04	17 3	0
A249	14 080	25 30	76 40	0 0	0 0	4 60	0 737E-04	8 1	10
A250	14 080	7 60	79 80	0 0	0 0	5 00	0 103E-03	8 7	0
A250	14 080	355 10	78 20	0 0	0 0	3 90	0 750E-04	6 8	10
A251	14 190	8 90	79 50	0 0	0 0	3 60	0 753E-04	6 3	0
A251	14 190	350 10	79 90	0 0	0 0	5 50	0 514E-04	9 8	10
A252	14 190	352 40	81 70	0 0	0 0	5 40	0 763E-04	9 4	0
A252	14 190	336 00	80 70	0 0	0 0	2 90	0 562E-04	5 1	10

A253	14	200	54	70	78	30	0.0	0.0	3.10	0.112E-03	5.5	0
A253	14	200	31	90	77	90	0.0	0.0	2.80	0.790E-04	4.8	10
A254	14	200	50	20	78	00	0.0	0.0	3.50	0.101E-03	6.1	0
A254	14	200	23	40	78	60	0.0	0.0	4.90	0.683E-04	7.8	10
A255	14	280	19	90	76	80	0.0	0.0	4.00	0.107E-03	6.9	0
A255	14	280	3	60	76	90	0.0	0.0	3.00	0.775E-04	5.2	10
A256	14	280	38	70	80	30	0.0	0.0	4.80	0.116E-03	8.5	0
A256	14	280	17	80	79	50	0.0	0.0	3.50	0.808E-04	6.2	10
A257	14	370	18	10	75	00	0.0	0.0	4.40	0.850E-04	7.6	0
A257	14	370	16	60	75	40	0.0	0.0	4.60	0.565E-04	8.1	10
A258	14	370	51	50	76	90	0.0	0.0	3.70	0.899E-04	6.5	0
A258	14	370	30	30	77	20	0.0	0.0	4.10	0.587E-04	7.1	10
A259	14	460	29	40	71	50	0.0	0.0	4.70	0.932E-04	8.2	0
A259	14	460	24	60	72	30	0.0	0.0	3.10	0.618E-04	5.4	10
A260	14	460	33	30	70	40	0.0	0.0	4.40	0.950E-04	7.7	0
A260	14	460	34	70	70	40	0.0	0.0	5.20	0.634E-04	9.1	10
A261	14	560	34	60	68	50	0.0	0.0	5.10	0.993E-04	8.8	0
A261	14	560	30	30	68	40	0.0	0.0	4.90	0.699E-04	8.6	10
A262	14	560	33	90	71	20	0.0	0.0	6.10	0.104E-03	10.7	0
A262	14	560	25	90	70	50	0.0	0.0	6.00	0.748E-04	10.4	10
A263	14	710	24	40	73	40	0.0	0.0	6.50	0.136E-03	11.3	0
A263	14	710	25	30	75	30	0.0	0.0	6.40	0.872E-04	11.2	10
A264	14	710	28	60	77	00	0.0	0.0	7.10	0.120E-03	12.3	0
A264	14	710	14	90	77	80	0.0	0.0	5.00	0.885E-04	8.7	10
A265	14	820	7	60	74	40	0.0	0.0	4.30	0.105E-03	7.5	0
A265	14	820	0	10	73	30	0.0	0.0	4.30	0.771E-04	7.5	10
A266	14	820	1	00	77	60	0.0	0.0	3.00	0.110E-03	5.3	0
A266	14	820	341	20	77	20	0.0	0.0	3.30	0.830E-04	5.7	10
A267	15	880	343	20	75	70	0.0	0.0	5.80	0.927E-04	10.1	0
A267	15	880	333	00	76	10	0.0	0.0	5.10	0.647E-04	8.9	10
A268	15	880	311	60	84	40	0.0	0.0	3.70	0.909E-04	6.5	0
A268	15	880	305	90	80	50	0.0	0.0	3.90	0.633E-04	6.9	10
A269	16	000	4	00	84	50	0.0	0.0	3.80	0.610E-04	6.7	0
A269	16	000	352	70	86	90	0.0	0.0	3.70	0.469E-04	6.5	10
A270	16	000	303	60	86	10	0.0	0.0	3.50	0.938E-04	6.2	0
A270	16	000	291	90	85	50	0.0	0.0	3.00	0.685E-04	5.2	10
A271	16	270	212	60	84	20	0.0	0.0	5.50	0.922E-04	9.6	0
A271	16	270	224	50	82	30	0.0	0.0	5.90	0.686E-04	10.3	10
A272	16	270	86	70	86	20	0.0	0.0	5.40	0.891E-04	9.3	0
A272	16	270	328	20	83	60	0.0	0.0	6.20	0.652E-04	10.9	10
A273	16	710	18	10	68	20	0.0	0.0	4.70	0.964E-04	8.2	0
A273	16	710	15	40	67	50	0.0	0.0	4.00	0.595E-04	6.9	10
A274	16	710	13	50	64	80	0.0	0.0	6.10	0.888E-04	10.6	0
A274	16	710	10	60	62	90	0.0	0.0	5.20	0.617E-04	9.1	10
A275	16	820	11	40	71	60	0.0	0.0	5.50	0.899E-04	9.6	0
A275	16	820	9	50	70	60	0.0	0.0	3.10	0.566E-04	5.5	10
A276	16	820	356	90	67	00	0.0	0.0	4.50	0.148E-03	7.8	0
A276	16	820	355	00	66	50	0.0	0.0	3.80	0.105E-03	6.7	10
A277	16	920	7	30	76	30	0.0	0.0	3.30	0.108E-03	5.7	0
A277	"		4	50	77	90	0.0	0.0	5.00	0.861E-04	10.5	2
A277	"		8	10	76	50	0.0	0.0	5.60	0.841E-04	9.7	5
A277	16	920	4	50	75	80	0.0	0.0	6.70	0.711E-04	11.6	10
A277	"		4	70	78	00	0.0	0.0	5.90	0.634E-04	10.3	15
A277	"		359	70	75	30	0.0	0.0	6.20	0.526E-04	10.7	20
A277	"		5	80	75	50	0.0	0.0	6.00	0.378E-04	10.5	30
A277	"		5	30	71	40	0.0	0.0	7.40	0.256E-04	12.9	40
A277	"		305	60	79	50	0.0	0.0	8.80	0.207E-04	15.3	50
A278	16	920	10	30	73	00	0.0	0.0	1.90	0.863E-04	3.3	0
A278	"		12	40	75	80	0.0	0.0	2.90	0.741E-04	5.1	2
A278	"		7	70	75	50	0.0	0.0	1.90	0.711E-04	3.2	5
A278	16	920	5	00	77	00	0.0	0.0	3.80	0.653E-04	6.7	10
A278	"		8	90	75	80	0.0	0.0	2.90	0.523E-04	5.1	15
A278	"		6	70	76	20	0.0	0.0	3.80	0.458E-04	6.6	20
A278	"		5	90	76	00	0.0	0.0	4.40	0.351E-04	7.6	30
A278	"		16	60	76	50	0.0	0.0	7.20	0.219E-04	12.6	40
A278	"		42	90	42	90	0.0	0.0	10.80	0.131E-04	18.9	50
A279	16	980	35	80	78	00	0.0	0.0	5.40	0.131E-03	9.4	0

A279	16	980	22	40	78	50	0.0	0.0	6.40	0.718E-04	11.1	10
A280	16	980	36	60	75	50	0.0	0.0	6.20	0.116E-03	10.8	0
A280	16	980	18	90	75	50	0.0	0.0	3.70	0.721E-04	6.5	10
A281	17	100	36	10	79	60	0.0	0.0	3.40	0.775E-04	6.0	0
A281	17	100	13	80	77	70	0.0	0.0	3.40	0.532E-04	6.0	10
A282	17	100	3	10	75	10	0.0	0.0	7.70	0.894E-04	13.3	0
A282	17	100	355	10	72	50	0.0	0.0	7.20	0.641E-04	12.5	10
A283	17	200	357	70	75	40	0.0	0.0	4.80	0.169E-03	8.3	0
A283	17	200	350	90	73	80	0.0	0.0	5.60	0.115E-03	9.7	10
A284	17	200	26	10	73	90	0.0	0.0	1.70	0.143E-03	3.0	0
A284	17	200	16	80	71	90	0.0	0.0	2.50	0.970E-04	4.3	10
A285	17	300	334	70	63	40	0.0	0.0	3.00	0.194E-03	5.3	0
A285	17	300	332	00	59	90	0.0	0.0	2.70	0.141E-03	4.7	10
A286	17	300	359	40	68	20	0.0	0.0	2.30	0.180E-03	4.0	0
A286	17	300	355	70	62	30	0.0	0.0	5.40	0.122E-03	9.4	10
A287	17	400	22	20	79	20	0.0	0.0	1.20	0.235E-03	2.1	0
A287	17	400	359	00	78	80	0.0	0.0	2.10	0.144E-03	3.7	10
A288	17	400	48	30	82	60	0.0	0.0	2.10	0.129E-03	3.6	0
A288	17	400	25	00	85	00	0.0	0.0	2.30	0.860E-04	4.1	10
A289	17	500	27	30	82	10	0.0	0.0	2.40	0.235E-03	4.3	0
A289	17	500	357	70	81	40	0.0	0.0	2.20	0.158E-03	3.8	10
A290	17	500	74	50	83	20	0.0	0.0	2.10	0.288E-03	3.7	0
A290	17	500	76	90	86	00	0.0	0.0	1.90	0.186E-03	3.2	10
A291	17	610	28	30	81	10	0.0	0.0	2.20	0.359E-03	3.8	0
A291	17	610	358	30	80	90	0.0	0.0	2.60	0.235E-03	4.6	10
A292	17	610	7	20	82	50	0.0	0.0	1.70	0.359E-03	3.1	0
A292	17	610	345	00	82	60	0.0	0.0	3.10	0.229E-03	5.3	10
A293	17	700	28	20	83	40	0.0	0.0	1.90	0.299E-03	3.4	0
A293	"		8	40	83	40	0.0	0.0	1.80	0.255E-03	3.3	2
A293	"		8	00	83	50	0.0	0.0	2.00	0.248E-03	3.5	5
A293	17	700	4	60	83	50	0.0	0.0	1.70	0.223E-03	2.9	10
A293	"		8	70	83	10	0.0	0.0	1.80	0.177E-03	3.4	15
A293	"		1	30	83	50	0.0	0.0	2.30	0.150E-03	4.0	20
A293	"		5	50	84	20	0.0	0.0	4.30	0.884E-04	7.4	30
A293	"		11	20	86	60	0.0	0.0	4.10	0.657E-04	7.1	40
A293	"		333	60	86	40	0.0	0.0	12.00	0.481E-04	20.7	90
A294	17	700	16	30	78	90	0.0	0.0	2.80	0.388E-03	4.8	0
A294	"		9	00	79	30	0.0	0.0	2.70	0.321E-03	4.7	2
A294	"		7	70	78	70	0.0	0.0	2.80	0.213E-03	5.1	5
A294	17	700	6	90	79	00	0.0	0.0	3.00	0.195E-03	5.2	10
A294	"		8	00	79	10	0.0	0.0	2.60	0.158E-03	4.5	15
A294	"		6	90	79	20	0.0	0.0	3.70	0.128E-03	6.4	20
A294	"		4	70	77	00	0.0	0.0	3.50	0.800E-04	6.2	30
A294	"		8	20	77	20	0.0	0.0	3.50	0.542E-04	6.2	40
A294	"		24	30	79	10	0.0	0.0	3.40	0.361E-04	6.0	50
A295	17	800	121	10	82	20	0.0	0.0	2.40	0.243E-03	4.2	0
A295	17	800	147	60	84	50	0.0	0.0	2.50	0.172E-03	4.3	10
A296	17	800	60	10	82	20	0.0	0.0	2.70	0.260E-03	4.7	0
A296	17	800	334	80	86	80	0.0	0.0	2.70	0.174E-03	4.6	10
A297	17	900	136	10	77	00	0.0	0.0	1.70	0.266E-03	2.9	0
A297	"		152	30	75	40	0.0	0.0	2.00	0.224E-03	3.6	2
A297	"		153	00	75	40	0.0	0.0	1.70	0.219E-03	2.8	5
A297	17	900	153	80	74	80	0.0	0.0	2.10	0.195E-03	3.7	10
A297	"		155	00	75	30	0.0	0.0	1.90	0.163E-03	3.4	15
A297	"		151	40	73	30	0.0	0.0	2.80	0.130E-03	4.9	20
A297	"		154	80	73	60	0.0	0.0	6.40	0.878E-04	11.1	30
A297	"		157	40	73	60	0.0	0.0	5.00	0.572E-04	8.8	40
A297	"		161	00	72	40	0.0	0.0	3.80	0.351E-04	6.6	50
A298	17	900	122	50	78	20	0.0	0.0	1.90	0.242E-03	3.3	0
A298	"		141	30	76	10	0.0	0.0	3.30	0.208E-03	5.7	2
A298	"		141	70	75	80	0.0	0.0	3.90	0.196E-03	6.7	5
A298	17	900	144	30	75	90	0.0	0.0	3.10	0.179E-03	5.4	10
A298	"		144	20	74	80	0.0	0.0	4.30	0.145E-03	7.5	15
A298	"		142	50	74	00	0.0	0.0	6.00	0.122E-03	10.5	20
A298	"		147	20	76	10	0.0	0.0	5.40	0.818E-04	9.4	30
A298	"		149	70	73	70	0.0	0.0	3.80	0.484E-04	6.7	40
A298	"		148	80	72	00	0.0	0.0	4.90	0.487E-04	8.5	50

A299	18.000	101.10	77.70	0.0	0.0	1.70	0.282E-03	3.0	0
A299	18.000	116.00	75.70	0.0	0.0	2.60	0.192E-03	4.6	10
A300	18.000	95.40	78.30	0.0	0.0	2.50	0.270E-03	4.3	0
A300	18.000	112.60	78.30	0.0	0.0	3.30	0.194E-03	5.8	10
A301	18.100	118.50	82.50	0.0	0.0	2.90	0.276E-03	5.1	0
A301	18.100	144.10	80.60	0.0	0.0	4.00	0.178E-03	7.0	10
A302	18.100	113.30	79.40	0.0	0.0	4.10	0.291E-03	7.2	0
A302	18.100	125.00	79.50	0.0	0.0	5.80	0.202E-03	10.0	10
A303	18.200	112.60	67.20	0.0	0.0	3.50	0.234E-03	6.1	0
A303	18.200	119.30	66.00	0.0	0.0	9.30	0.139E-03	16.1	10
A304	18.200	103.90	75.60	0.0	0.0	2.50	0.192E-03	4.4	0
A304	18.200	120.30	77.30	0.0	0.0	3.70	0.125E-03	6.5	10
A305	18.300	48.30	80.60	0.0	0.0	4.30	0.139E-03	7.4	0
A305	18.300	51.60	83.10	0.0	0.0	4.50	0.885E-04	7.8	10
A306	18.300	23.70	85.60	0.0	0.0	3.90	0.118E-03	6.7	0
A306	18.300	46.10	86.30	0.0	0.0	3.60	0.714E-04	6.3	10
A307	18.400	14.60	75.20	0.0	0.0	4.30	0.109E-03	7.6	0
A307	18.400	17.70	77.10	0.0	0.0	5.50	0.699E-04	9.6	10
A308	18.400	59.60	80.90	0.0	0.0	9.40	0.129E-03	16.3	0
A308	18.400	72.80	78.90	0.0	0.0	6.00	0.728E-04	10.4	10
A309	18.500	56.50	71.60	0.0	0.0	2.60	0.758E-04	4.5	0
A309	"	57.70	73.50	0.0	0.0	2.60	0.552E-04	4.6	2
A309	"	56.70	73.70	0.0	0.0	2.20	0.533E-04	3.9	5
A309	18.500	57.60	74.40	0.0	0.0	2.70	0.461E-04	4.7	10
A309	"	65.80	74.30	0.0	0.0	3.70	0.356E-04	6.5	15
A309	"	59.00	72.90	0.0	0.0	3.00	0.283E-04	5.3	20
A309	"	52.20	71.40	0.0	0.0	2.80	0.219E-04	4.9	30
A309	"	53.30	74.40	0.0	0.0	7.70	0.163E-04	13.4	40
A309	"	85.90	66.10	0.0	0.0	8.10	0.154E-04	14.1	50
A310	18.500	59.70	73.80	0.0	0.0	2.30	0.542E-04	4.1	0
A310	"	49.40	78.60	0.0	0.0	4.80	0.434E-04	8.3	2
A310	"	54.10	77.70	0.0	0.0	4.80	0.419E-04	8.3	5
A310	18.500	46.60	79.50	0.0	0.0	4.50	0.361E-04	7.9	10
A310	"	38.80	79.60	0.0	0.0	5.70	0.300E-04	10.0	15
A310	"	999.00	99.00	0.0	0.0	0.0	0.0	0.0	20
A310	"	61.20	75.60	0.0	0.0	4.80	0.187E-04	8.4	30
A310	"	46.70	77.50	0.0	0.0	4.80	0.151E-04	8.4	40
A310	"	84.50	74.30	0.0	0.0	7.50	0.146E-04	13.0	50
A311	18.600	24.30	71.30	0.0	0.0	4.00	0.758E-04	7.0	0
A311	18.600	20.00	69.80	0.0	0.0	3.80	0.423E-04	6.6	10
A312	18.600	37.90	71.90	0.0	0.0	3.30	0.630E-04	5.7	0
A312	18.600	40.30	74.40	0.0	0.0	7.40	0.324E-04	12.9	10
A313	18.700	6.40	79.20	0.0	0.0	6.80	0.966E-04	11.8	0
A313	18.700	2.80	76.10	0.0	0.0	5.00	0.548E-04	8.7	10
A314	18.700	55.70	78.80	0.0	0.0	9.30	0.602E-04	16.1	0
A314	18.700	56.90	83.00	0.0	0.0	4.60	0.389E-04	8.0	10
A315	18.800	33.80	78.70	0.0	0.0	6.70	0.944E-04	11.7	0
A315	18.800	14.90	83.70	0.0	0.0	5.90	0.563E-04	10.3	10
A316	18.800	83.40	81.70	0.0	0.0	13.30	0.913E-04	23.0	0
A316	18.800	7.10	87.20	0.0	0.0	4.60	0.569E-04	8.1	10
A317	18.900	173.40	87.40	0.0	0.0	5.10	0.117E-03	8.9	0
A317	18.900	275.20	86.50	0.0	0.0	5.00	0.854E-04	8.7	10
A318	18.900	3.00	84.10	0.0	0.0	4.70	0.591E-04	8.3	0
A318	18.900	347.10	81.60	0.0	0.0	6.40	0.447E-04	11.1	10
B 1	0.0	15.80	70.10	0.0	0.0	8.70	0.160E-04	15.2	0
B 2	0.0	38.70	71.30	0.0	0.0	7.60	0.182E-04	13.2	0
B 3	0.160	39.90	72.30	0.0	0.0	6.80	0.155E-04	11.8	0
B 4	0.160	30.80	68.30	0.0	0.0	8.60	0.140E-04	15.0	0
B 5	0.250	19.30	67.90	0.0	0.0	7.70	0.169E-04	13.4	0
B 6	0.250	355.70	67.50	0.0	0.0	6.70	0.151E-04	11.6	0
B 7	0.350	85.10	85.50	0.0	0.0	6.40	0.135E-04	11.1	0
B 8	0.350	46.10	74.30	0.0	0.0	11.60	0.138E-04	20.1	0
B 9	0.450	61.80	81.30	0.0	0.0	11.40	0.106E-04	19.8	0
B 10	0.450	49.80	79.10	0.0	0.0	8.70	0.264E-04	15.1	0
B 11	0.770	40.00	72.90	0.0	0.0	7.20	0.881E-05	12.6	0
B 12	0.770	143.70	71.80	0.0	0.0	18.10	0.940E-05	31.0	0
B 13	0.890	75.70	71.60	0.0	0.0	6.90	0.109E-04	12.1	0
B 14	0.890	45.00	81.90	0.0	0.0	6.00	0.108E-04	10.5	0
B 15	1.240	59.90	71.30	0.0	0.0	21.30	0.268E-05	36.3	0
B 16	1.240	70.40	65.40	0.0	0.0	17.30	0.223E-05	29.8	0
B 17	1.360	65.10	77.80	0.0	0.0	29.40	0.665E-05	49.1	0
B 18	1.360	160.40	77.00	0.0	0.0	10.00	0.712E-05	17.3	0
B 19	1.540	1.80	66.60	0.0	0.0	74.70	0.145E-05	96.5	0
B 20	1.540	1.80	66.60	0.0	0.0	40.10	0.190E-05	64.5	0
B 21	1.680	13.10	59.90	0.0	0.0	47.40	0.108E-05	73.6	0
B 22	1.680	13.10	59.90	0.0	0.0	12.70	0.247E-05	22.1	0
B 23	2.010	309.10	78.50	0.0	0.0	24.20	0.480E-05	41.0	0
B 24	2.010	10.60	81.70	0.0	0.0	16.00	0.422E-05	27.5	0
B 25	2.180	13.20	70.40	0.0	0.0	38.60	0.193E-05	62.4	0
B 26	2.180	354.90	70.30	0.0	0.0	19.00	0.283E-05	32.5	0
B 27	2.410	334.30	81.20	0.0	0.0	18.40	0.384E-05	31.6	0
B 28	2.410	31.80	81.00	0.0	0.0	6.60	0.746E-05	11.5	0
B 29	2.760	61.40	78.40	0.0	0.0	16.00	0.921E-05	27.5	0
B 30	2.760	138.00	74.40	0.0	0.0	20.10	0.799E-05	47.2	0
B 31	2.840	30.40	70.80	0.0	0.0	5.10	0.842E-05	8.9	0
B 32	2.840	62.00	77.60	0.0	0.0	9.90	0.803E-05	17.2	0
B 33	2.930	31.30	81.10	0.0	0.0	14.40	0.502E-05	24.8	0
B 34	2.930	88.10	78.90	0.0	0.0	10.90	0.599E-05	18.8	0
B 35	3.060	88.10	78.90	0.0	0.0	90.00	0.509E-05	100.0	0
B 36	3.060	325.00	56.50	0.0	0.0	65.80	0.512E-05	91.2	0
B 37	3.170	302.00	87.10	0.0	0.0	8.60	0.698E-05	14.8	0
B 38	3.190	9.20	87.70	0.0	0.0	11.80	0.830E-05	20.4	0
B 39	3.360	114.50	81.80	0.0	0.0	5.10	0.748E-05	9.0	0
B 40	3.360	34.90	81.60	0.0	0.0	11.50	0.866E-05	20.0	0
B 41	3.560	49.60	85.40	0.0	0.0	10.30	0.627E-05	17.8	0
B 42	3.560	39.40	84.40	0.0	0.0	17.10	0.662E-05	29.4	0
B 43	20.710	40.40	80.60	0.0	0.0	4.10	0.295E-03	7.1	0
B 43	20.710	46.70	82.50	0.0	0.0	3.40	0.235E-03	6.0	10
B 44	20.710	31.20	82.30	0.0	0.0	3.50	0.333E-03	6.2	0
B 44	20.710	56.50	76.70	0.0	0.0	3.60	0.232E-03	6.2	10
B 45	20.650	48.30	83.60	0.0	0.0	2.10	0.270E-03	3.6	0
B 45	"	46.20	83.90	0.0	0.0	3.00	0.257E-03	5.2	2
B 45	"	45.00	84.00	0.0	0.0	2.30	0.248E-03	4.1	5
B 45	20.650	46.70	84.20	0.0	0.0	3.70	0.218E-03	6.5	10
B 45	"	43.10	84.90	0.0	0.0	2.40	0.178E-03	4.3	15
B 45	"	43.40	84.80	0.0	0.0	2.30	0.157E-03	3.9	20
B 45	"	40.30	85.80	0.0	0.0	2.80	0.114E-03	4.9	30
B 45	"	20.80	85.50	0.0	0.0	5.10	0.868E-04	8.8	40
B 45	"	56.60	81.10	0.0	0.0	5.50	0.706E-04	9.6	50
B 46	20.650	21.60	84.00	0.0	0.0	1.90	0.269E-03	3.3	0
B 46	"	13.30	83.50	0.0	0.0	2.80	0.255E-03	4.8	2
B 46	"	18.70	84.00	0.0	0.0	2.90	0.248E-03	5.0	5
B 46	20.650	23.80	84.90	0.0	0.0	3.10	0.217E-03	5.5	10
B 46	"	16.50	84.80	0.0	0.0	4.10	0.183E-03	7.2	15
B 46	"	29.20	84.60	0.0	0.0	3.60	0.158E-03	6.2	20
B 46	"	21.50	84.00	0.0	0.0	4.00	0.114E-03	7.1	30
B 46	"	53.00	82.40	0.0	0.0	3.70	0.881E-04	6.4	40
B 46	"	347.80	82.90	0.0	0.0	10.20	0.719E-04	17.7	50
B 47	20.590	12.40	68.20	0.0	0.0	5.20	0.271E-03	9.0	0
B 47	20.590	11.70	69.40	0.0	0.0	4.80	0.201E-03	8.4	10
B 48	20.590	7.80	70.00	0.0	0.0	3.70	0.365E-03	6.4	0
B 48	20.590	8.50	70.50	0.0	0.0	3.50	0.282E-03	6.0	10
B 49	20.530	0.90	77.20	0.0	0.0	3.40	0.325E-03	5.9	0
B 49	"	1.20	78.30	0.0	0.0	4.50	0.300E-03	7.8	2
B 49	"	359.90	78.00	0.0	0.0	4.60	0.293E-03	8.0	5
B 49	20.530	358.30	77.00	0.0	0.0	4.90	0.262E-03	8.5	10
B 49	"	1.50	79.10	0.0	0.0	4.60	0.221E-03	8.1	15
B 49	"	0.90	78.30	0.0	0.0	4.60	0.184E-03	8.0	20
B 49	"	8.90	81.30	0.0	0.0	5.60	0.125E-03	9.8	30
B 49	"	7.20	81.60	0.0	0.0	7.00	0.847E-04	12.2	40
B 49	"	324.60	83.90	0.0	0.0	6.30	0.644E-04	11.0	50
B 50	20.530	12.90	75.20	0.0	0.0	3.00	0.283E-03	5.2	0
B 50	"	6.10	76.60	0.0	0.0	4.60	0.209E-03	8.0	2
B 50	"	11.30	76.10	0.0	0.0	2.60	0.293E-03	4.6	5
B 50	20.530	11.50	75.80	0.0	0.0	2.80	0.257E-03	4.8	10
B 50	"	11.40	75.40	0.0	0.0	3.60	0.216E-03	6.2	15
B 50	"	9.50	76.80	0.0	0.0	2.50	0.184E-03	4.3	20
B 50	"	8.30	75.70	0.0	0.0	2.60	0.128E-03	4.6	30

8 50	"	15.20	74.90	0.0	0.0	6.20	0.946E-04	10.8	40		
8 50	"	1.60	77.70	0.0	0.0	5.00	0.582E-04	8.8	50		
8 51	20.450	6.00	72.60	0.0	0.0	2.10	0.214E-03	3.7	0		
8 51	"	6.90	71.50	0.0	0.0	3.10	0.202E-03	5.5	2		
8 51	"	6.60	71.10	0.0	0.0	2.60	0.201E-03	4.5	5		
8 51	20.450	6.60	71.60	0.0	0.0	3.10	0.177E-03	5.4	10		
8 51	"	8.40	71.30	0.0	0.0	3.50	0.150E-03	6.1	15		
8 51	"	9.30	72.10	0.0	0.0	2.90	0.129E-03	5.1	20		
8 51	"	7.60	69.60	0.0	0.0	4.60	0.866E-04	8.1	30		
8 51	"	9.80	69.20	0.0	0.0	4.50	0.607E-04	7.8	40		
8 51	"	6.90	71.80	0.0	0.0	5.50	0.438E-04	9.5	50		
8 52	20.450	3.00	72.30	0.0	0.0	1.60	0.223E-03	2.8	0		
8 52	"	0.80	72.30	0.0	0.0	2.00	0.217E-03	3.5	2		
8 52	"	1.80	72.00	0.0	0.0	2.20	0.204E-03	3.8	5		
8 52	20.450	1.90	72.80	0.0	0.0	2.70	0.192E-03	4.7	10		
8 52	"	2.90	72.60	0.0	0.0	3.10	0.157E-03	5.4	15		
8 52	"	3.00	73.40	0.0	0.0	2.40	0.136E-03	4.2	20		
8 52	"	354.60	73.90	0.0	0.0	3.40	0.923E-04	6.0	30		
8 52	"	359.20	72.20	0.0	0.0	3.60	0.626E-04	6.2	40		
8 52	"	8.90	74.70	0.0	0.0	4.00	0.431E-04	7.0	50		
8 53	20.390	12.20	74.20	0.0	0.0	1.60	0.371E-03	2.8	0		
8 53	"	12.80	74.30	0.0	0.0	3.10	0.369E-03	5.4	2		
8 53	"	10.10	74.30	0.0	0.0	3.10	0.362E-03	5.4	5		
8 53	20.390	11.60	74.70	0.0	0.0	3.50	0.326E-03	6.2	10		
8 53	"	14.40	75.20	0.0	0.0	5.10	0.268E-03	8.8	15		
8 53	"	12.00	75.40	0.0	0.0	2.20	0.231E-03	3.9	20		
8 53	"	7.40	73.50	0.0	0.0	4.00	0.162E-03	7.0	30		
8 53	"	15.00	78.00	0.0	0.0	4.60	0.112E-03	8.0	40		
8 53	"	6.50	76.20	0.0	0.0	4.70	0.854E-04	8.2	50		
8 54	20.390	26.00	77.90	0.0	0.0	2.50	0.301E-03	4.4	0		
8 54	"	28.60	77.60	0.0	0.0	3.60	0.293E-03	6.2	2		
8 54	"	30.30	78.00	0.0	0.0	3.90	0.283E-03	6.7	5		
8 54	20.390	31.30	77.90	0.0	0.0	3.40	0.251E-03	6.0	10		
8 54	"	33.80	79.00	0.0	0.0	5.70	0.209E-03	10.0	15		
8 54	"	30.70	78.90	0.0	0.0	4.60	0.180E-03	8.0	20		
8 54	"	28.20	78.40	0.0	0.0	4.30	0.132E-03	7.6	30		
8 54	"	43.30	79.10	0.0	0.0	6.20	0.970E-04	10.8	40		
8 54	"	36.60	75.00	0.0	0.0	5.70	0.685E-04	9.9	50		
8 55	20.310	3.70	70.00	0.0	0.0	2.90	0.356E-03	5.0	0		
8 55	"	1.10	70.10	0.0	0.0	3.40	0.350E-03	5.9	2		
8 55	"	2.00	69.90	0.0	0.0	3.30	0.342E-03	5.8	5		
8 55	20.310	0.50	70.30	0.0	0.0	3.50	0.305E-03	6.1	10		
8 55	"	359.90	69.90	0.0	0.0	3.40	0.251E-03	6.0	15		
8 55	"	359.00	71.10	0.0	0.0	3.60	0.215E-03	6.3	20		
8 55	"	1.70	69.50	0.0	0.0	3.40	0.149E-03	6.0	30		
8 55	"	4.10	68.50	0.0	0.0	4.70	0.109E-03	8.3	40		
8 55	"	4.00	69.00	0.0	0.0	3.10	0.830E-04	5.4	50		
8 56	20.310	4.40	69.80	0.0	0.0	2.30	0.331E-03	4.0	0		
8 56	"	2.10	69.80	0.0	0.0	3.60	0.327E-03	6.3	2		
8 56	"	2.20	70.10	0.0	0.0	4.40	0.319E-03	7.7	5		
8 56	20.310	3.10	69.10	0.0	0.0	3.20	0.291E-03	5.6	10		
8 56	"	3.40	70.40	0.0	0.0	3.60	0.239E-03	6.2	15		
8 56	"	4.00	70.00	0.0	0.0	3.30	0.199E-03	5.8	20		
8 56	"	4.90	70.50	0.0	0.0	3.50	0.139E-03	6.1	30		
8 56	"	1.90	71.60	0.0	0.0	4.50	0.942E-04	7.9	40		
8 56	"	1.30	71.50	0.0	0.0	3.30	0.709E-04	5.7	50		
8 57	20.210	341.30	65.40	29.70	67.20	1.60	0.425E-03	2.9	0		
8 57	20.210	339.60	65.20	28.30	67.70	1.50	0.337E-03	2.7	10		
8 58	20.210	338.30	59.80	17.30	64.40	2.80	0.509E-03	4.8	0		
8 58	20.210	337.50	59.40	16.00	64.40	2.60	0.406E-03	4.5	10		
8 59	20.130	349.40	63.90	32.40	63.60	7.10	0.324E-03	12.3	0		
8 59	20.130	347.80	63.70	30.90	63.90	8.50	0.246E-03	14.7	10		
8 60	20.130	356.00	61.50	33.30	59.70	6.40	0.323E-03	11.2	0		
8 60	20.130	353.60	61.60	31.80	60.60	7.20	0.249E-03	12.5	10		
8 61	20.050	349.20	59.30	25.40	60.30	2.20	0.365E-03	3.8	0		
8 61	20.050	348.90	59.60	25.60	60.70	2.00	0.286E-03	3.6	10		
8 62	20.050	345.20	64.50	30.60	65.30	2.40	0.311E-03	4.2	0		
8 62	20.050	342.40	64.10	0.0	0.0	2.80	0.238E-03	4.8	10		
8 63	20.100	340.50	67.10	32.90	68.40	2.60	0.120E-03	4.6	0		
8 63	20.100	337.50	67.10	31.20	69.40	3.50	0.886E-04	6.2	10		
8 64	20.100	341.30	67.60	34.50	68.50	5.90	0.167E-03	10.4	0		
8 64	20.100	338.70	64.10	26.10	66.90	5.90	0.123E-03	10.3	10		
8 65	20.030	350.70	60.50	28.10	60.70	2.70	0.267E-03	4.8	0		
8 65	20.030	350.60	59.20	26.40	59.80	2.70	0.206E-03	4.7	10		
8 66	20.030	341.40	58.50	18.00	62.40	2.40	0.267E-03	4.2	0		
8 66	20.030	340.40	57.50	15.60	62.00	2.30	0.206E-03	4.1	10		
8 67	19.900	334.80	64.80	24.00	69.00	3.10	0.178E-03	5.3	0		
8 67	19.900	331.80	62.60	16.90	68.60	2.80	0.132E-03	4.9	10		
8 68	19.900	321.40	56.60	355.50	67.90	7.00	0.216E-03	12.2	0		
8 68	19.900	336.70	54.80	8.80	61.20	11.10	0.183E-03	19.3	10		
8 69	19.780	329.20	35.20	344.20	46.60	2.00	0.330E-03	3.5	0		
8 70	19.780	334.20	37.80	351.10	47.40	3.80	0.387E-03	6.7	0		
8 70	19.780	327.80	24.90	337.80	37.40	3.20	0.265E-03	5.6	10		
8 71	19.550	338.60	51.00	6.30	57.40	5.10	0.847E-04	8.8	0		
8 71	19.550	332.80	45.70	355.40	54.90	11.60	0.704E-04	20.1	10		
8 72	19.550	341.10	48.20	6.00	54.20	4.20	0.118E-03	7.4	0		
8 72	19.550	333.40	43.20	354.00	52.80	3.50	0.926E-04	8.1	10		
8 73	19.440	337.90	45.60	0.60	53.10	2.50	0.152E-03	4.4	0		
8 73	19.440	333.70	44.70	355.50	53.70	5.50	0.118E-03	9.6	10		
8 74	19.440	337.30	49.20	3.20	56.40	5.60	0.158E-03	9.8	0		
8 74	19.440	330.30	46.90	353.80	56.80	10.10	0.125E-03	17.5	10		
8 75	19.700	318.00	55.90	5.30	72.90	3.80	0.269E-03	6.7	0		
8 75	19.700	314.70	53.00	353.70	72.30	5.30	0.214E-03	9.2	10		
8 76	19.700	326.10	56.50	15.20	69.60	2.90	0.287E-03	5.1	0		
8 76	19.700	323.80	53.40	6.10	68.70	4.10	0.222E-03	7.1	10		
8 77	19.610	334.20	53.10	16.00	63.90	4.10	0.244E-03	7.2	0		
8 77	19.610	330.30	48.80	5.40	62.50	3.80	0.195E-03	6.6	10		
8 78	19.610	332.40	56.60	20.90	66.90	2.20	0.284E-03	3.8	0		
8 78	19.610	332.40	53.80	15.50	65.20	2.50	0.233E-03	4.4	10		
8 79	19.550	329.70	49.10	5.00	63.00	2.80	0.239E-03	4.9	0		
8 79	19.550	328.90	46.20	0.30	61.10	3.60	0.201E-03	6.3	10		
8 80	19.550	329.60	56.70	18.80	68.20	2.40	0.281E-03	4.1	0		
8 80	19.550	326.20	52.50	7.00	67.00	4.10	0.227E-03	7.2	10		
8 81	19.470	328.90	48.60	3.60	63.00	8.80	0.345E-03	15.3	0		
8 81	19.470	329.50	49.90	6.00	63.70	4.70	0.309E-03	8.1	10		
8 82	19.470	332.00	46.20	3.60	59.80	2.30	0.384E-03	4.0	0		
8 82	19.470	328.90	41.00	354.40	56.90	2.10	0.314E-03	3.6	10		
8 83	19.360	343.10	68.30	53.80	67.50	5.70	0.281E-03	10.0	0		
8 83	19.360	338.70	64.60	43.20	68.00	8.70	0.218E-03	15.2	10		
8 84	19.360	351.30	64.00	47.40	62.80	4.40	0.303E-03	7.6	0		
8 84	19.360	347.20	62.60	42.70	63.70	7.10	0.236E-03	12.4	10		
8 85	19.250	340.70	61.90	37.80	66.10	4.10	0.161E-03	7.2	0		
8 85	19.250	336.50	58.50	27.90	66.10	6.40	0.127E-03	11.2	10		
8 86	19.250	341.10	62.80	40.10	66.30	6.60	0.140E-03	11.5	0		
8 86	19.250	335.30	61.60	34.20	68.20	6.60	0.116E-03	11.5	10		
8 87	19.170	353.50	64.50	49.30	62.20	3.80	0.125E-03	6.6	0		
8 87	19.170	347.90	61.80	41.40	63.00	5.70	0.948E-04	9.9	10		
8 88	19.170	2.50	67.80	56.90	60.50	4.70	0.141E-03	8.3	0		
8 88	19.170	348.50	65.40	48.90	64.50	7.40	0.109E-03	12.8	10		
8 89	19.060	344.70	68.30	41.20	70.00	6.10	0.136E-03	10.6	0		
8 89	19.060	340.10	67.30	50.40	68.30	3.80	0.119E-03	6.7	10		
8 90	19.060	353.10	65.20	50.50	62.60	2.40	0.110E-03	4.1	0		
8 90	19.060	343.20	61.00	37.40	64.60	4.60	0.832E-04	8.1	10		
8 91	18.960	326.70	55.60	13.60	68.80	4.80	0.113E-03	8.3	0		
8 91	18.960	324.20	54.00	7.80	68.90	3.80	0.875E-04	6.7	10		
8 92	18.960	331.40	59.40	10.70	69.00	4.00	0.122E-03	7.0	0		
8 92	18.960	350.00	55.30	16.10	67.20	3.20	0.947E-04	5.6	10		
8 93	18.760	7.10	66.90	50.90	62.30	3.30	0.500E-03	5.8	0		
8 93	18.760	0.50	65.60	54.30	60.10	7.70	0.340E-03	13.5	10		
8 94	18.760	346.00	66.90	51.30	66.00	3.60	0.426E-03	6.3	0		
8 94	18.760	342.20	64.90	45.20	66.70	3.40	0.334E-03	6.0	10		
8 95	18.690	10.10	69.60	64.60	59.00	3.10	0.385E-03	5.4	0		
8 95	18.690	4.80	68.60	61.10	60.10	3.10	0.281E-03	5.4	10		
8 96	18.690	359.60	73.30	68.90	63.60	4.30	0.343E-03	7.5	0		
8 96	18.690	350.20	71.60	63.30	65.90	8.10	0.245E-03	14.2	10		
8 97	18.560	54.10	75.60	0.0	0.0	3.20	0.801E-04	5.7	0		
8 97	18.560	38.00	76.80	0.0	0.0	2.80	0.543E-04	5.0	10		
8 98	18.560	53.10	70.80	0.0	0.0	3.90	0.563E-04	8.1	0		

B 98	18 560	46 00	71 20	0 0	0 0	2 50	0 455E-04	4 3	10
B 99	18 470	90 40	69 50	0 0	0 0	2 20	0 993E-04	3 8	0
B 99	18 470	91 70	70 50	0 0	0 0	3 40	0 799E-04	5 9	10
B100	18 470	52 10	76 60	0 0	0 0	3 20	0 702E-04	5 5	0
B100	18 470	47 50	78 10	0 0	0 0	2 40	0 552E-04	4 2	10
B101	18 370	76 10	64 10	0 0	0 0	3 90	0 196E-03	6 7	0
B101	18 370	79 40	65 00	0 0	0 0	3 20	0 145E-03	5 5	10
B102	18 370	85 50	62 10	0 0	0 0	6 40	0 118E-03	11 1	0
B102	18 370	84 00	64 60	0 0	0 0	10 40	0 838E-04	18 0	10
B103	18 270	96 10	58 50	0 0	0 0	4 10	0 225E-03	7 1	0
B103	18 270	98 60	56 90	0 0	0 0	4 50	0 178E-03	7 9	10
B104	18 270	92 50	53 10	0 0	0 0	5 60	0 219E-03	9 8	0
B104	18 270	93 40	51 70	0 0	0 0	4 10	0 156E-03	7 2	10
B105	18 150	89 70	72 60	0 0	0 0	3 80	0 231E-03	6 6	0
B105	18 150	90 50	73 30	0 0	0 0	5 70	0 165E-03	10 0	10
B106	18 150	90 20	64 50	0 0	0 0	3 40	0 185E-03	5 9	0
B106	18 150	91 30	66 10	0 0	0 0	2 40	0 131E-03	4 2	10
B107	18 030	105 30	35 60	0 0	0 0	5 10	0 118E-03	8 9	0
B107	18 030	106 50	34 50	0 0	0 0	4 60	0 783E-04	7 9	10
B108	18 030	113 70	45 20	0 0	0 0	7 50	0 173E-03	13 0	0
B108	18 030	118 70	40 00	0 0	0 0	3 80	0 119E-03	6 6	10
B109	17 980	88 70	66 70	0 0	0 0	2 80	0 919E-04	4 9	0
B109	17 980	86 50	64 10	0 0	0 0	4 20	0 580E-04	7 4	10
B110	17 980	100 70	55 30	0 0	0 0	5 90	0 862E-04	10 3	0
B110	17 980	92 70	57 90	0 0	0 0	5 10	0 529E-04	8 8	10
B111	17 870	22 10	71 80	0 0	0 0	5 30	0 118E-03	9 2	0
B111	17 870	4 70	68 10	0 0	0 0	20 90	0 829E-04	35 7	10
B112	17 870	23 70	70 70	0 0	0 0	4 20	0 129E-03	7 3	0
B112	17 870	9 90	70 30	0 0	0 0	4 60	0 918E-04	7 9	10
B113	17 770	87 20	67 40	0 0	0 0	5 40	0 107E-03	9 4	0
B113	17 770	80 20	67 20	0 0	0 0	6 50	0 744E-04	11 3	10
B114	17 770	88 70	81 30	0 0	0 0	3 50	0 937E-04	6 0	0
B114	17 770	72 90	85 50	0 0	0 0	3 10	0 595E-04	5 4	10
B115	17 660	62 70	75 80	0 0	0 0	5 30	0 162E-03	9 2	0
B115	17 660	46 20	78 20	0 0	0 0	4 40	0 112E-03	7 6	10
B116	17 660	108 10	80 00	0 0	0 0	4 40	0 127E-03	7 7	0
B116	17 660	117 30	80 00	0 0	0 0	2 90	0 901E-04	5 1	10
B117	17 550	48 50	76 50	0 0	0 0	3 20	0 128E-03	5 6	0
B117	17 550	30 80	76 90	0 0	0 0	4 30	0 915E-04	7 4	10
B118	17 550	47 10	76 00	0 0	0 0	4 30	0 111E-03	7 5	0
B118	17 550	26 40	72 90	0 0	0 0	6 30	0 725E-04	10 9	10
B119	17 460	19 70	76 50	0 0	0 0	7 00	0 135E-03	12 2	0
B119	17 460	14 50	73 50	0 0	0 0	3 10	0 102E-03	5 5	10
B120	17 460	25 70	77 60	0 0	0 0	4 90	0 141E-03	8 5	0
B120	17 460	20 80	73 70	0 0	0 0	3 30	0 968E-04	5 7	10
B121	17 360	39 80	72 10	0 0	0 0	2 20	0 128E-03	3 8	0
B121	17 360	0 0	0 0	0 0	0 0	2 40	0 945E-04	4 1	10
B122	17 360	61 80	76 90	0 0	0 0	7 00	0 115E-03	12 2	0
B122	17 360	28 90	76 10	0 0	0 0	7 90	0 840E-04	13 8	10
B123	17 260	15 60	80 10	0 0	0 0	2 80	0 939E-04	4 9	0
B123	17 260	111 50	69 30	0 0	0 0	4 20	0 760E-04	7 3	10
B124	17 260	28 90	76 90	0 0	0 0	4 90	0 122E-03	8 5	0
B124	17 260	344 80	75 70	0 0	0 0	7 00	0 868E-04	12 2	10
B125	17 170	14 90	64 60	0 0	0 0	8 90	0 678E-04	15 5	0
B125	17 170	15 90	63 90	0 0	0 0	4 30	0 615E-04	7 4	10
B126	17 170	5 70	73 50	0 0	0 0	7 00	0 579E-04	12 3	0
B126	17 170	0 90	69 10	0 0	0 0	8 70	0 471E-04	15 1	10
B127	17 100	1 20	61 10	0 0	0 0	4 80	0 684E-04	8 4	0
B127	17 100	1 60	57 80	0 0	0 0	3 90	0 644E-04	6 7	10
B128	17 100	3 30	54 90	0 0	0 0	4 80	0 937E-04	8 5	0
B128	17 100	2 70	53 10	0 0	0 0	4 40	0 857E-04	7 7	10
B129	17 000	350 30	66 20	0 0	0 0	6 70	0 682E-04	11 7	0
B129	17 000	356 50	64 00	0 0	0 0	5 10	0 620E-04	8 9	10
B130	17 000	13 50	62 60	0 0	0 0	6 30	0 609E-04	11 0	0
B130	17 000	11 40	61 30	0 0	0 0	6 70	0 529E-04	11 6	10
B131	16 910	10 90	64 30	0 0	0 0	6 40	0 693E-04	11 1	0
B131	16 910	11 40	61 00	0 0	0 0	4 60	0 624E-04	8 0	10
B132	16 910	357 50	62 10	0 0	0 0	4 60	0 566E-04	8 0	0
B132	16 910	2 60	57 00	0 0	0 0	4 00	0 512E-04	7 0	10

B133	16 820	359 90	79 60	0 0	0 0	5 30	0 556E-04	9 3	0
B133	16 820	1 90	76 10	0 0	0 0	2 90	0 488E-04	5 1	10
B134	16 820	3 20	66 50	0 0	0 0	4 10	0 610E-04	7 2	0
B134	16 820	5 00	65 10	0 0	0 0	5 20	0 516E-04	9 0	10
B135	16 720	20 40	77 30	0 0	0 0	2 10	0 174E-03	3 7	0
B135	16 720	20 70	77 50	0 0	0 0	2 70	0 162E-03	4 8	10
B136	16 720	15 40	73 20	0 0	0 0	4 30	0 132E-03	7 6	0
B136	16 720	14 80	73 50	0 0	0 0	4 90	0 957E-04	8 6	10
B137	16 640	355 50	69 20	0 0	0 0	3 70	0 156E-03	6 5	0
B137	16 640	351 40	67 30	0 0	0 0	3 60	0 117E-03	6 3	10
B138	16 630	10 10	74 80	0 0	0 0	14 60	0 986E-04	25 2	0
B138	16 630	4 00	77 60	0 0	0 0	4 90	0 821E-04	8 6	10
B139	16 540	9 40	76 00	0 0	0 0	4 10	0 619E-04	7 2	0
B139	16 540	1 40	74 00	0 0	0 0	5 10	0 404E-04	8 9	10
B140	16 540	9 50	74 70	0 0	0 0	5 00	0 621E-04	8 7	0
B140	16 540	355 20	72 80	0 0	0 0	4 50	0 412E-04	7 9	10
B141	16 440	1 40	80 10	0 0	0 0	5 10	0 305E-04	8 8	0
B141	16 440	355 20	72 80	0 0	0 0	6 90	0 192E-04	12 0	10
B142	16 440	11 20	72 90	0 0	0 0	5 20	0 367E-04	9 1	0
B142	16 440	355 20	72 80	0 0	0 0	9 00	0 239E-04	15 7	10
B143	16 360	20 40	76 80	0 0	0 0	7 60	0 531E-04	13 2	0
B143	16 360	16 30	76 80	0 0	0 0	5 00	0 346E-04	8 6	10
B144	16 360	20 10	75 20	0 0	0 0	5 40	0 567E-04	9 4	0
B144	16 360	16 10	72 30	0 0	0 0	4 90	0 391E-04	7 8	10
B145	16 260	11 80	78 10	0 0	0 0	4 90	0 505E-04	8 6	0
B145	16 260	5 20	79 90	0 0	0 0	5 00	0 342E-04	8 7	10
B146	16 260	14 50	79 80	0 0	0 0	7 00	0 488E-04	12 1	0
B146	16 260	359 00	77 70	0 0	0 0	4 80	0 315E-04	8 4	10
B147	16 150	31 50	79 00	0 0	0 0	6 40	0 528E-04	11 2	0
B147	16 150	15 80	79 40	0 0	0 0	7 30	0 330E-04	12 7	10
B148	16 150	30 30	75 00	0 0	0 0	6 60	0 512E-04	11 5	0
B148	16 150	24 10	75 00	0 0	0 0	4 40	0 340E-04	7 7	10
B149	15 960	347 80	74 90	0 0	0 0	2 90	0 553E-04	5 0	0
B149	15 960	351 30	73 90	0 0	0 0	5 60	0 325E-04	9 8	10
B150	15 950	20 20	76 70	0 0	0 0	5 20	0 573E-04	9 0	0
B150	15 950	8 50	70 90	0 0	0 0	9 40	0 330E-04	16 4	10
B151	15 840	23 80	78 40	0 0	0 0	5 40	0 534E-04	9 2	0
B151	15 840	11 90	75 30	0 0	0 0	6 80	0 317E-04	11 8	10
B152	15 830	10 30	79 00	0 0	0 0	3 90	0 504E-04	6 7	0
B152	15 830	26 00	81 90	0 0	0 0	5 40	0 313E-04	9 4	10
B153	15 670	31 60	77 50	0 0	0 0	3 50	0 657E-04	6 1	0
B153	15 670	24 30	80 80	0 0	0 0	3 90	0 525E-04	6 8	10
B154	15 680	28 00	75 10	0 0	0 0	8 30	0 625E-04	14 4	0
B154	15 680	22 60	79 00	0 0	0 0	3 90	0 514E-04	6 8	10
B155	15 450	333 40	82 90	0 0	0 0	2 90	0 834E-04	5 0	0
B155	15 450	302 20	80 70	0 0	0 0	3 80	0 575E-04	6 6	10
B156	15 450	356 70	75 20	0 0	0 0	4 10	0 868E-04	7 2	0
B156	15 450	353 30	78 00	0 0	0 0	5 90	0 566E-04	10 3	10
B157	15 280	340 10	82 40	0 0	0 0	11 10	0 937E-04	19 2	0
B157	15 280	320 40	80 50	0 0	0 0	3 20	0 778E-04	5 6	10
B158	15 280	349 90	81 30	0 0	0 0	3 80	0 123E-03	6 6	0
B158	15 280	328 10	79 10	0 0	0 0	5 60	0 870E-04	9 8	10
B159	15 150	313 40	76 40	0 0	0 0	3 60	0 649E-04	6 2	0
B159	15 150	309 80	71 70	0 0	0 0	4 20	0 616E-04	7 4	10
B160	15 150	351 30	75 80	0 0	0 0	8 00	0 732E-04	13 8	0
B160	15 150	345 20	74 80	0 0	0 0	4 40	0 683E-04	7 6	10
B161	14 830	0 70	76 30	0 0	0 0	4 90	0 788E-04	8 6	0
B161	14 830	351 20	75 10	0 0	0 0	4 80	0 741E-04	8 5	10
B162	14 820	341 10	80 20	0 0	0 0	7 50	0 613E-04	13 0	0
B162	14 820	350 60	76 50	0 0	0 0	5 10	0 880E-04	8 9	10
B163	14 640	5 30	68 40	0 0	0 0	4 40	0 655E-04	7 6	0
B163	14 640	353 40	69 00	0 0	0 0	5 70	0 640E-04	9 8	10
B164	14 650	11 00	68 70	0 0	0 0	4 40	0 800E-04	7 7	0
B164	14 650	356 50	69 30	0 0	0 0	6 10	0 696E-04	10 6	10
B165	14 540	23 50	71 10	0 0	0 0	4 30	0 740E-04	7 5	0
B165	14 540	16 50	69 90	0 0	0 0	6 50	0 648E-04	11 3	10
B166	14 540	15 30	74 40	0 0	0 0	5 60	0 606E-04	9 7	0
B166	14 540	14 60	73 00	0 0	0 0	3 50	0 612E-04	6 2	10

8167	14	450	32	60	75	80	0 0	0 0	6 00	0 781E-04	10 5	0
8167	14	450	8	80	76	20	0 0	0 0	5 50	0 580E-04	9 6	10
8168	14	450	20	10	76	70	0 0	0 0	1 70	0 785E-04	3 0	0
8168	14	450	8	30	75	70	0 0	0 0	3 50	0 657E-04	6 2	10
8169	14	330	32	70	72	00	0 0	0 0	4 50	0 622E-04	7 9	0
8169	14	330	13	40	77	50	0 0	0 0	5 00	0 551E-04	8 7	10
8170	14	330	48	80	67	70	0 0	0 0	4 90	0 722E-04	8 6	0
8170	14	330	36	70	73	70	0 0	0 0	5 10	0 641E-04	8 8	10
8171	14	230	19	10	71	60	0 0	0 0	9 70	0 102E-03	16 8	0
8171	14	230	358	00	73	80	0 0	0 0	7 70	0 609E-04	13 4	10
8172	14	230	40	60	68	10	0 0	0 0	5 40	0 537E-04	9 5	0
8172	14	230	19	00	75	20	0 0	0 0	4 90	0 339E-04	8 6	10
8173	14	110	36	20	75	70	0 0	0 0	3 50	0 512E-04	6 1	0
8173	14	110	358	60	82	40	0 0	0 0	3 70	0 347E-04	6 5	10
8174	14	110	29	30	72	50	0 0	0 0	5 10	0 547E-04	9 0	0
8174	14	110	13	80	77	50	0 0	0 0	5 30	0 378E-04	9 2	10
8175	14	010	27	00	68	60	0 0	0 0	4 80	0 550E-04	8 4	0
8175	14	010	7	90	71	70	0 0	0 0	4 80	0 371E-04	8 4	10
8176	14	010	38	40	73	30	0 0	0 0	4 30	0 586E-04	7 5	0
8176	14	010	9	80	79	10	0 0	0 0	5 00	0 386E-04	8 7	10
8177	13	900	22	50	74	20	0 0	0 0	3 40	0 484E-04	5 9	0
8177	13	900	16	00	78	10	0 0	0 0	4 90	0 309E-04	8 6	10
8178	13	900	9	60	78	50	0 0	0 0	3 10	0 494E-04	5 5	0
8178	13	900	0	20	79	90	0 0	0 0	5 40	0 343E-04	9 4	10
8179	13	900	19	40	83	60	0 0	0 0	7 10	0 493E-04	12 3	0
8179	13	900	342	20	82	80	0 0	0 0	5 40	0 317E-04	9 4	10
8180	13	900	3	30	80	80	0 0	0 0	6 50	0 451E-04	11 4	0
8180	13	900	342	70	80	30	0 0	0 0	7 30	0 302E-04	12 7	10
8181	13	840	13	30	82	50	0 0	0 0	10 00	0 139E-03	17 4	0
8181	13	840	24	70	80	30	0 0	0 0	7 70	0 378E-04	13 4	10
8182	13	840	14	80	83	30	0 0	0 0	8 50	0 225E-03	14 8	0
8182	13	840	350	50	80	70	0 0	0 0	7 40	0 482E-04	12 9	10
8183	13	740	30	30	84	30	0 0	0 0	4 50	0 641E-04	7 9	0
8183	13	740	10	80	86	30	0 0	0 0	6 10	0 441E-04	10 6	10
8184	13	740	340	10	80	40	0 0	0 0	9 50	0 657E-04	16 5	0
8184	13	740	333	20	82	70	0 0	0 0	9 10	0 303E-04	15 7	10
8185	13	610	40	30	83	00	0 0	0 0	10 00	0 134E-03	17 4	0
8185	13	610	8	30	83	10	0 0	0 0	7 00	0 905E-04	12 2	10
8186	13	610	32	10	80	30	0 0	0 0	3 80	0 107E-03	6 7	0
8186	13	610	27	00	81	30	0 0	0 0	3 80	0 743E-04	6 5	10
8187	13	500	11	40	80	70	0 0	0 0	4 00	0 929E-04	7 0	0
8187	13	500	5	20	80	70	0 0	0 0	3 00	0 664E-04	5 2	10
8188	13	500	4	70	78	30	0 0	0 0	4 50	0 106E-03	7 8	0
8188	13	500	344	60	78	40	0 0	0 0	5 50	0 834E-04	9 7	10
8189	13	400	10	80	79	40	0 0	0 0	2 60	0 105E-03	4 6	0
8189	13	400	344	40	78	90	0 0	0 0	4 60	0 505E-04	8 0	10
8190	13	400	24	60	76	90	0 0	0 0	3 30	0 989E-04	5 8	0
8190	13	400	8	50	76	60	0 0	0 0	4 90	0 548E-04	8 6	10
8191	12	950	10	20	72	10	0 0	0 0	5 50	0 298E-04	9 5	0
8191	12	950	4	80	69	70	0 0	0 0	4 00	0 183E-04	7 0	10
8192	12	950	0	30	64	50	0 0	0 0	7 00	0 262E-04	12 2	0
8192	12	950	5	60	61	90	0 0	0 0	3 70	0 174E-04	6 5	10
8193	12	840	19	00	64	90	0 0	0 0	7 10	0 310E-04	12 3	0
8193	12	840	17	60	60	60	0 0	0 0	6 20	0 220E-04	10 8	10
8194	12	840	14	80	68	60	0 0	0 0	6 00	0 302E-04	10 5	0
8194	12	840	7	40	62	50	0 0	0 0	7 60	0 209E-04	13 2	10
8195	12	750	21	70	72	30	0 0	0 0	8 00	0 314E-04	13 8	0
8195	12	750	21	60	70	70	0 0	0 0	6 10	0 227E-04	10 7	10
8196	12	750	25	30	72	20	0 0	0 0	8 70	0 288E-04	15 1	0
8196	12	750	22	70	74	00	0 0	0 0	5 20	0 220E-04	9 0	10
8197	12	650	11	30	64	10	0 0	0 0	8 80	0 335E-04	15 3	0
8197	12	650	3	90	61	70	0 0	0 0	5 10	0 242E-04	8 9	10
8198	12	650	11	70	64	00	0 0	0 0	8 40	0 295E-04	14 6	0
8198	12	650	8	00	57	50	0 0	0 0	5 00	0 195E-04	8 7	10
8199	12	550	17	50	72	70	0 0	0 0	6 40	0 216E-04	11 2	0
8199	12	550	2	40	75	50	0 0	0 0	4 80	0 163E-04	8 3	10
8200	12	550	38	80	67	00	0 0	0 0	6 40	0 168E-04	11 2	0
8200	12	550	30	20	71	60	0 0	0 0	4 10	0 127E-04	7 2	10
8201	12	450	358	80	57	10	0 0	0 0	17 20	0 301E-04	29 5	0

8201	12	450	355	40	58	80	0 0	0 0	9 10	0 227E-04	15 8	10
8202	12	450	359	40	63	70	0 0	0 0	7 00	0 310E-04	12 2	0
8202	12	450	344	20	54	50	0 0	0 0	7 00	0 192E-04	12 3	10
8203	12	250	354	30	68	00	0 0	0 0	9 50	0 211E-04	16 5	0
8203	12	250	355	20	59	80	0 0	0 0	5 30	0 168E-04	9 2	10
8204	12	250	357	00	67	00	0 0	0 0	4 80	0 237E-04	8 3	0
8204	12	250	355	30	61	10	0 0	0 0	6 10	0 172E-04	10 7	10
8205	12	150	78	00	75	50	0 0	0 0	14 30	0 141E-04	24 7	0
8206	12	150	8	80	63	10	0 0	0 0	20 80	0 123E-04	35 6	0
8206	12	150	37	80	74	00	0 0	0 0	9 10	0 731E-05	15 8	10
8207	12	000	333	40	66	20	0 0	0 0	37 50	0 844E-05	60 8	0
8207	12	000	343	50	62	80	0 0	0 0	10 80	0 603E-05	18 8	10
8208	12	000	359	80	83	60	0 0	0 0	15 80	0 981E-05	27 2	0
8208	12	000	332	20	80	10	0 0	0 0	19 20	0 521E-05	32 8	10
8209	11	880	53	50	76	40	0 0	0 0	7 60	0 144E-04	13 2	0
8209	11	880	44	80	73	20	0 0	0 0	6 20	0 783E-05	10 7	10
8210	11	880	66	70	78	10	0 0	0 0	6 30	0 124E-04	11 0	0
8210	11	880	111	00	76	90	0 0	0 0	9 00	0 650E-05	15 7	10
8211	11	700	78	30	72	20	0 0	0 0	4 80	0 850E-05	8 4	0
8211	11	700	99	00	68	60	0 0	0 0	9 00	0 446E-05	15 7	10
8212	11	700	105	20	76	00	0 0	0 0	6 50	0 897E-05	11 3	0
8212	11	700	82	00	80	40	0 0	0 0	7 60	0 521E-05	13 2	10
8213	11	570	69	10	74	50	0 0	0 0	6 80	0 911E-05	11 8	0
8213	11	570	39	80	79	90	0 0	0 0	6 20	0 499E-05	10 8	10
8214	11	570	80	60	77	30	0 0	0 0	8 20	0 108E-04	14 3	0
8214	11	570	83	20	86	70	0 0	0 0	9 60	0 503E-05	16 7	10
8215	11	460	40	40	74	80	0 0	0 0	10 40	0 992E-05	18 1	0
8215	11	460	27	80	80	30	0 0	0 0	8 90	0 610E-05	15 5	10
8216	11	460	51	40	79	40	0 0	0 0	6 80	0 106E-04	11 8	0
8216	11	460	357	90	85	40	0 0	0 0	7 40	0 617E-05	12 8	10
8217	11	350	70	40	81	00	0 0	0 0	12 20	0 885E-05	21 1	0
8217	11	350	53	80	81	50	0 0	0 0	6 40	0 688E-05	11 1	10
8218	11	350	326	10	75	20	0 0	0 0	9 30	0 709E-05	16 2	0
8218	11	350	345	50	84	10	0 0	0 0	9 50	0 598E-05	16 5	10
8219	11	250	25	10	72	90	0 0	0 0	9 70	0 925E-05	16 9	0
8219	11	250	24	00	74	40	0 0	0 0	8 50	0 823E-05	14 8	10
8220	11	250	39	80	72	70	0 0	0 0	4 50	0 120E-04	7 8	0
8220	11	250	28	40	72	10	0 0	0 0	8 00	0 107E-04	14 0	10
8221	11	150	35	90	74	80	0 0	0 0	12 80	0 906E-05	22 2	0
8221	11	150	21	60	79	40	0 0	0 0	6 40	0 801E-05	11 2	10
8222	11	150	347	60	72	60	0 0	0 0	11 60	0 747E-05	20 2	0
8222	11	150	351	80	64	80	0 0	0 0	10 20	0 514E-05	17 8	10
8223	11	050	39	70	68	20	0 0	0 0	18 10	0 122E-04	31 1	0
8223	11	050	20	40	64	80	0 0	0 0	17 30	0 736E-05	29 7	10
8224	11	050	0	0	69	60	0 0	0 0	11 30	0 114E-04	19 5	0
8225	10	940	29	70	75	20	0 0	0 0	11 20	0 826E-05	19 4	0
8225	10	940	343	00	85	30	0 0	0 0	8 60	0 485E-05	15 0	10
8226	10	940	37	70	65	10	0 0	0 0	8 00	0 876E-05	13 9	0
8226	10	940	13	20	74	60	0 0	0 0	13 60	0 401E-05	23 5	10
8227	10	820	34	30	79	70	0 0	0 0	5 60	0 198E-04	9 8	0
8227	10	820	8	20	78	80	0 0	0 0	5 80	0 125E-04	10 1	10
8228	10	820	340	50	71	30	0 0	0 0	9 60	0 106E-04	16 6	0
8229	10	710	17	70	64	40	0 0	0 0	12 10	0 112E-04	21 0	0
8229	10	710	9	80	71	60	0 0	0 0	6 70	0 668E-05	11 6	10
8230	10	710	12	70	69	20	0 0	0 0	12 70	0 105E-04	22 1	0
8230	10	710	13	30	66	50	0 0	0 0	9 40	0 731E-05	16 4	10
8231	10	600	43	40	66	50	0 0	0 0	6 80	0 718E-05	11 8	0
8231	10	600	28	70	72	30	0 0	0 0	7 60	0 483E-05	13 2	10
8232	10	600	33	60	67	50	0 0	0 0	8 90	0 779E-05	15 4	0
8232	10	600	16	80	65	50	0 0	0 0	15 40	0 481E-05	26 5	10
8233	10	500	8	10	71	70	0 0	0 0	10 80	0 136E-04	18 7	0
8233	10	500	350	10	66	80	0 0	0 0	8 70	0 912E-05	15 9	10
8234	10	500	4	90	70	20	0 0	0 0	5 60	0 170E-04	9 8	0
8234	10	500	355	80	69	40	0 0	0 0	6 90	0 117E-04	12 0	10
8235	10	350	8	80	65	90	0 0	0 0	3 80	0 852E-05	6 7	0
8235	10	350	2	10	62	00	0 0	0 0	5 50	0 575E-05	9 5	10
8236	10	350	355	10	67	50	0 0	0 0	5 40	0 833E-05	9 3	0
8236	10	350	344	50	65	10	0 0	0 0	6 30	0 580E-05	10 9	10
8237	10	250	8	00	61	20	0 0	0 0	12 30	0 522E-05	21 3	0

8237	10	250	350	80	69	10	0 0	0 0	10 60	0.348E-05	18 4	10
8238	10	250	11	20	63	50	0 0	0 0	12 40	0.636E-05	21 5	0
8238	10	250	0	40	52	40	0 0	0 0	16 70	0.375E-05	28 8	10
8239	10	140	317	10	78	30	0 0	0 0	11 80	0.464E-05	20 4	0
8239	10	140	300	80	80	20	0 0	0 0	12 00	0.310E-05	20 8	10
8240	10	140	358	30	64	00	0 0	0 0	11 10	0.121E-04	19 3	0
8241	10	020	42	40	61	80	0 0	0 0	10 50	0.501E-05	18 1	0
8241	10	020	40	70	61	60	0 0	0 0	11 50	0.360E-05	19 9	10
8242	10	020	24	70	52	10	0 0	0 0	10 80	0.496E-05	18 8	0
8243	9	880	25	30	66	40	0 0	0 0	9 60	0.112E-04	16 7	0
8244	9	880	25	60	62	10	0 0	0 0	9 90	0.199E-04	17 2	0
8245	9	040	353	20	64	60	0 0	0 0	11 80	0.469E-05	20 4	0
8246	9	040	30	90	53	80	0 0	0 0	10 90	0.434E-05	18 9	0
8247	8	940	36	60	78	50	0 0	0 0	20 30	0.359E-05	34 7	0
8248	8	940	36	60	73	90	0 0	0 0	90 00	0.279E-05	100 0	0
8249	8	860	53	60	73	40	0 0	0 0	8 60	0.521E-05	14 9	0
8250	8	860	62	80	79	60	0 0	0 0	8 50	0.101E-04	14 8	0
8251	8	700	14	30	64	50	0 0	0 0	22 70	0.500E-05	38 6	0
8252	8	700	30	00	73	80	0 0	0 0	21 50	0.545E-05	36 7	0
8253	8	580	335	90	76	90	0 0	0 0	10 50	0.672E-05	18 2	0
8254	8	580	28	20	65	90	0 0	0 0	5 60	0.777E-05	9 7	0
8255	8	340	28	20	69	00	0 0	0 0	52 40	0.376E-05	79 2	0
8256	8	340	76	30	63	30	0 0	0 0	14 10	0.426E-05	24 3	0
8257	8	210	353	80	71	20	0 0	0 0	8 80	0.944E-05	15 2	0
8258	8	210	340	70	66	00	0 0	0 0	10 30	0.947E-05	17 9	0
8259	8	120	25	90	74	00	0 0	0 0	14 60	0.479E-05	25 2	0
8260	8	120	24	50	70	20	0 0	0 0	23 20	0.440E-05	39 3	0
8261	8	030	356	80	65	00	0 0	0 0	5 90	0.254E-04	10 3	0
8261	8	030	359	90	65	70	0 0	0 0	9 00	0.180E-04	15 6	10
8262	8	030	346	60	64	90	0 0	0 0	5 40	0.254E-04	9 4	0
8262	8	030	337	30	68	00	0 0	0 0	9 10	0.180E-04	15 8	10
8263	7	920	325	00	72	20	0 0	0 0	6 80	0.123E-04	11 9	0
8264	7	920	350	70	63	70	0 0	0 0	14 20	0.148E-04	24 5	0
8265	7	820	357	60	67	40	0 0	0 0	6 50	0.118E-04	11 4	0
8265	7	820	356	10	67	00	0 0	0 0	6 20	0.851E-05	10 8	10
8266	7	820	347	40	55	30	0 0	0 0	4 50	0.157E-04	7 8	0
8266	7	820	338	50	51	60	0 0	0 0	5 00	0.127E-04	8 8	10
8267	7	720	352	30	64	10	0 0	0 0	4 10	0.223E-04	7 1	0
8267	7	720	347	20	59	40	0 0	0 0	5 30	0.186E-04	9 2	10
8268	7	720	349	10	63	00	0 0	0 0	8 40	0.228E-04	14 6	0
8268	7	720	350	70	60	60	0 0	0 0	7 50	0.183E-04	13 1	10
8269	7	620	343	70	54	00	0 0	0 0	4 90	0.290E-04	8 5	0
8269	7	620	339	60	53	00	0 0	0 0	6 80	0.239E-04	11 8	10
8270	7	620	338	00	63	60	0 0	0 0	4 60	0.193E-04	7 9	0
8270	7	620	336	00	61	90	0 0	0 0	6 90	0.137E-04	12 1	10
8271	7	520	354	70	68	80	0 0	0 0	8 90	0.839E-05	15 5	0
8272	7	510	0	40	71	10	0 0	0 0	4 90	0.867E-05	8 5	0
8273	7	420	34	50	61	20	0 0	0 0	8 50	0.570E-05	14 8	0
8274	7	410	359	00	70	80	0 0	0 0	8 20	0.609E-05	14 2	0
8275	7	240	345	40	64	80	0 0	0 0	5 80	0.266E-04	10 1	0
8275	7	240	337	60	61	20	0 0	0 0	4 20	0.196E-04	7 3	10
8276	7	230	339	10	66	60	0 0	0 0	8 30	0.228E-04	14 4	0
8276	7	230	339	50	62	40	0 0	0 0	12 70	0.157E-04	21 9	10
8277	7	130	19	30	73	60	0 0	0 0	12 40	0.416E-05	21 5	0
8278	7	130	29	00	77	80	0 0	0 0	20 20	0.452E-05	34 6	0
8279	7	030	60	00	54	10	0 0	0 0	17 40	0.341E-05	30 0	0
8280	7	030	347	20	70	30	0 0	0 0	12 00	0.451E-05	20 8	0
8281	6	740	6	70	73	90	0 0	0 0	5 70	0.352E-04	9 9	0
8281	6	740	2	10	71	00	0 0	0 0	5 60	0.257E-04	9 7	10
8282	6	730	345	50	58	70	0 0	0 0	4 50	0.324E-04	7 9	0
8282	6	730	343	10	58	40	0 0	0 0	4 30	0.249E-04	7 4	10
8283	6	410	356	80	63	50	0 0	0 0	5 60	0.260E-04	9 7	0
8283	6	410	345	30	63	90	0 0	0 0	9 00	0.192E-04	15 7	10
8284	6	400	357	80	66	70	0 0	0 0	3 80	0.275E-04	6 6	0
8284	6	400	349	60	64	80	0 0	0 0	8 40	0.196E-04	14 7	10
8285	6	060	49	60	79	30	0 0	0 0	9 90	0.546E-05	17 2	0
8286	6	060	53	40	62	40	0 0	0 0	11 90	0.426E-05	20 7	0
8287	5	930	8	20	78	00	0 0	0 0	6 50	0.645E-05	11 2	0
8288	5	930	291	30	59	70	0 0	0 0	34 90	0.683E-05	97 3	0
8289	5	720	7	30	68	70	0 0	0 0	12 10	0.544E-05	21 0	0
8290	5	720	29	80	65	40	0 0	0 0	44 80	0.124E-04	70 5	0
8291	5	570	335	80	53	60	0 0	0 0	5 60	0.234E-04	9 7	0
8291	5	570	332	70	53	40	0 0	0 0	7 30	0.176E-04	12 7	10
8292	5	570	319	10	57	40	0 0	0 0	5 40	0.458E-04	9 5	0
8292	5	570	317	30	58	50	0 0	0 0	4 30	0.320E-04	7 5	10
8293	5	430	8	30	40	60	0 0	0 0	38 60	0.454E-05	62 4	0
8294	5	430	55	20	72	20	0 0	0 0	43 20	0.191E-05	68 5	0
8295	5	280	148	70	80	90	0 0	0 0	41 70	0.263E-05	66 5	0
8296	5	280	17	20	63	60	0 0	0 0	32 40	0.330E-05	53 6	0
8297	5	190	9	80	82	30	0 0	0 0	27 20	0.439E-05	45 8	0
8298	5	190	153	20	83	90	0 0	0 0	14 80	0.306E-05	25 5	0
8299	5	080	48	70	88	60	0 0	0 0	28 40	0.245E-05	47 5	0
8300	5	080	27	60	79	90	0 0	0 0	14 50	0.284E-05	25 1	0
8301	4	900	42	40	73	40	0 0	0 0	11 40	0.415E-05	19 7	0
8302	4	900	68	20	73	70	0 0	0 0	7 60	0.390E-05	13 2	0
8303	4	730	61	00	68	10	0 0	0 0	7 40	0.557E-05	12 9	0
8304	4	730	222	00	37	20	0 0	0 0	90 00	0.545E-05	100 0	0
8305	4	520	329	00	79	80	0 0	0 0	7 90	0.701E-05	13 7	0
8306	4	520	357	80	72	40	0 0	0 0	11 20	0.817E-05	18 5	0
8307	4	240	5	00	67	90	0 0	0 0	10 80	0.763E-05	18 8	0
8308	4	240	317	10	70	20	0 0	0 0	6 30	0.101E-04	11 0	0